DETERMINATION OF
TOTAL RESPIRATORY COMPLIANCE
DURING ARTIFICIAL VENTILATION

BEPALING VAN LONG EN THORAX
COMPLIANTIE TIJDENS BEADEMING

PROEFSCHRIFT

TER VERKRIJGING VAN DE GRAAD VAN DOCTOR
AAN DE ERASMUS UNIVERSITEIT ROTTERDAM
OP GEZAG VAN DE RECTOR MAGNIFICUS
PROF. DR. A.H.G. RINNOOY KAN
EN VOLGENS BESLUIT VAN HET COLLEGE VAN DEKANEN.
DE OPENBARE VERDEDIGING ZAL PLAATSVINDEN OP
WOENSDAG 14 JUNI 1989 OM 13.45 UUR

DOOR

JEROEN VAN GOUDOEVER

GEBOREN TE LEIDEN

Promotiecommissie

Promotor: : Prof. Dr. A. Versprille

Overige leden : Prof. Dr. C. Hilvering
                       Prof. Dr. S.C.M. Luijendijk, R.U. Limburg
                       Prof. Dr. A. van Oosterom, K.U. Nijmegen

Co-promotor   : Dr. J.M. Bogaard

Aan mijn ouders,
aan Cynthia

CONTENTS

List of abbreviations

ATPD	ambient temperature and pressure, dry
BTPS	body temperature and pressure, saturated
C_{CW}	compliance of the chest wall
C_{DEFL}	compliance derived from the deflation limb of a SID procedure
C_{INFL}	compliance derived from the inflation limb of a SID procedure
$C_{IP,sl}$	compliance derived from the slope of the PV_{IP} curve
$C_{IP,1.5}$	compliance derived from an inspiratory pause using $P_{T,1.5}$
$C_{IP,8.5}$	compliance derived from an inspiratory pause using $P_{T,8.5}$
C_L	compliance of the lungs
C_P	pulse compliance
C_{RS}	total respiratory compliance, i.e. compliance of lungs and chestwall
E	expiration; in chapter 7 also the elastic modulus [N.m^{-2}]
$F_{E,He}$	He fraction of expiratory gas
F_{E,N_2}	N_2 fraction of expiratory gas
$F_{EE,He}$	$F_{E,He}$ at the end of expiration
$F_{I,He}$	He fraction of inspiratory gas
F_{I,N_2}	N_2 fraction of inspiratory gas
F_{I,O_2}	O_2 fraction of inspiratory gas
FRC	functional residual capacity
IP	inspiratory pause
I	inspiration
L_0,L	resting length and current length respectively
min	time in minutes
P	pressure
P_1	magnitude of the slow exponential decay in P_T during an IP
P_2	magnitude of the fast exponential decay in P_T during an IP
P_A	alveolar pressure
P_{ao}	systemic arterial pressure measured in aorta
P_{AW}	airway pressure
P_{a,CO_2}	arterial CO_2 tension
P_{A,CO_2}	alveolar CO_2 tension
P_{CO_2}	CO_2 tension
P_{cv}	central venous pressure
P_{CW}	recoil pressure of the chest wall
P_{EE}	end-expiratory pressure
P_L	recoil pressure of the lungs
P_{pa}	pulmonary artery pressure
P_{RS}	total recoil pressure of lungs and thorax
P_{stat}	estimate of the static recoil pressure
P_T	tracheal pressure

$P_{T,1.5}$, $P_{T,8.5}$	P_T after 1.5 s and 8.5 s IP respectively
PV_{IP}	quasi-static pressure-volume curve
PEEP	positive end-expiratory pressure
R	respiratory exchange ratio
s	time in seconds
SD	standard deviation
SID	slow inflation-deflation
STPD	standard temperature and pressure, dry
t	time
TLC	total lung capacity
V	volume
$V_{CO_2}^{n}$, $V_{N_2}^{n}$, $V_{O_2}^{n}$	volume of CO_2, N_2 and O_2 respectively, in ventilator and tubes during rebreathing cycle n
V_E	expiratory volume
V_{FL}	change in lung volume derived from integration of $\dot{V}$
V_L	lung volume
$V_{L,EE}$	end-expiratory lung volume
V_{MC}	change in lung volume derived from the mercury cord
V_{RBR}	rebreathing volume
V_{RB1}	first inflation volume in the rebreathing procedure
V_T	tidal volume
Vd,eff	effective dead space in tubing between ventilator and lungs
Vd,bellows	dead space in the bellows
$\dot{V}$	ventilatory flow rate
$\dot{V}_E$	expiratory flow rate
$\dot{V}_{CO_2}$	CO_2 output
$\dot{V}_{O_2}$	O_2 uptake
Ya,Yb,Yc	Y–pieces in tubes
ZEEP	zero end-expiratory pressure
ΔR_{MC}	change in the resistance of the mercury cord
Δt_{RBR}	cycle time of rebreathing (2 s)
ϵ	strain $(L-L_0)/L_0$
η	viscosity-modulus $[N.s.m^{-2}]$)
σ	stress $[N.m^{-2}]$
τ_1	time constant of the slow exponential decay [s]
τ_2	time constant of the fast exponential decay [s]

CHAPTER 1

INTRODUCTION

In mechanical ventilation the function of the respiratory muscles to change lung volume is taken over by a ventilator. In most types of mechanical ventilation changes in lung volume coincide with pressure changes at the airway opening. The ventilator inflates the lungs either to a pre-set pressure, which is called pressure controlled ventilation, or to a pre-set volume, which is called volume controlled ventilation. The goal of mechanical ventilation is the maintenance of respiratory gas exchange. A disadvantage of the increase in lung volume and the concomitant rise in intra-thoracic pressure during mechanical ventilation is a reduction in cardiac output [37,104], and therefore a reduction in oxygen transport, since this value is determined by the product of the oxygen content of arterial blood and cardiac output.

The recoil pressure of the total respiratory system, P_{RS}, is determined by the recoil pressure of the lungs, P_L, and the recoil pressure of the thorax or chest wall, P_{CW} from [32,85,87]

$$P_{RS} = P_L + P_{CW} \qquad (1)$$

The recoil pressure of the thorax is composed of recoil pressures from the structures which surround the lungs such as the rib cage and the abdominal compartment. During mechanical ventilation the recoil pressure of the total respiratory system can be estimated by measurement of the pressure at the airway opening (P_{AW}). P_{AW} approximates P_{RS} provided that the airflow rate in the respiratory system is zero and muscle activity is absent. In measurements of the relationship between P_{RS} and the changes in lung volume V the activity of respiratory muscles is either assumed to be absent [90,98], or suppressed by muscle relaxants [31,68]. This thesis is confined to the studies on the relationship between P_{RS} and V, i.e. the P_{RS}-V or the P-V relationship of the respiratory system in paralysed piglets.

The total recoil pressure can be divided into a contribution of lung recoil pressure and thoracic recoil pressure, by measuring the difference between alveolar pressure and intra-thoracic pressure for the estimation of the lung recoil and by measuring the difference between intra-thoracic pressure and ambient air pressure for the estimation of the thoracic recoil. Intra-thoracic pressure is usually measured by means of an oesophageal balloon

[57,72]. However, this technique has been proved to be less accurate in supine subjects because of substantial cardiac interference and changes in absolute pressure due to the weight of the heart and the surrounding structures [71,102,106,109].

It is a common observation that the relationship between the thoracic recoil pressure and the change in lung volume is approximately linear in the volume range which is used for mechanical ventilation [1]. Although changes in the pressure-volume relationship of the thorax were reported in abdominal distension and chest-wall edema [57], the most common cause of a change in the respiratory P-V relationship in patients with acute respiratory failure is a change in elasticity of the lungs [26,68,100]. Changes in the relationship between P_{RS} and lung volume were often found to be the first indication of the development of pulmonary or pleural disorders in patients under mechanical ventilation, like pneumothorax, atelectasis and pulmonary oedema [17].

Total respiratory compliance C_{RS} is the measure which quantifies the relationship between the change in lung volume and the change in alveolar pressure. C_{RS} is defined as the ratio between a change in lung volume and the concomitant change in alveolar pressure, and can be estimated from $C_{RS} = \Delta V / \Delta P_{RS}$. This compliance can be divided into the thoracic compliance C_{CW} and the lung compliance C_L. In one of the methods to estimate C_{RS} during mechanical ventilation an inspiratory pause is applied. This inspiratory pause method has also been called 'inflation hold method' or 'end-inflation occlusion method' by other investigators. During the inspiratory pause airflow rate was zero and hence lung volume was assumed to be constant, provided changes in volume by gas exchange or changes in pulmonary blood volume were negligible. After 1.5 s during an inspiratory pause stable airway pressures have been reported [57,58,90,98]. However, some investigators reported a slowly decreasing pressure during an inspiratory pause of 2.5 s to more than 5 s [17,22]. Such a gradual decrease in pressure could indicate a potential error in the estimation of C_{RS} by the inspiratory pause method for several reasons. Incomplete equilibration of gas pressure in the lungs and viscoelastic forces will contribute to an overestimation of the characteristic elastic pressure for a given lung volume, resulting in an underestimation of compliance. A larger oxygen uptake than CO_2 output will contribute to an overestimation of lung volume when the inflation volume is used, resulting in an overestimation of compliance.

1.1 Objectives of the study.

The main objective of the study presented in this thesis has been the investigation of mechanisms related to the decrease in airway pressure during an inspiratory pause in mechanically ventilated subjects. In particular, we have paid attention to two of these mechanisms, i.e. viscoelasticity and the influence of continuous gas exchange on lung volume. We aimed at estimating the errors in the determination of C_{RS} when assuming the pressure after an inspiratory pause of 1.5 s to be equal to 'the' static recoil pressure of the respiratory system, which is a common assumption in clinical practice [57,90,98]. In addition we aimed at an evaluation of other methods for the estimation of C_{RS} during mechanical ventilation.

This study was performed in animals for reasons of large series of observations in each subject in order to evaluate the accuracy and the reliability of a diversity of standardized methods for the estimation of C_{RS}. We have used piglets.

1.2 Outline of the thesis.

In Chapter 2 a review of the literature on the estimation of C_{RS} during mechanical ventilation is presented.

In Chapter 3 the computer controlled ventilator is described with emphasis on its operation during special ventilatory manoeuvres. Moreover, two different methods for the estimation of the end-expiratory lung volume are discussed.

In Chapter 4 the change in pressure during an inspiratory pause is related to the change in thoracic volume. This change in volume was measured by means of a mercury strain gauge around the rib cage of the piglet.

In Chapter 5 the pulse method and the slow inflation-deflation method are evaluated.

In Chapter 6 those experiments are discussed in which the loss of lung volume by continuous gas exchange was estimated from special ventilatory ('rebreathing') manoeuvres performed at different volume levels above end-expiratory lung volume.

In Chapter 7 an attempt was made to model the airway pressure decay during 'post mortem' inspiratory pauses with a bi-exponential decay process. Also the contribution of lungs and thorax to the total recoil pressure is discussed.

CHAPTER 2

REVIEW OF THE LITERATURE

Several methods can be used to estimate total respiratory compliance C_{RS} during mechanical ventilation. In general, C_{RS} is derived from the relationship between the changes in airway pressure and the changes in lung volume. In the next subsections a number of methods for the estimation of C_{RS} are discussed and special attention is paid to the underlying assumptions of these methods.

2.1 Inspiratory pause method.

In the inspiratory pause method the airway is occluded at the end of an insufflation. In this way C_{RS} can be derived from the ratio of the inflation volume and the difference in airway pressure between inspiratory pause and end-expiration [22,89,100]. This principle is illustrated in Fig. 2.1. Such an inspiratory pause is necessary to approximate the static compliance of the respiratory system. C_{RS} cannot be derived from P_{AW} during insufflation because this pressure is not only due to the static recoil pressure of the respiratory system but is also affected by the flow resistance of the airways, the viscoelasticity of the tissues and equilibration of gas pressures in the lungs [12,22,66]. Peak pressure at end-inflation is considered to be inadequate as a determinant for the derivation of compliance, because this pressure includes a component due to airflow resistance. Therefore, peak pressure does not separate parenchymal disease from airway disease [17,100]. In normal human lungs the dynamic component in the airway pressure decays within 1.5 s from the start of the inspiratory pause [35,63,89,100]. Subsequently, a gradual flattening of the pressure-time course occurs. A pressure measurement after an inspiratory pause of 0.55 s [3] to 1.5 s is usually considered adequate for clinical applications [35,89,100]. Nevertheless, some investigators consider such a pause too short and have applied inspiratory pauses of several seconds [17,22].

Recent publications on intrinsic- or auto PEEP (positive end-expiratory pressure) have showed that in many intensive care patients the time for expiration, allowed by the ventilator, was insufficient for mean alveolar pressure P_A to return to the pre-set end-expiratory pressure. The alveolar pressure will then remain markedly higher than its pre-set value [83,90]. Under such
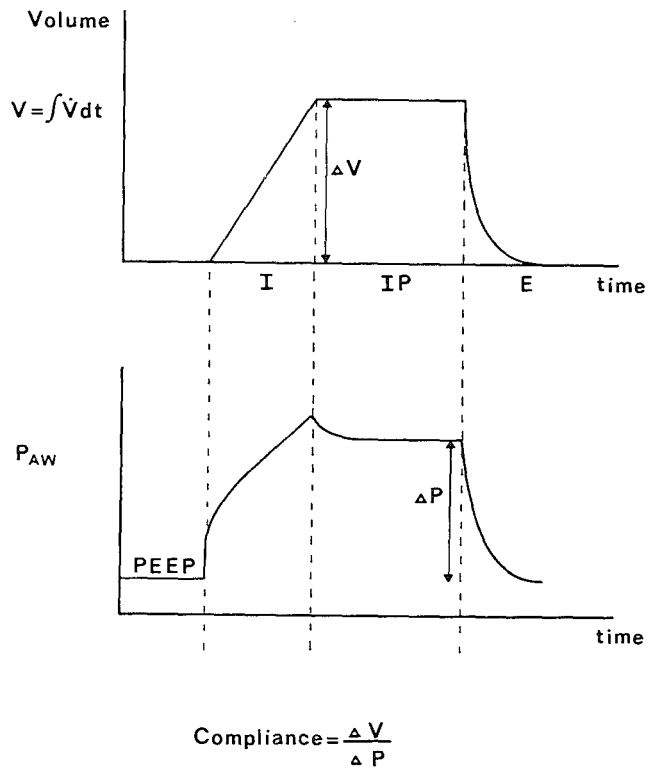
Fig 2.1 Inspiratory pause method.

In the upper panel the imposed lung volume change V, obtained from airflow $\dot{V}$ is plotted as a function of time during the inflation (I), the inspiratory pause (IP) and the subsequent expiration (E).

In the lower panel the corresponding airway pressure P_{AW} is plotted. C_{RS} is derived from the ratio $\Delta V / \Delta P$.

circumstances end-expiratory alveolar pressure should be derived from the airway pressure, obtained by means of a *pause* at end-expiration to equilibrate P_{AW} with P_A [83]. The value of intrinsic PEEP could also be obtained from the rise in airway pressure immediately before the start of the inspiratory flow during insufflation [90].

The P-V curve of the total respiratory system is S-shaped, implying a small increase in volume for a rather large increase in pressure, which inclines to a larger volume rise for a small increase in pressure followed by a declination of the curve to larger rises in pressure per volume increase (cf. e.g. Fig. 2.2). The part at low lung volume where the curve inclines to a steeper approximately linear part has been attributed to recruitment of previously closed lung regions. Because of this nonlinearity in the P-V curve, changes in end-expiratory lung volume and tidal volume will affect the value of compliance [1,17,23,26,27,45,64,100]. A change in lung volume will occur by application of positive end-expiratory pressure, PEEP. In spite of the aforementioned dependence on volume the inspiratory pause method is usually based on the application of a single volume change, corresponding to tidal volume [31,57,63,90]. Therefore, such estimates of C_{RS} pertain to the entire tidal volume. As a consequence total respiratory compliance derived from the inspiratory pause method will underestimate the compliance derived from the slope of the linear part of the quasi-static P-V curve. This situation is visualized in Fig. 2.2. The underestimation will be even more pronounced when the nonlinearity of the P-V relationship is larger at low lung volumes.

An evident advantage of this method is its fast and safe performance with most ventilators without having to disconnect the patient from the ventilator in normal mechanical ventilation [17]. When a stable plateau pressure is found during an inspiratory pause an absence of muscular activity can be concluded [89,110]. Therefore, muscle paralysis is not required in the inspiratory pause method.

2.2   Multiple inspiratory pause procedures.

If inspiratory pause procedures are performed at different volumes the plateau pressures and the inflation volumes can be used to construct a quasi-static P-V curve as in Fig. 2.2 [17,51,100]. During mechanical ventilation changes in alveolar pressure are a consequence of changes in lung volume. Therefore, the volume axis should be the abscissa. In pulmonary physiology, however, volume is usually presented on the ordinate because an easier comparison

15
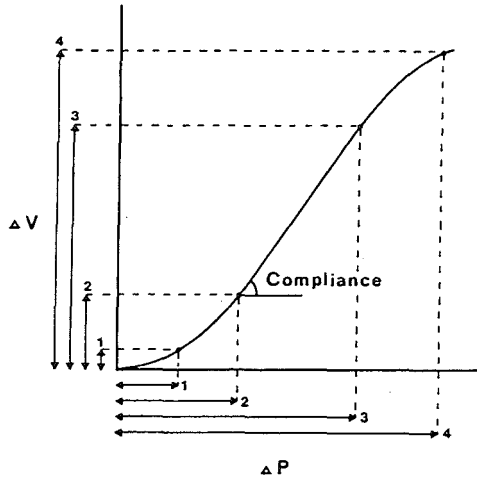
Fig 2.2 The multiple inspiratory pause method.
The pressure differences ΔP and the volume differences ΔV, as obtained from a series of inspiratory pause procedures (Fig. 2.1) can be combined to calculate the quasi-static P-V curve. Four examples (1–4) are given. C_{RS} can be derived from the linear part of the curve.

with P-V curves is obtained during spontaneous breathing. For this reason we plot all relationships between pressure and volume with pressure on the X–axis and volume on the Y–axis. Detection of a change in the slope and in the position of P-V curves in the diagram is considered to be a useful diagnostic tool during mechanical ventilation, because it provides early indications for e.g. atelectasis, pneumothorax, pulmonary edema, progressive pneumonia and other pulmonary diseases affecting pulmonary compliance [17]. Hylkema and coworkers [51] performed a linear regression analysis on the different pressure-volume points, and they argued that the slope of such a line is probably a more realistic estimate of the compliance of the respiratory system than compliance derived from a single inspiratory pause. The multiple inspiratory pause technique can be performed comparatively easy, although some investigators find the technique 'fastidious' [69,101].

2.3 Pulse method.

When lung volume is increased at a constant flow rate and when airway pressure is rising linearly in time after an initial transient, compliance can be directly calculated from the ratio of the flow $\dot{V}$ and the slope of the pressure-
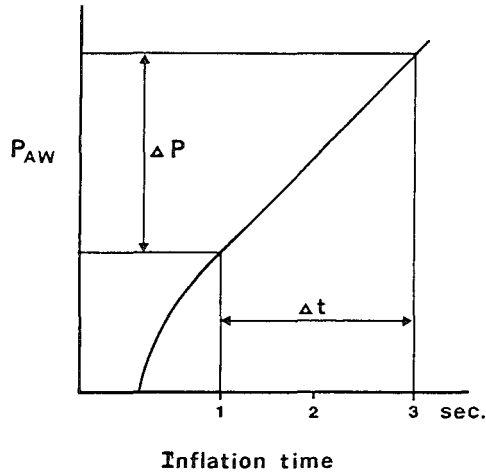
16

Inflation time

Fig 2.3 Pulse method
Pulse compliance can be derived from the ratio of airflow $\dot{V}$ during an inflation at constant flow rate and the slope of the corresponding airway pressure-time course ($\Delta P/\Delta t$): compliance $= \dot{V}/(\Delta P/\Delta t)$

time course ($\Delta P/\Delta t$) [10,86,97,98]. This concept of compliance measurement is called the pulse method and is visualized in Fig. 2.3. Undoubtedly, during the inflation P_{AW} is affected by the airflow resistance but it is assumed that this contribution is constant over the considered volume range and, therefore, does not affect ΔP [10,97]. The pulse method should be applied within a limited volume range [10], considering: 1) the nonlinearity of the quasi-static P-V curve [45], 2) the decreasing airway resistance at increasing lung volumes [82,86,97] and 3) the increasing contribution of viscoelasticity at increasing volumes [22,49]. The 'pulse' method can also be performed in non paralysed subjects, because insufficient muscle relaxation is easily detected from an irregular increase in airway pressure during inflation. When this method is applied a linear relationship between pressure and time is a prerequisite [10]. Comparison of compliance estimates derived from the pulse method and the inspiratory pause method revealed virtually identical values, even in patients with obstructive lung disease [89,98,99]. Most volume controlled ventilators can provide a constant inspiratory flow [98]. However, from the very onset of inflation airflow is not always constant and, therefore, some time is needed to obtain a stable flow rate [89]. Apart from the actual compliance measurement a constant flow during inflation

17

offers the advantage that over-distention is easily detected by a nonlinear increase in pressure at a certain volume [101].

2.4   Slow inflation-deflation method.

C_{RS} can also be derived from quasi-static P-V curves which can be obtained by recording P_{AW} and the change in lung volume during a slow inflation and deflation of the respiratory system. Such a procedure can be performed either at a constant flow rate or step by step. Because of the low flow rate during the continuous inflation-deflation procedure, P_{AW} is virtually equal to the alveolar pressure P_A and static conditions are measured during the entire procedure [31,43,68]. In the stepwise inflation-deflation procedure it is assumed that P_{AW} equals P_A at the end of the pause after each step.

Pressure-volume curves are usually performed as described in the following paragraph [14,19,21,31,43,63,64,68,69].

Firstly, the subject is anaesthetized and paralysed. When a PEEP is used during normal mechanical ventilation this pressure is adjusted to zero end-expiratory pressure (ZEEP) about 15 minutes before the P-V curve determination. When hypoxemia is expected during the procedure, the inspiratory fraction of oxygen F_{I,O_2} is increased in advance, if necessary to $F_{I,O_2} = 1$. To perform the procedure, the patient is disconnected from the ventilator. Then, some type of ventilatory procedure is performed to standardize lung volume history. Different 'standardizing' procedures were used which consisted in the majority of studies of one or a sequence of hyper-inflations. Thereafter, inflation is started at a rate of approximately 0.5 ml.s^{-1}.kg^{-1} (about 2 l.min^{-1} in adults). Volume is insufflated either by stepwise increments of lung volume, 100-200 ml each 3-5 s with an inspiratory pause of 2-3 s in each step, or by means of a low constant flow. Inflation is continued until an increase in lung volume between 10 ml.kg^{-1} and 25 ml.kg^{-1} is reached or until airway pressure has reached 40-50 cm H_2O. Then, deflation is started with the same flow rate. An entire 'slow inflation-deflation procedure' takes between 40 and 90 s. Deflation is continued either until zero airway pressure is observed or until the entire inflation volume has been recollected. The volume can be insufflated by means of a constant flow device [14], a modified ventilator [43], or an (automated) super syringe [21,31,63,69].

For a long time the change in lung volume was derived from the change in volume measured at the airway opening, e.g. by integration of the airflow rate. Publications of Butler and Smith [18], Gattinoni et al. [30] and

Dall'Ava Santucci et al. [21] demonstrated clearly that the actual change in lung volume was different from the change in volume measured at the airway opening. This was attributed to a continuous oxygen uptake and a decreasing CO_2 output during the slow inflation-deflation procedure [21,30]. Different solutions were proposed to avoid this problem. Butler and Smith [18] measured the change in lung volume in apnoeic patients by means of a sensitive spirometer which was filled with expired gas. They used this value, which was about 0.2-0.3 $l.min^{-1}$ in adults, as a standard correction for the P-V curves. According to Sharp et al. [92] such a volume correction may be too large, because alveolar gas is continuously diluted by fresh gas during inflation causing a steady instead of a decreasing CO_2 output during the slow inflation. They assumed that lung volume decreases about 25 ml during a 60 s slow inflation-deflation procedure. Recently, Gattinoni et al. [30] estimated the loss of volume due to gas exchange during slow inflation-deflation procedures by calculating the decrease in the amount of oxygen and the increase in the amount of CO_2. The decrease in volume due to oxygen uptake was assumed to be equal to the steady oxygen uptake multiplied by the time required to perform the slow inflation-deflation procedure. The increase in lung volume due to CO_2-exchange was derived from measurements of arterial blood gases just before and after the slow inflation-deflation procedure and from a determination of the end-expiratory lung volume. Gattinoni et al. [30] estimated the decrease in lung volume during a slow inflation-deflation procedure to be about 170 ± 120 (SD) ml in 30-90 s in patients. This value corresponds better with the correction of Butler and Smith than the value of 25 ml assumed by Sharp et al. [92]. The changes in intra-thoracic volume measured by means of respiratory inductive plethysmography (RIP) [21] confirmed the findings of Gattinoni et al. [30]. In slow inflation-deflation procedures the authors [21] were able to demonstrate obvious differences between the changes in volume based on airflow and changes in volume based on RIP.

Total compliance estimates have usually been derived from both inflation and deflation limbs of the pressure-volume loop. They were obtained from the approximately linear segment of the curve, which was between 0.5 and 1 l above the end-expiratory lung volume in adults. These compliance estimates are illustrated in Fig. 2.4. The compliance values for inflation and deflation (C_{INFL} and C_{DEFL}, respectively) correlated well with the compliance values derived from the inspiratory pause method [63], in spite of small differences between the values. Gattinoni et al. [31] found no significant differences between these compliance estimates after proper corrections for continuous
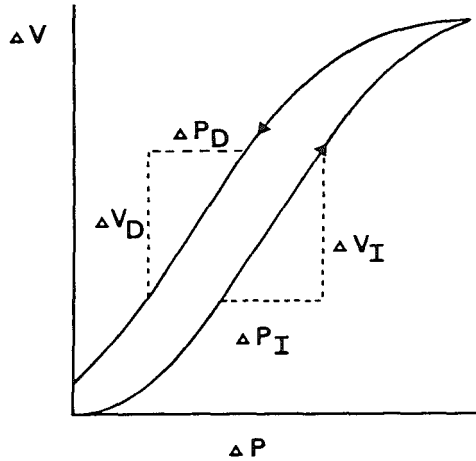
19

ΔV

ΔP_D

ΔV_D

ΔV_I

ΔP_I

ΔP

Fig 2.4 Slow inflation-deflation procedure.
Airway pressure plotted versus the change in lung volume, measured by integration of airflow at the mouth, during a slow inflation-deflation procedure. Compliance can be derived from the slope of the approximately linear part of the inflation limb ($\Delta V_I/\Delta P_I$) and similarly from the deflation limb ($\Delta V_D/\Delta P_D$).

gas exchange.

The inflation and deflation limb of pressure-volume loops are thought to contain different information. The inflation limb is often characterized by an initial part with a relatively large pressure change ('low compliance'), which has been attributed to opening of previously closed lung units or recruitment, followed after an inflection by a steeper part [31,33,68]. The deflation limb is generally found without the characteristic nonlinearity in the pressure-volume relationship and is therefore thought to reflect physiological compliance better than the inflation limb [68]. However, compliance estimates derived from volume measurements without corrections for the decrease in lung volume due to gas exchange during the procedure are more affected during deflation than during inflation [21,31]. This is probably due to the difference in CO_2 output during inflation and deflation caused by addition of fresh gas during inflation which is absent during deflation. Compliance estimates derived from the deflation limb are dependent on the total inflation volume [14] and larger values have been found after larger inflations. This increase in compliance values suggests that during inflation at the large volumes sequential opening of closed lung units still occurred

20

[14,33,70]. Therefore, Benito et al. [14] suggested to standardize inflation volume at 25 ml.kg^{-1}.

2.5 Interrupter technique during a passive expiration.

The interrupter technique [76,80] was originally proposed to estimate airway resistance during spontaneous breathing. The method is based on the following assumptions:

- The pressure rapidly equilibrates between the airway opening (P_{AW}) and the alveoli (P_A) when the airway is occluded for 100 ms during breathing.

- The so obtained measurement of P_A is only minimally disturbed by movement of lung and chest-wall.

Several studies, however, indicated that airway resistance was overestimated with respect to the values of the airway resistance obtained by body plethysmography [52].

In contrast with studies during spontaneous breathing, the interrupter technique yielded reliable values of airway resistance during passive expirations in mechanically ventilated patients, in whom part of the upper airways was bypassed by an endo-tracheal tube or tracheal cannula [35,110]. This difference in reliability has mainly been attributed to the faster transmission of alveolar pressure to the airways when the compliant upper airways were eliminated [35,74].

Gottfried and coworkers [34] have demonstrated that with this technique 'static' mechanical properties of the respiratory system could be measured in anaesthetized human beings. During relaxed expirations they applied several short expiratory pauses (of 100 ms) with a rapid pneumatic valve. During these pauses they observed plateau values in airway pressure, which were preceded by transient oscillations due to inertial properties. Although in patients with chronic obstructive pulmonary disease (COPD) a longer pause was required, a pause of 0.3 s was always sufficient to obtain a stable plateau pressure [34]. Gottfried et al. interpreted these plateau values as an indication both for equilibration between alveolar and airway pressure, and for relaxation of the respiratory muscles. In paralysed human beings all expiratory pauses yielded stable plateau pressures, whereas during spontaneous breathing plateaus were only found during the last part of the expirations, indicating respiratory muscle activity early in expiration. Quasi-static P-V

curves were obtained by plotting the plateau pressures versus the respective volumes levels above end-expiratory lung volume. This P-V relationship appeared to be linear in most cases. Gottfried et al. compared the slope of this P-V curve with estimates of C_{RS} from the inspiratory pause method. They found no significant differences [34,35].

The short pause (100-300 ms) in the interrupter method seems in contradiction with the required pause (1.5 s) in the inspiratory pause method. Although this issue has not been covered in the publications on the interrupter technique [34,35,74,110] we assume this difference to be caused by differences in stress-relaxation, which is the gradual decrease in pressure after a stepwise increase in lung volume. The interrupter technique is usually performed during a passive expiration after an inspiratory pause of a few seconds. Therefore, the influence of viscoelastic pressures during the subsequent passive expiration might be small.

However, in a study by Bates et al. [11] tracings of tracheal pressure have been presented obtained from passive expirations in which the outlet of the airway was occluded at 0.2 s after the beginning of expiration, which coincided approximately with mid-expiration. During the next expiratory pause of 5 s, airway pressure was not constant but increased gradually with a time constant of about 1 s [11]. This slow pressure change indicates that significant errors can be made when the pressure after a pause of only 100-300 ms is assumed to be equal to the recoil pressure of the total respiratory system.

CHAPTER 3

# VENTILATORY MANOEUVRES

3.1 Introduction.

During the experiments presented in the following chapters we have used a computer controlled ventilator [56] for normal mechanical ventilation as well as for all special ventilatory manoeuvres to determine total respiratory compliance. In this chapter the operation of the ventilator is described. Additionally, the procedures and essentials of two helium-dilution methods used for the estimation of end-expiratory lung volume are discussed.

3.2 The ventilator.

3.2.1 Basics

The most essential parts of the ventilator (Fig. 3.1) are two concertina bellows (numbered 1 en 2) coupled together to move simultaneously. One side of each bellows has been mounted on a fixed plate (FP), which is part of the frame of the ventilator, whereas the other side has been attached to a movable plate or piston (P). The maximum volume of each bellows ($\approx$ 300 ml) is large enough to perform all respiratory manoeuvres. In the fixed plate four holes have been made, two in front of each bellows, to permit inflow and outflow of gas. Volume of the bellows is changed by a motor (M), which moves the piston by turning the ballscrew (K). Two electromagnetic solenoid valves control the 'inlet' A, and 'outlet' B of the bellows. Via valves A fresh gas is taken into the bellows, via valves B this gas is insufflated into the animal. Two additional valves (C) have been mounted in the frame of the ventilator to permit outflow of expiratory gas. In addition to these six electromagnetic valves connections have been provided for the control of two external valves, which can be used for different purposes in the ventilatory system (cf. valve X in section 3.3).

When the piston is in its most forward position the concertina bellows are folded. The folds prevent the movable plate to approach the fixed plate closely. In order to reduce the remaining extra volume within each bellows a 'soft filling body' has been attached to the fixed plate.
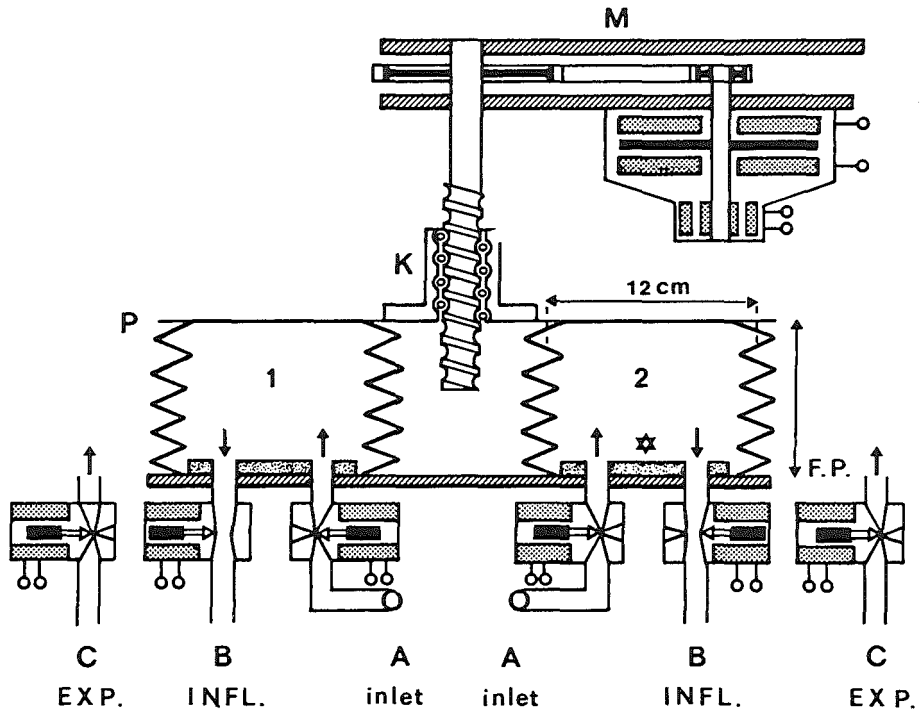
Figure 3.1 Schematic drawing of the computer controlled ventilator.
M: Motor, K: Ballscrew, P: Piston, F.P.: Fixed plate, ⋆: soft-filling body, 1,2: Bellows 1 and 2 respectively, A: inlet valve, B: valve in inspiratory tube, C: valve in expiratory tube.

The ventilator was based on a motor servo system [56]. The motor and electromagnetic valves are controlled by a computer (Olivetti, M24). The user interactive part of the program was written in FORTRAN, the actual control of the ventilator is performed by a set of routines, written in assembly language.

In the next section the functioning of the ventilator is explained on the basis of the normal mechanical ventilation. Also some of the elementary aspects of the software are described to elucidate the versatility of this ventilator.

3.2.2 *Normal mechanical ventilation*

Normal mechanical ventilation is usually performed by one of the bellows (e.g. number 1) leaving the other bellows (number 2) in 'flush' mode. In flush mode inflow and outflow of gas occurs via valve A, because valves B and C are closed. Therefore, no gas flow is possible between the 'flushing' bellows and the animal. In the following description of normal mechanical ventilation the opening and closing of valves A, B and C refer only to bellows 1.

The starting point of a ventilatory cycle is defined to be the moment that the piston is in the most forward position and ready to move backwards. Thus, the starting point of the cycle coincides with the beginning of expiration. This moment differs from a starting point at the beginning of insufflation, which is usually chosen in physiological and clinical studies. A normal ventilatory cycle in our experiments took 6 s, i.e. 10 breaths per minute. In the first phase of a ventilatory cycle the piston moves backwards until the volume increase of the bellows is equal to the volume which has to be insufflated subsequently. During this phase, the valves A and C are open and B is closed to permit both a gas flow into the bellows and a passive expiration by the animal via valve C. Valve B is closed to avoid inflow of expiratory gas into the bellows when the piston is returning to its position for insufflation. After this 'expiratory' phase, which usually lasted 3.6 s in our experiments, 'inflation' is started by moving the piston again to the forward position, with valves A and C closed and valve B open. During this phase the tidal volume is directed via valve B into the animal. This insufflation usually took 2.4 s in our experiments. When the piston is in the most forward position at end-inflation, an optional inspiratory pause can be inserted, with all valves closed. Thereafter, the next cycle is again performed automatically.

3.2.3 *Software*

The ventilator is controlled by a computer program commanding the valves
and the position of the piston. All commands for an entire ventilatory cycle
are stored in a buffer in the computer. The buffer has a fixed length and
contains 200 different positions and valve states. In order to handle different
ventilatory cycle times the commands of the valves and the piston positions
are transmitted to the ventilator at intervals depending on the cycle time.
The program uses four buffers in total, two for normal mechanical ventilation
and two additional buffers for special ventilatory manoeuvres, which are
meant to be inserted in between normal ventilatory cycles. Most ventilatory
manoeuvres for estimation of compliance, end-expiratory lung volume and
gas exchange (cf. Chapter 6) were defined as special manoeuvres. In practice
these special procedures were always performed by bellows 2 (Fig. 3.1).

   During normal mechanical ventilation only one of the four buffers is in
use. The operator may change the commands of any of the three remaining
buffers by supplying the following data to the program:

1. the kind of buffer to be used, i.e. to change normal mechanical
   ventilation or to define a special ventilatory procedure

2. the number of the bellows,

3. the ventilatory volume,

4. the ventilatory cycle time,

5. the percentages of the ventilatory cycle for inflation (I) and for
   expiration (E) respectively. The remaining time, if any, is auto-
   matically reserved for an inspiratory pause.

6. the inspiratory flow profile, which can be either constant flow or
   sinusoidal flow. Although technically any flow profile is possible,
   only two different flow types are installed in the program. In case
   of a controlled deflation the expiratory flow profile can be defined
   too.

7. the number of normal ventilatory cycles after which a special
   procedure has to be repeated automatically.

With the use of these data, the program defines one of the buffers and uses
the data in this buffer to perform the next ventilatory cycle. Therefore, it is
possible to change parameters as ventilatory cycle time, ventilatory volume,
I:E ratio etc. per cycle, without any delay. Even the gas mixture can be

changed instantaneously by switching, between two ventilatory cycles from the ventilating bellows to the other bellows, which was previously flushed with an other gas mixture. This feature has been used in the helium dilution measurements to estimate end-expiratory lung volume. It is also possible to control the ventilator so that both bellows can be used during ventilation. In this way the movement and acceleration of the piston can be reduced by the smaller displacement, which is important when short inflation times are required.

The ventilator can be controlled both by keyboard and by remote computer. In our experiments the experimental protocol of an entire experiment could be stored in the remote computer. In this way the protocol could be performed automatically during the experiment and similar in each animal.

3.3   The ventilator as part of the experimental set-up.

The tubes, the additional equipment and the connections to the experimental animal and the ventilator are presented schematically in Fig. 3.2. The figure represents the situation in normal mechanical ventilation and in most special procedures. In the case of end-expiratory lung volume determinations the set-up was slightly different, this is to be discussed later in this section.

The gas mixture to ventilate the animals was obtained from two cylinders with compressed gas, containing usually N_2 and O_2 respectively. The gases were directed through a blender into a large Douglas bag (D) of about 50 l. Collection of the gases in the Douglas bag provided a stable mixture with a large enough volume for buffering slight inlet changes in gas fraction. When no measurements of end-expiratory lung volume with the use of He dilution were performed both bellows of the ventilator were filled with the same gas mixture from the Douglas bag. In that situation the bellows in flush mode continuously 'rebreathed' the gas in the Douglas bag. The tubes between the valves (1B, 2B, 1C and 2C) and the animal contained three Y pieces (Ya, Yb and Yc in Fig. 3.2). In the tube between Yc and the tracheal cannula inspiratory and expiratory airflow ($\dot{V}$) was monitored by means of a Fleisch pneumotachometer (Sensormedics (Godart), Holland, nr 0). An extra valve (X), also controlled by the ventilator program, was mounted at the tracheal cannula. This valve was closed only during the inspiratory pauses to eliminate the effect of extra-thoracic compliance of the ventilator and the tubes on the measurement of tracheal pressure during the pause. The extra valve X was open in other special procedures and in normal
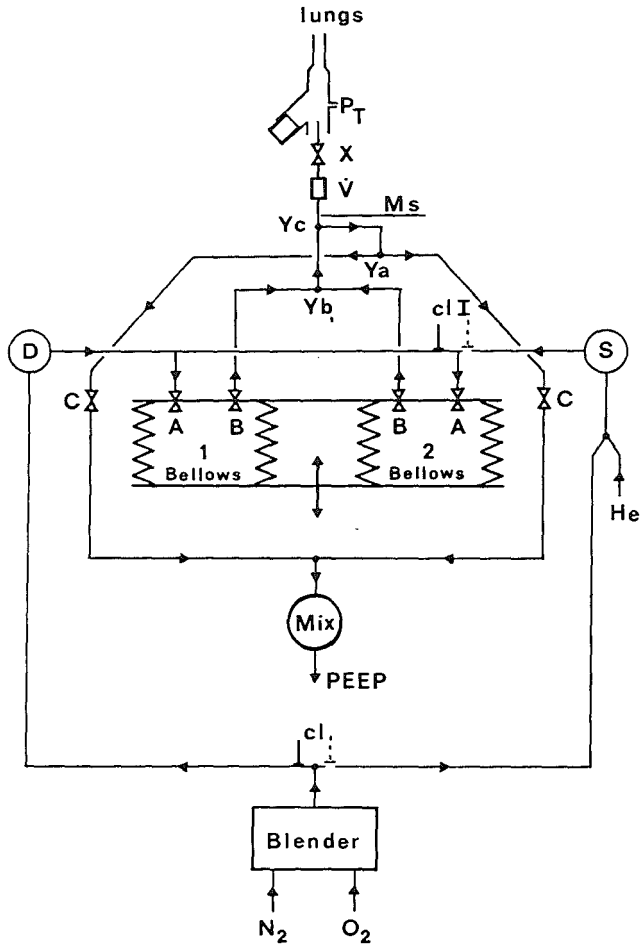
Figure 3.2 The ventilator as used in its experimental function.

A,B,C	: Valves, electromagn. controlled (cf. Fig. 3.1)
Blender	: Blender for mixing N_2 and O_2
D	: Douglas Bag
cl.	: Clamp, cl. I for He wash-in procedures
Mix	: Mixing box to collect expiratory gases
Ms	: Mass-spectrometer sampling site
PEEP	: Waterseal for application of positive end-expiratory
	: pressure (PEEP)
P_T	: Measuring site of the tracheal pressure,
S	: Spirometer
$\dot{V}$	: Flow head of pneumotachometer
X	: Extra valve at tracheal cannula
Ya Yb Yc	: Y-pieces in tubes.

mechanical ventilation. In the experiments described in Chapters 6 and 7 a Capnometer (Hewlett Packard) was inserted between the extra valve and the pneumotachometer. The P_{CO_2} signal was only used during the experiments to check stability of end-tidal P_{CO_2}. Airway pressure (P_{AW}) was measured at a small side arm of the tracheal cannula with the use of a gas pressure transducer (Hewlett Packard type 270). This pressure is also called tracheal pressure P_T in the following chapters. Another side arm of the tracheal cannula could be used for suctioning.

Expiratory gas was directed via 1C or 2C to a small gas mixing box, to permit measurement of mean expiratory gas fractions. The outlet of this mixing box was attached to a water seal for application of PEEP.

A few minutes before lung volume measurements were started a spirometer S (Lode, D53/R, The Netherlands) was thoroughly flushed with the same gas mixture as was used during the ventilation. For that purpose the tube between the blender and the spirometer was opened and the other tube from the blender to the Douglas bag was closed by switching a clamp manually. After flushing the spirometer a small volume of helium was added to obtain a helium concentration of about 5 %. Thereafter, the spirometer was attached to the inlet of bellows 2 and the previous pathway between this inlet and the large Douglas bag was closed by switching the clamp at 'I' (Fig. 3.2). Within a few minutes the helium concentration in the spirometer and bellows 2 was found to be stable, due to the continuous gas mixing by the movement of the bellows. Next, the inlet capillary of the mass-spectrometer (Perkin Elmer, MGA 1100) was attached to Y piece Yc to permit sampling of gases during the lung volume measurements. The helium washin procedures are treated in section 3.5.

3.4   The ventilatory procedures for the estimation of compliance.

3.4.1   *Pulse inflation and inspiratory pause*

The inspiratory pause method (cf. Chapter 2) for the estimation of C_{RS} was applied in all experiments. A special ventilatory procedure with an inspiratory pause was defined for this method. Such a procedure always started with an insufflation at the end of an expiratory phase in the normal mechanical ventilation. The inspiratory pause procedure consisted of 1) an inspiratory phase of 1-5 s at a constant flow rate, 2) an inspiratory pause of several seconds, 3) an expiratory phase of 3.6 s. Because insufflation was always performed at a constant flow rate, the pulse method in which C_{RS} is
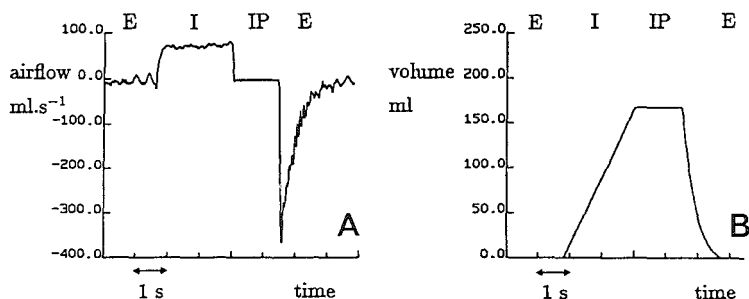
Figure 3.3 Airflow and changes in volume during an inspiratory pause procedure.
A) Airflow plotted as a function of time. I: Inspiratory phase (2.4 s), inflation volume 180 ml, IP: Inspiratory Pause (1.5 s), E: Expiratory phase (3.6 s). In the last seconds of each expiration airflow rate is close to zero. However, fluctuations around zero level are usually observed due to movement of water in the waterseal (for the application of PEEP) and cardiac interference.
B) Integrated airflow rate (volume-time course) during an inspiratory pause procedure. The volume increase during inflation is linear.

derived from the pressure increase at constant flow (cf. Chapter 2), could be applied simultaneously in these procedures. In Fig. 3.3A an example of an inspiratory pause procedure is presented with an insufflation at constant flow rate of a normal tidal volume during normal mechanical ventilation. At the end of an insufflation the airway was occluded for 1.5 s. After this inspiratory pause the piglet was allowed to breathe out passively. The flow rate was observed to be constant within 0.3 s after the start of insufflation. Due to small irregularities in the movement of the piston and the concertina bellows small fluctuations in the 'constant' flow rate were often observed. During the inflation, as presented in Fig. 3.3, the mean flow rate was 73 ml.s^{-1} with a standard deviation of 3 ml.s^{-1}. In Fig. 3.3B the integrated signal of flow rate is presented, giving a linear volume increase. After the inflation the airway was occluded and airflow returned to zero causing a transient phase between pulse flow level and zero level of maximally 0.3 s. The insufflated volume, calculated by integration of the rate of airflow, was always found to be identical to the volume imposed via the program controlling the ventilator.
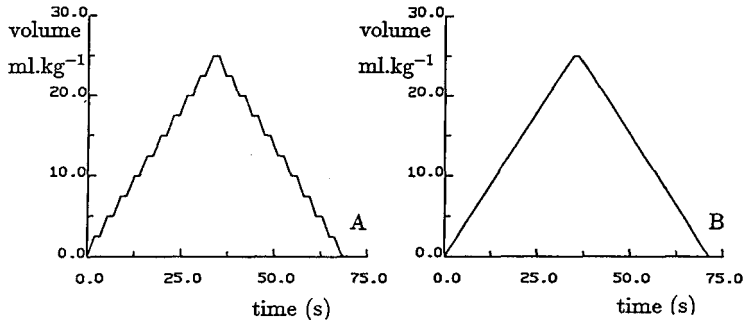
Figure 3.4 Ventilatory volume during two slow inflation-deflation procedures.
A) Stepwise inflation and deflation. In each step the volume change is 2.5 ml.kg^{-1} in 2.0 s followed by a pause of 1.5 s.
B) Continuous slow inflation-deflation procedure. The rate of volume change is 2.5 ml.kg^{-1} per 3.5 s. At end-inflation (25 ml.kg^{-1}) an inspiratory pause of 1.5 s was inserted.

3.4.2 *Slow inflation-deflation procedure*

A *stepwise* slow inflation-deflation (SID) procedure was performed by defining 10 volume steps with an inspiratory or expiratory phase respectively of 2.0 s followed by a ventilatory pause of 1.5 s. Such a ventilatory pause was performed by holding the position of the piston, however, without closing the valve 2B. A slow deflation of the lungs was performed by commanding a backward movement of the piston at the same valve states as during insufflation (2B open, 2A and 2C closed). A *continuous* inflation (or deflation) could be performed by defining 10 volume-'steps' with an inspiratory phase (or expiratory phase) of 3.5 s without ventilatory pauses. Examples of the imposed volume-time course of a stepwise and a continuous SID procedure are presented in Fig. 3.4.

In the SID procedures we cancelled the concept of using only one buffer for one ventilatory cycle, because the combination of a rather long ventilatory cycle time ($\approx$ 60 s) and a large inflation volume (25 ml.kg^{-1}) caused an irregular movement of the piston, when only 200 positions could be set. At the end of each volume step in the SID procedure we selected alternately one of the special buffers, containing the positions of the piston and the valve states of the next volume step. By updating these buffers at each step during the SID procedure the piston was found to move 'smoothly'.

Since the slow inflation-deflation procedures could be performed by the

31

same ventilator, it was not necessary to disconnect the animal from the ventilator or to change from a PEEP to a ZEEP, as was reported in the majority of studies mentioned in section 2.4.

3.5   End-expiratory lung volume measurements.

We applied two methods to estimate the end-expiratory lung volume $V_{L,EE}$: an open-circuit and a closed-circuit method. Both methods were based on the dilution of an inert gas (helium) in the lung volume and the mass balance for that gas.

3.5.1   *The open circuit wash-in/wash-out method*

Introduction. In the open circuit helium wash-in method the lungs were ventilated during several cycles with a gas mixture containing about 5% He. This ventilation usually took 15 cycles, i.e. 90 s. During the wash-in period $V_{L,EE}$ could be estimated at the end of each expiration by relating 1) the inspired amount of helium since the start of the wash-in, 2) the expired amount of helium since the start of the wash-in and 3) the helium fraction which remained in the lung at the end of the expiration. This helium fraction was assumed to be equal to the fraction at the end of that expiration, $F_{EE,He}$. $V_{L,EE}$ was calculated from [111]

$$V_{L,EE} = \frac{\int \dot{V}.F_{I,He}.dt - \int \dot{V}.F_{E,He}.dt}{F_{EE,He}} \tag{1}$$

where $\dot{V}$ is the airflow rate, $F_{I,He}$ the inspiratory fraction of helium, $F_{E,He}$ the expiratory fraction of helium and $F_{EE,He}$ the end-expiratory helium fraction.

Although we calibrated the mass-spectrometer carefully, it would not have been necessary in this situation to have an accurate calibration of the He concentration. It is, however, of crucial importance to obtain 1) an accurate estimate of tidal volume, 2) a correct zero level of the helium signal and 3) a linear relation between the He concentration and the output signal. Tidal volume was calibrated before each experiment and could also be determined by integration of the airflow. The zero level of helium was determined before each wash-in procedure. Since the measurement of the helium concentration was performed with the use of a mass-spectrometer the linearity of the relationship between the concentration and the output signal was assumed. We chose for a gas concentration of about 5% to obtain

a reasonable signal-to-noise ratio which would not affect the concentrations of the respiratory gases in the lungs too much.

Methods. To accomplish the open circuit wash-in, mechanical ventilation was switched at end-expiration from bellows 1 with the normal ventilatory gas mixture to bellows 2 containing 5% He in the normal gas mixture. During a wash-in period the ventilatory cycles were the same as during normal mechanical ventilation. Therefore, we did not program a special ventilatory procedure but merely switched from one bellows to the other. A constant inspiratory helium concentration was maintained during the wash-in period because for each cycle the bellows was filled with a gas mixture from the spirometer. Although, theoretically, the inspiratory fraction of helium ($F_{I,He}$) for each ventilatory cycle does not need to be the same during a wash-in procedure, we used a constant $F_{I,He}$ because it simplified the data analysis and enabled us to recognize an equilibration in the intra-pulmonary helium concentration more easily. In this situation the advantage of a spirometer over a Douglas bag was its check on the tidal volume, delivered by the ventilator.

A wash-in procedure could be ended and switched to a wash-out procedure either after a pre-set number of ventilatory cycles or by hand. In the wash-out procedure ventilation was resumed by bellows 1. The alveolar helium concentration gradually returned to zero. The wash-out of helium from the lungs could also be used to estimate $V_{L,EE}$ with an equation comparable to equation 1. Fig. 3.5 shows the He and CO_2 concentration signals as functions of time during a typical wash-in procedure.

Data-analysis.

Stability of lung volume. The calculation of $V_{L,EE}$ with equation (1) demanded a stable lung volume during the wash-in as well as during the wash-out procedure. Stability of end-expiratory lung volume was achieved by performing the wash-in ventilatory cycles during stationary conditions and with the same ventilatory cycles as during normal ventilation. In measurements with a mercury strain gauge around the rib cage of the piglets we did not detect any change in thoracic circumference at end-expiration throughout the procedure. This indicated a constant $V_{L,EE}$.

Alveolar helium concentration. The calculation of the amount of helium which remained in the lung at end-expiration was based on the assumption that the end-expiratory helium concentration reflected the average concentration in the entire lung. If this assumption was valid and if the inspired and expired amounts of helium could be accurately determined, then the estimates of $V_{L,EE}$ during subsequent ventilatory cycles in a wash-in should

33
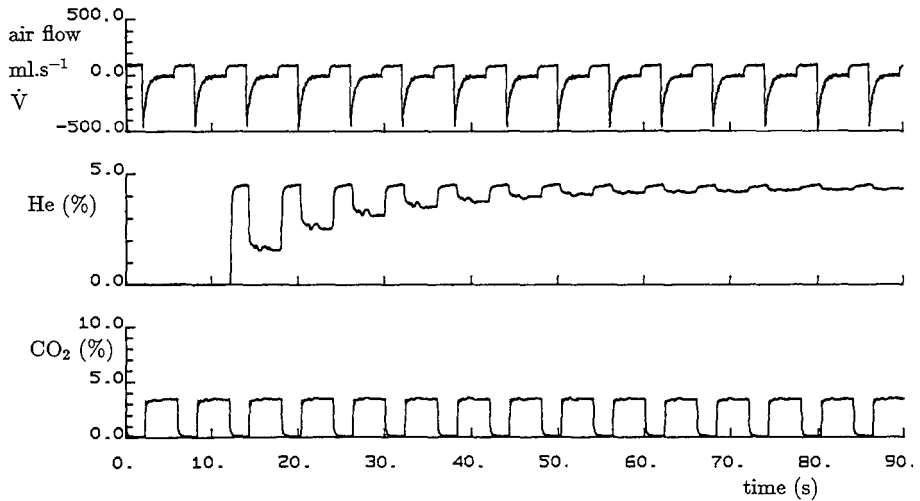
Figure 3.5 Gas concentrations during a open circuit wash-in procedure.
In this figure the respiratory airflow rate $\dot{V}$ and the gas concentrations of He and CO_2 (in percentages of total gas) are plotted as functions of time.

all have been the same. Probably this assumption was not valid, because mixing of helium in the lungs took more time than available during one cycle of a few seconds. As a consequence end-expiratory lung volume was under-estimated in the initial phase of a wash-in or wash-out period when changes in concentration between inspiration and expiration were relatively large. The estimates of $V_{L,EE}$ increased in the first 4-8 ventilatory cycles, where-after they became approximately constant. Therefore, $V_{L,EE}$ was taken as the mean value of these 'stable' values.

Inspired and expired amount of helium. We had serious problems in obtaining reliable estimates of the total amounts of helium which were insufflated and exhaled during each ventilatory cycle. This was caused by the uncertainties in the multiplication of the flow rate ($\dot{V}$) and the concentration of helium, obtained from the pneumotachometer and the mass-spectrometer respectively. Firstly, both signals were changing rapidly both during insufflation and expiration, and secondly, mass-spectrometers produce distorted signals due to time delays and finite rise times [9].

The response of the mass-spectrometer to a stepwise change in the helium concentration is shown in Fig. 3.6. Such a response was obtained by switching between different gases, by using fast valves with closing times of

34
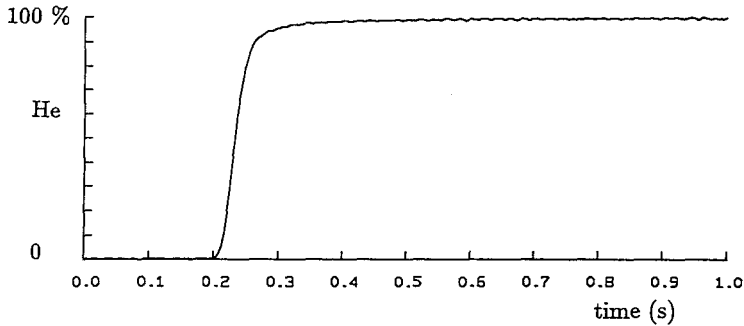
Figure 3.6 Response of the mass-spectrometer.
In this figure the response of the mass-spectrometer to a stepwise increase in helium concentration is presented. This response has been sampled at 250 Hz. The time delay (220 ms) between the stepwise change and the moment the concentration was at 50 % of the response was used to correct the mass-spectrometer signals.

10-15 ms (Kuhnke, micro-solenoid valves). The time delay of the He-signal with respect to the $\dot{V}$–signal was found to be 220 ± 10 (SD) ms. In all analyses we corrected the gas signals for this time delay. The step response had a rise time of ≈ 28 ms for an increase from 10 to 90% of the signal, which was considered sufficiently fast to calculate the expired amount of helium.

Fig. 3.7 shows the flow rate signal (Panel A) and the helium signal (Panel B) as functions of time during a typical expiration in a wash-out procedure. Because flow rate was high in the early phase of expiration 90% of the volume was expired within 1 s (see Panel C). An accurate estimation of the expired volume was jeopardized, because the sharp increase in the flow rate at the start of an expiration could have been beyond the linear response of the pneumotachometer [84]. Due to the dead space in the lungs a considerable volume of about 50 ml was exhaled before the concentration of helium was found to increase. In the same figure (Panel D) three calculations of the expired amount of helium are presented, in which the helium signal has been corrected for a delay of 200, 220 and 240 ms respectively. It is obvious that a small error in the estimation of the time delay between flow and concentration signal might cause errors in the estimation of the expired amount of helium, and thus of $V_{L,EE}$. Changing the delay time from 220 ms to 200 ms caused a shift of 8 ml at an end-expiratory lung volume of about 190 ml (4%).

To avoid the problems related to the determination of the expired volume
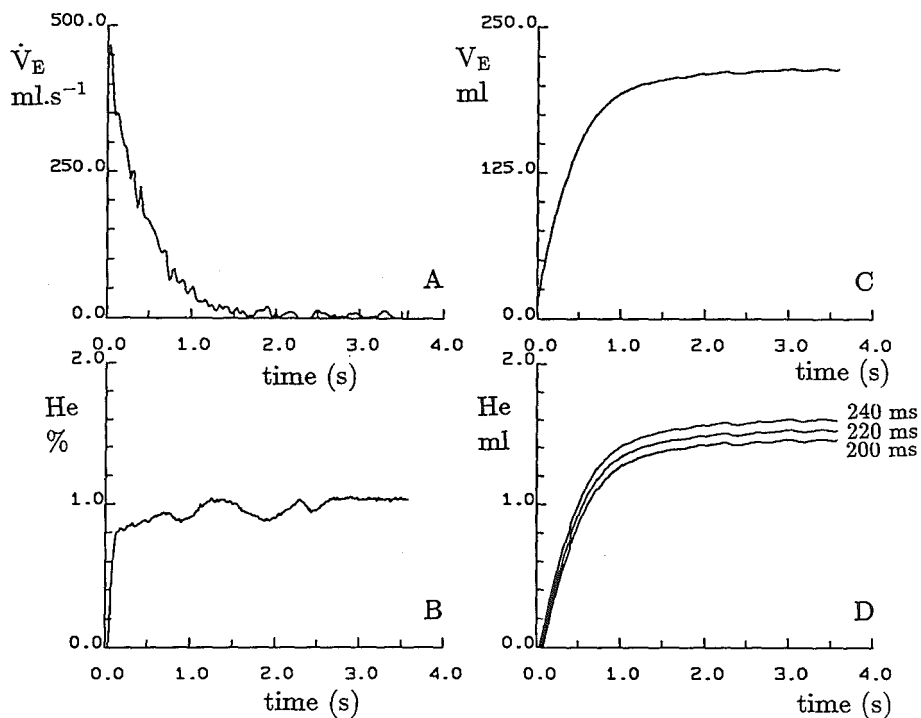
Figure 3.7 The influence of the time delay of the mass-spectrometer on the calculation of the expired amount of helium.

    A Airflow rate $\dot{V}_E$ during an expiration in an open circuit helium wash-out procedure

    B He concentration (corrected for a delay of 220 ms) during this expiration

    C Expired volume V_E obtained from integration of $\dot{V}_E$

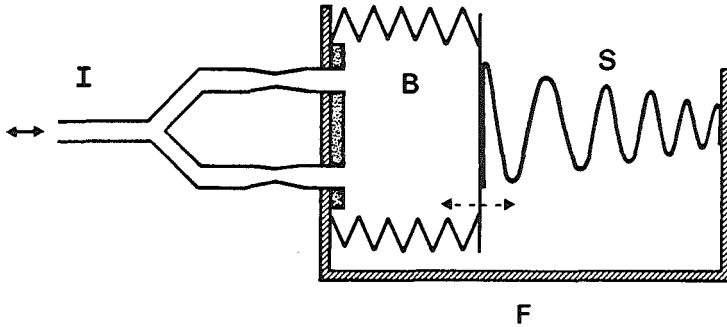   D Expired volume of helium, using the delay of 220 ms and two other delays of 200 and 240 ms respectively.

Figure 3.8 Schematic presentation of the test lung.
Components: B: Bellows, F: Frame, I: In and outlet of the bellows, S: Spring.

of helium the expiratory gas can be collected in a 'bag in box' system, in which the pressure around the bag, is held at the same positive end-expiratory pressure as is used during the normal mechanical ventilation. This method has been described by e.g. Hickham et al. [40] and Emmanuel et al. [25]. After collecting some expirations the amount of helium in the bag can be estimated by measuring the mixed helium concentration and by measuring the collected gas volume by means of a spirometer.

This collection could not be easily integrated in the rather complex experimental set-up of our experiments. Therefore, we calculated the expired volume of helium by numerical integration.

Effect of additional dead space in the sampling system.
In the experiments, to be presented in the following chapters, the inlet capillary of the mass-spectrometer was attached to a Y piece (see Fig. 3.2, component Yc) with a small sidearm on it. We investigated the effect of such a sidearm on the delay and rise time of the mass-spectrometer response and found that in this situation step responses were distorted. This was probably caused by a small amount of dead space (about 0.5 ml) in the sidearm of the Y–piece which affected the delay time. The distortion might have caused a systematic error in the estimation of the absolute lung volume in this 'open-circuit helium dilution' technique.

Therefore, we examined whether the open wash-in method could discriminate between small changes in lung volume, in spite of the aforementioned additional dead space in the sampling system. This was done by using a test lung. The test lung (Fig. 3.8) consisted of a prototype of a computer controlled ventilator with one bellows, which was used after removal of the

37

valves and disconnection from the ball screw between the motor and the piston, and after construction of a spring between the piston and the frame to introduce a recoil pressure acting on the bellows. With this set-up and with the additional 0.5 ml dead space in the mass-spectrometer sampling catheter the end-expiratory volume was estimated, $V_{L,EE}(e)$. The real end-expiratory volume of the test lung, $V_{L,EE}(r)$ was determined by relating the helium concentration in a syringe to the equilibrium concentration in the system formed by the test lung and the syringe after connecting the syringe to the test lung at end-expiration. This technique was essentially a closed helium dilution technique, which is treated in the next subsection. Both volume estimates were found to be related via

$$V_{L,EE}(e) = 31 + 0.78.V_{L,EE}(r) \quad (r = 0.999) \tag{2}$$

It was unclear whether this systematic error in the estimation of $V_{L,EE}$ could be used to correct the lung volume determinations in the experiments which are described in Chapters 4 and 5. However, since the estimates of end-expiratory lung volume were only used to monitor stability of lung volume in those experiments, we concluded that the open circuit helium dilution technique met our requirements satisfactorily. For the estimation of the absolute lung volumes (Chapter 6) we used the closed circuit helium dilution technique.

3.5.2 *The closed circuit wash-in method*

Introduction. The closed circuit method for the estimation of the end-expiratory lung volume is probably best explained by referring to the closed system He dilution technique with the use of a syringe. When a certain volume in a syringe (V_{syr}), which contains a fraction of helium, F_{syr}, is added to an unknown volume (V), this volume can be estimated according to the equation

$$V = V_{syr}.\frac{(F_{syr} - F_{eq})}{F_{eq}} \tag{3}$$

where F_{eq} is the helium fraction at equilibrium in the total volume, which is the volume of the syringe plus unknown volume. As in the open circuit method an accurate zero level is needed without the necessity to know the absolute concentration exactly. It is sufficient to know the relative changes in the helium concentration.

Methods. This method was automatically performed with the computer controlled ventilator. At the end of a normal expiration bellows 2 containing
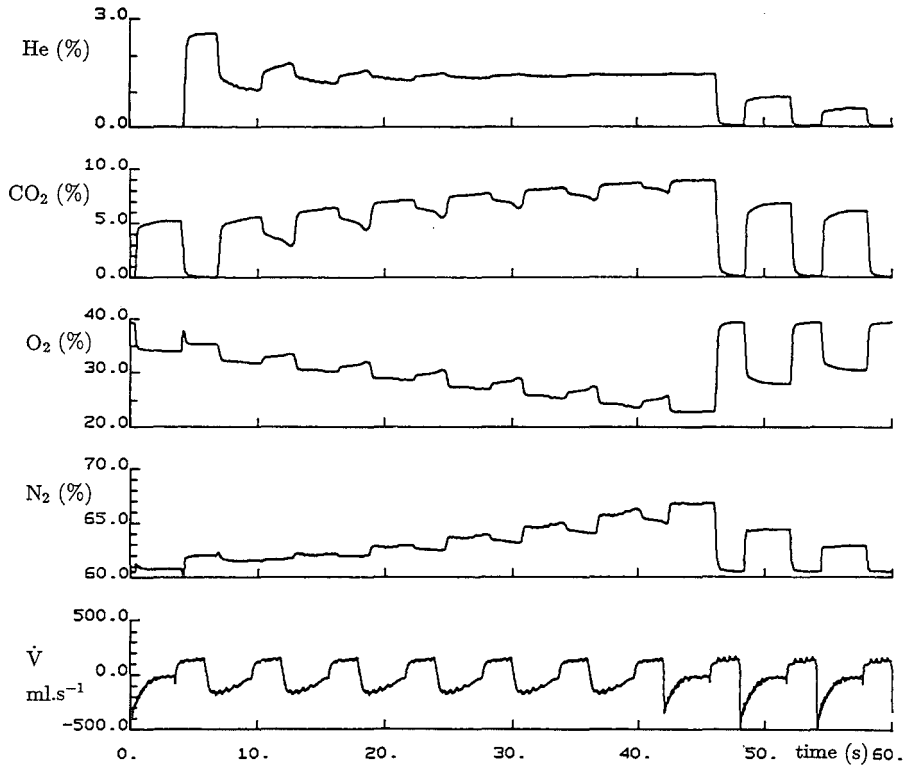
Figure 3.9 Gas concentrations during a closed circuit wash-in procedure.
In this figure the gas concentrations of He, CO_2, O_2 and N_2 (in percentages of total gas) and the respiratory airflow rate $\dot{V}$ are presented as functions of time during a closed system wash-in procedure.

39

about 5% He in the normal ventilatory gas mixture was connected to the lungs. Then, the piston continued as during normal mechanical ventilation, however, with a different state of the valves. Only valve 2B was opened and both inflation and deflation were controlled by the decreasing and increasing volume of bellows 2 (bellows 1 was in 'flush mode', see section 3.2.2). After a pre-set number of 'rebreathing' cycles, which was usually taken at 6 cycles, i.e. 36 s, normal mechanical ventilation was resumed by bellows 1 and was started as usual with a normal passive expiration. In the last part of this 36 s 'rebreathing' period the helium concentration was found to be constant, i.e. equilibrated, and $V_{L,EE}$ could be calculated via a formula comparable to equation 3, but with corrections for dead spaces in the 'rebreathing system'. Fig. 3.9 shows the gas concentrations as functions of time during a closed-circuit wash-in procedure.

Data-analysis. The calculation of the end-expiratory lung volume with the closed-circuit helium dilution technique required information 1) on the volume which was present in the bellows at the moment the wash-in was started, 2) on the concentration of He in the bellows at that time, 3) on the volume of the tubes between ventilator and lungs, 4) on the He fraction after equilibration (F_{eq}) and 5) on mechanisms acting on F_{eq}, as e.g. continuous gas exchange.

Volume of the bellows. The volume in the bellows was always larger than the volume which had to be insufflated, because a gap remained in the ventilator when the piston was in its "most" forward position, despite of the soft filling body mentioned in section 3.2.1. This remaining volume, which we have called the 'dead space' of the bellows, was calculated from a closed-circuit helium dilution procedure with the use of a small balloon with known volume directly attached to the B valve of the ventilator. The calculated dead space was 30 to 70 ml dependent on the experiment. This large range in dead space volume was primarily caused by adjustments to the electronics of the ventilator between experiments, which were sometimes needed to have optimal control of the servo-system of the ventilator. Before each experiment we have measured the dead space of the bellows.

Inspiratory helium concentration. The helium concentration in the bellows was measured during the first inflation of the wash-in period by means of the mass-spectrometer sampling at the Y piece (see Fig. 3.2, component Yc).

Dead space of the tubes. The dead space of the tubes (Vd,tube) between ventilator and lungs was determined by doing the wash-in technique on a balloon with known volume, using the earlier obtained value for the dead space in the bellows. Vd,tube was 29 ± 1 (SD) ml, n=3. This dead space

turned out to be significantly smaller than the total dead space in all tubes between ventilator and lungs, which was 47 ml (determined with water). We attributed the difference between both values to the sideways of tubes ('cul de sacs'), which did not participate in the wash-in, as for instance the tubes between bellows 1 and Y-piece Yc (see Fig. 3.2). Although end-expiratory lung volume measurements (and the 'rebreathing procedures', cf. Chapter 6) were done with different airflow rates and different ventilation volumes, which may have caused slight differences in mixing of the helium in the transitional zones of the sideways, it was assumed that effective dead space in the tubing was the same as that estimated with the balloon, i.e. $V_{d,eff} = 29$ ml. This value is used in the lung volume calculations.

Helium concentration after equilibration. The helium gas mixture was usually equilibrated after 6 ventilatory cycles. To avoid errors due to the small remaining fluctuations in the concentration, the equilibrium value was derived by averaging the helium concentration over the last ventilatory cycle.

Continuous gas exchange during the procedure. In general practice the closed-circuit helium dilution technique is accomplished at a constant volume. Expiratory CO_2 is removed by a soda-lime absorber and O_2 is supplied to compensate for the volume loss by oxygen uptake. Until now we did not use CO_2 absorbers during the closed-circuit helium dilution technique to remove the CO_2 from the gas mixture. As a consequence this technique has many similarities to the 'rebreathing procedures' mentioned in Chapter 6. In that chapter we have discussed aspects of gas exchange during such procedures and argued that a *sustained* oxygen uptake, and a *decreasing* CO_2 output are likely to occur. Assuming a constant amount of N_2 in the total system (bellows, tubing and lungs) the increasing concentration of N_2 during a closed-circuit helium dilution technique points to a decrease in volume of the total system. The volume loss caused a decrease of the fall in O_2 concentration and an increase of the rise in CO_2 concentration. The equilibrium concentration of helium, which was obtained after a closed system ventilation of about 36s, also will have been too high. We corrected the $V_{L,EE}$ value for the change in lung volume due to continuous gas exchange, based on the assumption of a constant amount of N_2 in the total system. This correction was found to be about 15 ml which was about 10 % of the end-expiratory lung volume.

Check of measurements with an artificial lung. It is an advantage of the closed-circuit method that the dynamic response of the mass-spectrometer is not crucial whereas it is in the 'open-circuit' method. The closed-circuit helium dilution method has been checked on an artificial lung as previ-

ously described (section 3.5.1). In test measurements the dead spaces in the bellows and tubes were separately determined in a way which was discussed earlier in this section. The real volume in the test lungs $V_{L,EE}(r)$ was also estimated by means of a closed circuit helium dilution technique with a syringe, without using the ventilator and the tubes between ventilator and lungs. This value was compared with the estimates $V_{L,EE}(e)$ derived from the closed-circuit helium dilution technique with the ventilator. At an $V_{L,EE}(r)$ of 85, 150 and 210 ml the maximum deviation between $V_{L,EE}(e)$ and $V_{L,EE}(r)$ was 7 ml in repeated measurements (at least 3 at each volume level), whereas the standard deviation of lung volume estimates in repeated measurements at the same volume level was 3 ml. This accuracy was considered good enough for our analysis.

CHAPTER 4

THE INSPIRATORY PAUSE
METHOD

4.1 Introduction.

In clinical routine and (patho-) physiological research several methods have been applied for the estimation of C_{RS} during mechanical ventilation. In this chapter our study on one of these methods, the inspiratory pause method is presented. Furthermore, quasi-static pressure-volume curves are described. These curves were obtained by combining the pressure and the volume data of the inspiratory pause procedures with different inflation volumes. Another estimate of total respiratory compliance was derived from the slope of these P-V curves.

Ventilatory manoeuvres with an inspiratory pause have been applied in our laboratory in several studies with healthy mechanically ventilated piglets [54,104]. A common, non discussed, finding in those studies was a sustained gradual decrease in airway pressure during pauses of a few seconds. However, in the literature stable plateau pressures were frequently reported in inspiratory pauses of 1.5 s [10,13,90].

Because of the sustained pressure fall during an inspiratory pause in our observations we wondered whether a pause of 1.5 s would cause an overestimation of the plateau pressure and, thus, would cause an underestimation of C_{RS}.

Therefore, we did a series of observations during inspiratory pause procedures in mechanically ventilated piglets. To study the effect of differences in inflation volume and inflation rate on the expected overestimation of the airway pressure after a pause of 1.5 s the procedures were performed by insufflation of volumes ranging from 0 to 25 ml.kg^{-1} in 1 to 5 s. An inspiratory pause of 9 s was chosen in all procedures, in order to obtain a reliable estimate of the plateau pressure. Using the pressure and volume data of the different inspiratory pauses we composed a quasi-static P-V curve of the respiratory system. The linear part of such a P-V curve was determined and the slope of this linear part was also interpreted as an estimate of C_{RS}.

Since the observed gradual decrease in pressure during an inspiratory pause might be related to changes in the volume of the respiratory system,

we used a mercury strain gauge around the thorax of the pig to measure changes in intra-thoracic volume. So, this strain gauge was used as a check on the stability of lung volume during the pause.

In the same experiments, different methods for the estimation of C_{RS} during mechanical ventilation were applied. The inflation at constant flow rate during the inspiratory pause procedures enabled us to estimate C_{RS} according to the pulse method. We also performed slow inflation-deflation procedures to derive compliance estimates from the inflation and the deflation limb of the P-V loop. The evaluation of these methods for estimation of C_{RS} is described in the next chapter. In this chapter we focus our attention on the time course of pressure and volume during inspiratory pauses.

4.2   Methods and material.

4.2.1   Surgical procedure

Four healthy Yorkshire pigs (5-7 wk old, 8.5-9.7 kg body weight) were anaesthetized with pentobarbital sodium (30 mg.kg^{-1} i.p.). After a tracheostomy between the second and third tracheal ring a metal Y-shaped cannula was inserted into the distal part of the trachea. Special attention was given to an airtight fixation. A four lumen catheter served for measuring central venous pressure, P_{cv}, and infusions of drugs. A Swan-Ganz catheter was inserted for monitoring the pulmonary arterial pressure, P_{pa}, and sampling mixed venous blood. A polythene one lumen catheter was used to obtain systemic arterial pressure, P_{ao}, and to sample arterial blood. After surgery anaesthesia was maintained by a continuous infusion of pentobarbital sodium (7.5 mg.h^{-1}.kg^{-1} , i.v.). Next, the animals were paralysed with a loading dose of d-tubocurarine hydrochloride (0.1 mg.kg^{-1} i.v. in 3 min.), followed by a continuous infusion of 0.2 mg.h^{-1}.kg^{-1} to avoid spontaneous breathing activity. The animals were mechanically ventilated in supine position on a thermo-controlled operating table for maintenance of body temperature.

Throughout the experiments the haemodynamic data were monitored continuously and the blood gases and the acid-base variables were measured intermittently in order to check the general condition of the animals.

4.2.2   Measurements and estimations

Blood pressures were measured with Statham transducers (P23De). The electrocardiogram (ECG) was used to monitor heart function, to calculate

heart rate and to average several signals over a cardiac cycle, derived from the R-R intervals.

Airflow ($\dot{V}$) was measured by a Fleisch pneumotachometer no. 0 (Sensormedics (Godart), Holland) close to the tracheal cannula. Inflation volumes were calculated by integration of the airflow rate signal. Changes in lung volume determined from the integration of $\dot{V}$ were called ΔV_{FL}.

The pneumotachometer was calibrated before each experiment by insufflating a calibrated spirometer via the flowhead of the pneumotachometer with the same gas mixture as was used during normal mechanical ventilation. The ventilator, used for the mechanical ventilation, was also calibrated by inflation of this spirometer.

The mercury strain gauge, which is also called 'mercury cord' (MC) in the next chapters, was positioned around the thorax at the level of the caudal part of the sternum. The mercury cord was fixed to the skin of the pig to avoid position changes during mechanical ventilation, yet without hindering length changes. Changes in lung volume determined from the mercury cord were called ΔV_{MC}.

Tracheal pressure (P_T) was measured at a small side arm of the tracheal cannula with the use of a pressure transducer (Hewlett-Packard type 270) and was calibrated in each experiment by means of a water manometer.

Blood gases and acid-base variables were measured in arterial and mixed venous blood by means of an automatic blood gas analyser (Radiometer ABL3). O_2 saturation and haemoglobin values were measured with an oximeter (Radiometer OSM2). Inspiratory and mixed expiratory gases were analysed with a mass-spectrometer (Perkin Elmer, MGA 1100), which sampled gas at a flow rate of 0.94 ml.s^{-1} from the tube between ventilator and tracheal cannula. The mass-spectrometer was frequently calibrated by means of an accurate gas mixing pump (H. Wösthoff, Bochum).

Lung volume at end-expiration was estimated by an open circuit helium dilution (wash-in and wash-out) technique (cf. Chapter 3, page 32).

Oxygen consumption during normal mechanical ventilation was calculated from the tidal volume and the inspiratory and mixed expiratory gas concentrations, assuming a constant amount of N_2 in the lungs [81].

Mechanical ventilation was performed with the use of the computer controlled ventilator as described in detail in Chapter 3. Ventilatory rate was $10.\text{min}^{-1}$ and the inspiration-expiration time ratio was 40:60. Tidal volume was adjusted to maintain arterial CO_2 tension (P_{a,CO_2}) between 38 and 45 Torr. Once such a P_{a,CO_2} was established, tidal volume was kept constant at 20.7 ± 0.8 (SD) ml.kg^{-1} BTPS throughout the experiment. The

animals were ventilated with a gas mixture of 95 % O2 and 5 % He to prevent hypoxemia during the special manoeuvres and in particular during the slow inflation-deflation procedures in these experiments. A PEEP of about 2 cm H_2O was applied by means of a waterseal to avoid atelectasis.

4.2.3 Observations

After a period of stabilization, following the surgical procedures, observations were started with two determinations of $V_{L,EE}$ by means of the open-circuit wash-in and wash-out technique. Thus, each determination produced two estimates. Then, three slow inflation-deflation procedures were performed at 15 minute intervals (series 'A'). These procedures were characterized by a slow inflation and subsequent deflation of a volume of 25 ml.kg^{-1} in about 70 s. They are described in detail in the next chapter. Fifteen minutes after the third slow inflation-deflation procedure lung volume was determined again and a series of twenty-two different inspiratory pause procedures was performed in a random sequence (series 'A'). During the inspiratory phase in these procedures a volume of 0 - 25 ml.kg^{-1} was insufflated in 1 - 5 s and flow rates varied from 0 - 17.5 ml.s^{-1}.kg^{-1}. An insufflation of zero volume means actually a prolonged pause at end-expiration. The inspiratory pause procedures were characterized by 1) a normal (passive) expiratory phase, 2) a constant flow rate during the inflation, and 3) an inspiratory pause of 9 s (cf. Chapter 3). Immediately after each inspiratory pause procedure normal mechanical ventilation was resumed for 5 min in order to maintain stable haemodynamic and ventilatory conditions throughout the experiment. After another determination of lung volume the three slow inflation-deflation procedures were performed again (series 'B') followed by a lung volume determination and a second series of 22 inspiratory pause procedures (series 'B'). Finally, another measurement of $V_{L,EE}$ was done. Maximally, 12 estimates of $V_{L,EE}$ were obtained throughout an experiment. However, as is specified in the results section, not all data were obtained because of various technical reasons.

4.2.4 Air leakage

A crucial condition for accurate estimations of compliance is an airtight pulmonary and ventilatory system during the procedures. Therefore, the tubes and ventilator were checked twice on air leakage during each experiment. After an inflation of 25 ml.kg^{-1} the tube between the tracheal cannula and

the ventilator was clamped manually for about 30 s. Gas pressure was monitored both at the side of the lungs and at the side of the ventilator. No significant changes in pressure in the ventilator and tubes were detected, whereas the pressure fall in the tracheal cannula was similar to the pressure fall without clamping the tube.

As an extra precaution and to eliminate the compliance of the ventilator and its tubing an electromagnetic valve was placed in the tubing at the tracheal cannula (cf. section 3.3). This extra valve was only closed during the pauses in the inspiratory pause procedures.

4.2.5 *Data analysis*

Monitoring. All signals were displayed on a Hewlett Packard 7758A chart recorder throughout the entire experiment to monitor the haemodynamic and ventilatory conditions of the animal. The signals were filtered by low pass filters (-3 dB frequency 10 Hz, 12 dB/oct) to suppress high frequency noise. During the special procedures the signals were stored on magnetic tape (RACAL Store 14 recorder) and sampled by a computer (DEC PDP 11/03) with a sample frequency of 100 Hz and stored on disk. All calculations and analyses were done off-line.

Calibration of the mercury cord. With the use of different inflation volumes in the 22 inspiratory pause procedures we could calibrate the mercury cord by relating its change in resistance (ΔR_{MC}) to the applied tidal volume, obtained by integration of the airflow signal (change in volume ΔV_{FL}). For the change in resistance ΔR_{MC} we took the difference between the resistance over the first 0.5 s of the inspiratory pause and the resistance at end-expiration. We took ΔR_{MC} as a substitute for the change in thoracic volume. The relationship between ΔV_{FL} and ΔR_{MC} could be compressed into a second degree polynomial function, which was used as the calibration characteristic for detection of changes in thoracic volume (ΔV_{MC}) by the mercury cord.

It has to be emphasized that ΔV_{FL} represents the input volume (= tidal volume), whereas ΔV_{MC} represents the actual change in thoracic volume. ΔV_{FL} and ΔV_{MC} may differ when there is a change in lung volume due to continuous gas exchange at a respiratory gas exchange ratio different from 1 or a loss of pulmonary blood volume during insufflation.

Considering a maximal expected volume decrease of ≈ 1 ml.s^{-1}, which is about equal to the oxygen uptake in mechanically ventilated piglets weighing 10 kg, the decrease in lung volume during the insufflation was calculated to

47

be maximally 5 % (no insufflation was longer than 2 s. at 5 ml.kg^{-1} and longer than 2.5 s at 7.5 ml.kg^{-1}). However, considering a steady state respiratory exchange ratio between 0.7 and 1.0 we may predict an error of maximally 1.5 %.

The loss of pulmonary blood volume may have caused a maximal error of 4%. Versprille et al. [105] observed under similar circumstances as in our experiments a loss of pulmonary blood volume of maximally 1.2 ml per 30 ml inflation volume.

We regarded a total error of 5-6 % acceptable for our analysis.

Volumes ΔV_{MC} and ΔV_{FL} are given in BTPS values, i.e. corrected for differences in temperature, humidity and pressure.

We have also studied the feasibility of a mercury cord around the abdomen for the estimation of changes in lung volume. We calculated the ratio between the change in resistance of a mercury cord around the rib cage and that of a mercury cord around the abdomen and found no significant differences in the ratios in the volume range from 0 to 20 ml.kg^{-1}, indicating no variation in thoracic-to-abdominal partitioning of volume. Therefore, the strain gauge around the rib cage could monitor changes in lung volume adequately for the selected volume interval between 4 and 12 ml.kg^{-1}.

Moreover, the abdominal strain gauge appeared not to be useful for detecting small gradual volume changes in the abdominal compartment during inspiratory pauses because of a rather poor signal-to-noise ratio very probably due to continuous peristaltic movements of the intestine.

Compliance estimates and quasi-static P-V curves. Total respiratory compliance was calculated at 1.5 and 8.5 s in the inspiratory pause. Because of the influence of cardiac oscillations on tracheal pressure tracings we always interpolated between two cardiac cycles when the pressure at a specific time had to be calculated. This is the reason why the pressure at 8.5 s instead of 9.0 s has been used for the calculations. These compliance estimates are called $C_{IP,1.5}$ and $C_{IP,8.5}$ respectively.

For the calculation of the compliance an accurate estimation of the change in lung volume between end-expiration and inspiratory pause was needed. Based on ΔV_{FL} this volume was always equal to the insufflated volume. However, when the change in lung volume was derived from the mercury strain gauge ΔV_{MC}, the volume at 1.5 and 8.5 s inspiratory pause usually deviated from the insufflated volume. Therefore, C_{RS} was derived both from 1.5 s and 8.5 s, using both estimates of changes in lung volume. All compliance values were normalized to the body weight of the piglets and are therefore expressed in ml.cm H$_2$O^{-1}.kg^{-1} (BTPS).

A quasi-static P-V curve (PV_{IP}) was composed out of each series of 22 inspiratory pause procedures by fitting a polynomial function of the third degree to all inflation volumes and tracheal pressures at 8.5 s inspiratory pause ($P_{T,8.5}$). Such a third degree polynomial function appeared to be a satisfactory mathematical description. A higher order function did not improve the minimal errors of the fit. The curve yielded an approximately linear relationship between 4 and 12 ml.kg^{-1}. The slope of this linear part of the curve was calculated by a linear regression technique, using only those inspiratory pause procedures with volumes between 4 and 12 ml.kg^{-1}, and was considered to be an estimate of the slope of the static P-V curve of the respiratory system. This compliance estimate is called $C_{IP,sl}$ (sl = slope).

Statistical analysis. Statistical analyses were performed using the test procedure of Fisher-Behrens, which tests the equality of means with unequal sample size and possibly unequal variances [91]. p values of ≤ 0.05 were regarded as significant.

4.3 Results.

4.3.1 *Lung volume measurements*

A systematic trend in the end-expiratory lung volume throughout the experiments could not be detected. Normalized to body weight, lung volume was 17.4 ± 0.7 (SD) ml.kg^{-1} (n=10), 16.4 ± 1.4 (SD) ml.kg^{-1} (n=12) and 15.0 ± 1.8 (SD) ml.kg^{-1} (n=11) in piglets 2 to 4 respectively (n: the number of observations per experiment). In piglet 1 end-expiratory lung volume could not be measured because of technical problems. As was discussed in Chapter 3 (page 37) a systematic error in the open circuit wash-in and wash-out technique probably affected the above mentioned lung volume estimates.

4.3.2 *Pressure and thoracic volume during an inspiratory pause*

Pressure change during an inspiratory pause. Pressure was generally found to decrease gradually during the entire inspiratory pause of 9 seconds and consequently no unambiguous plateau pressure could be defined. In Fig. 4.1 the pressure decay in pauses at different inflation volumes is displayed by plotting the actual pause pressure with respect to the pressure at 8.5 s in the respective inspiratory pauses. Therefore, all tracings intercept the X–axis at 8.5 s. We have pooled procedures of all experiments in which inflation volume was 5, 15 or 25 ml.kg^{-1} (tracings A, B and C respectively
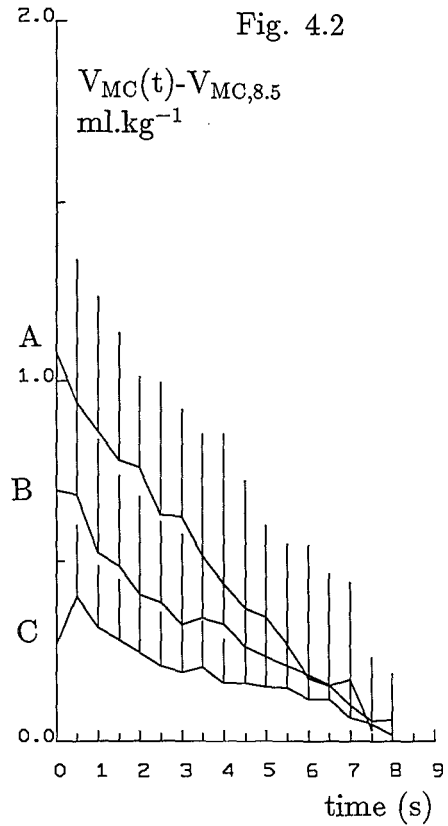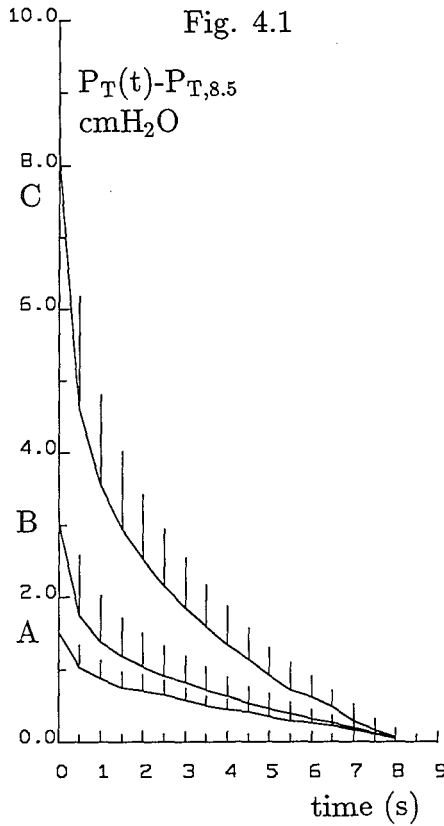
Figure 4.1 Changes in tracheal pressure during an inspiratory pause.
Tracheal pressure P_T above the tracheal pressure at 8.5 s pause ($P_{T,8.5}$) versus time for inflation volumes of 5, 15 and 25 ml.kg^{-1} (tracings A, B and C respectively). The vertical bars represent the standard deviations plotted at 0.5 s intervals in the inspiratory pauses.

Figure 4.2 Changes in thoracic volume during an inspiratory pause.
Change in intra-thoracic volume, obtained from the mercury cord, with respect to the volume at 8.5 s pause as a function of time for inflation volumes of 5, 15 and 25 ml.kg^{-1} (tracings A, B and C respectively). The vertical bars represent the standard deviations plotted at 0.5 s intervals in the inspiratory pauses.

50

in Fig. 4.1). It is obvious that pressure was not constant during any part of the inspiratory pause. Larger changes in pressure during the inspiratory pauses were observed after larger inflation volumes. Visual inspection of all pressure decay curves gave us the strong impression that the slow gradual decrease in pressure during an inspiratory pause at low inflation volumes (e.g. 5 ml.kg^{-1}, tracing A) behaved like a linear function of time, whereas the pressure decrease at large inflation volumes (25 ml.kg^{-1}, tracing C) was curved like an exponential function.

Thoracic volume changes during an inspiratory pause. The inspiratory pause method for estimation of C_{RS} started from the assumption of a constant volume of the respiratory system during the inspiratory pause. This assumption appeared to be invalid in our experiments. In all procedures we detected a slow gradual decrease in volume throughout the pause. To demonstrate the changes in intra-thoracic volume we have plotted (Fig. 4.2) the volume-time course with respect to the intra-thoracic volume after a pause of 8.5 s, similar to the plot of the decrease in pressure in Fig. 4.1. We also chose for the same procedures as were used in that figure, i.e. we have pooled procedures with volumes of inflation of 5, 15 and 25 ml.kg^{-1}, respectively. In contrast with the changes of P_T the largest changes of volume during the inspiratory pauses were found after insufflation with the lowest volumes (5 ml.kg^{-1}, tracing A).

We have quantified the rate of the slow volume decrease by calculating the slope of volume-time course between 6 and 9 s in the inspiratory pause by means of a linear regression technique. The slope of the volume-time course was found to be negative in all inspiratory pauses. The rate of the change in lung volume was found to be on average -0.11 $\pm$ 0.05 (SD) ml.s^{-1}.kg^{-1} (n=14) after 5 ml.kg^{-1} inflations and -0.05 $\pm$ 0.02 (SD) ml.s^{-1}.kg^{-1} (n=35) after 25 ml.kg^{-1} inflations. Using insufflation volumes in between we found rates of volume decrease between both values.

4.3.3 *Quasi-static pressure-volume curves*

Pressure-volume (PV$_{IP}$) curves of the respiratory system were obtained in each series 'A' and 'B' by fitting a polynomial function through the pressure and volume pairs at the end of the 22 different inspiratory pauses. In Fig. 4.3 such a P-V curve (continuous line) is presented in combination with the 22 P-V pairs of one series. For this continuous curve we used the ΔV_{MC} values. The P-V curve intercepts the pressure axis at the PEEP level. When we used the ΔV_{FL} values for the determination of the P-V curve this curve
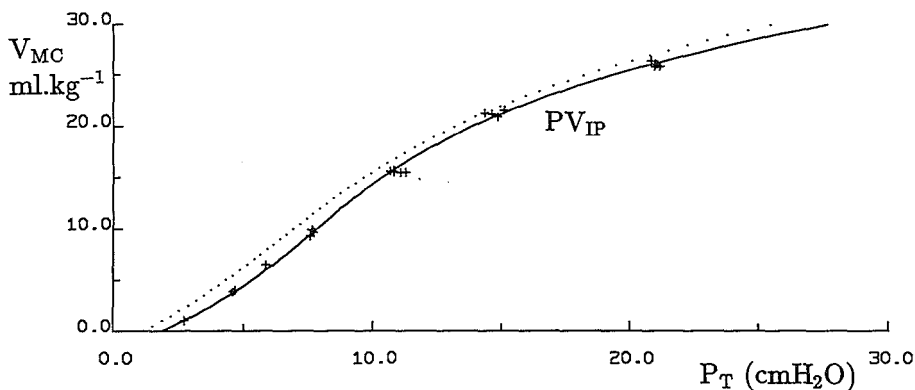
Figure 4.3 Quasi-static P-V curves PV_{IP}.
The continuous line is the polynomial fit through the individual data of airway pressure and change in lung volume, based on the mercury cord, obtained at 8.5 s pause in 22 different inspiratory pause procedures. The '+' symbols represent individual data. The dotted line represents the P-V curve from the same procedures but with changes in volume based on integration of the airflow.

shifted upwards (dotted line), because then the change in lung volume was overestimated.

4.3.4 The relationship between pressure and volume decrease

To investigate whether the pressure decrease during an inspiratory pause depended on a decrease in volume or not, we plotted the changes in P_T and V_{MC} of three inspiratory pause procedures in a diagram of the PV_{IP} curve (Fig. 4.4). This curve was also based on ΔV_{MC}. The inflation volume of the three procedures was 5, 15 and 25 $ml.kg^{-1}$ respectively. Inspiratory flow rate was 5 $ml.s^{-1}.kg^{-1}$ in these procedures. During the last few seconds of the inspiratory pause after insufflation of the low volume the pressure-volume course coincided with the quasi-static P-V curve (PV_{IP}). This coincidence indicates that this part of the decrease in pressure was mainly due to a decrease in lung volume. At the largest insufflation volume, however, the fall in lung volume and pressure during an inspiratory pause did only coincide with the PV_{IP} curve after 8.5 s, indicating that the fall in pressure was mainly based on other mechanisms than a loss of lung volume.
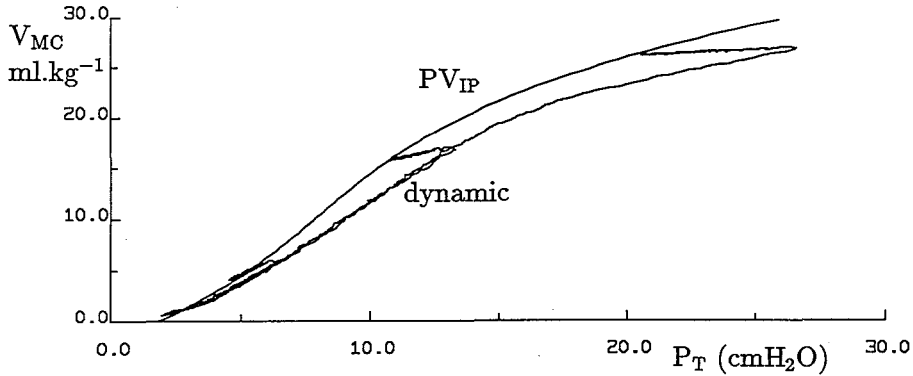
Figure 4.4 P-V tracings during inspiratory pause procedures.
P_T and the change in intra-thoracic volume during inflation and subsequent inspiratory pause for three different procedures. Inflation volumes were 5, 15 and 25 ml.kg^{-1} (ATPD) at a flow rate of 5 ml.s^{-1}.kg^{-1}. The continuous line PV$_{IP}$ is the quasi-static P-V curve as obtained for Fig. 4.3.

4.3.5 Comparison of compliance estimates based on the inspiratory pause method

Because of the overall nonlinearity of the P-V relationship of the respiratory system we compared compliance estimates only when inflation volume was in the range from 4 to 12 ml.kg^{-1}. In this volume range the quasi-static P-V curve was approximately linear. Therefore, only part of the inspiratory pause procedures was used for the comparison. All estimates of compliance were normalized to body weight (ml.cm H_2O^{-1}.kg^{-1}). The mean values and standard deviations are presented in Table 4.1. In the third experiment series 'B' was not measured.

The loss of thoracic volume during the pause points to a gradually increasing difference between lung volume after inflation and the actual lung volume during the pause. This volume difference determines the differences found between the corresponding compliance estimates. When integration of the airflow was used for the calculation of the change in lung volume, the compliance estimate $C_{IP,8.5}$ derived from the 8.5 s pause period was significantly higher than the compliance $C_{IP,1.5}$ derived from the 1.5 s pause period.

However, when the volume change was measured by means of the mercury strain gauge the compliance estimates at 1.5 and 8.5 s inspiratory pause were not significantly different. Both estimates ($C_{IP,1.5}$ and $C_{IP,8.5}$)

53

TABLE 4.1
Estimates of total respiratory compliance.

Pig	$C_{IP,8.5}$		$C_{IP,1.5}$		$C_{IP,sl}$	
	ΔV_{FL}	ΔV_{MC}	ΔV_{FL}	ΔV_{MC}	ΔV_{FL}	ΔV_{MC}
1A	1.60	1.41	1.42	1.36	1.55	1.63
	(0.04)	(0.08)	(0.05)	(0.20)	(0.06)	(0.07)
1B	1.57	1.40	1.42	1.37	1.55	1.70
	(0.04)	(0.16)	(0.07)	(0.23)	(0.06)	(0.09)
2A	2.11	1.66	1.73	1.55	1.88	1.91
	(0.11)	(0.11)	(0.08)	(0.09)	(0.10)	(0.06)
2B	2.14	1.69	1.75	1.60	1.90	1.89
	(0.10)	(0.08)	(0.06)	(0.06)	(0.07)	(0.04)
3A	1.44	1.29	1.27	1.22	1.38	1.43
	(0.04)	(0.06)	(0.06)	(0.06)	(0.08)	(0.03)
4A	1.63	1.31	1.34	1.26	1.56	1.63
	(0.06)	(0.12)	(0.07)	(0.08)	(0.08)	(0.05)
4B	1.28	1.06	1.07	1.01	1.06	1.14
	(0.12)	(0.09)	(0.09)	(0.07)	(0.20)	(0.14)
mean	1.68	1.40	1.43	1.34	1.55	1.62
	(0.31)	(0.22)	(0.23)	(0.22)	(0.29)	(0.27)
	n=42	n=42	n=42	n=42	n=7	n=7

Compliance estimates, expressed in $ml.cmH_2O^{-1}.kg^{-1}$, obtained from inspiratory pause procedures, with inflation volumes between 4 and 12 $ml.kg^{-1}$ in four experiments. The standard deviations are give in parentheses. In the third experiment series 'B' was not measured. $C_{IP,8.5}$ is the estimate of C_{RS} derived from inspiratory pauses of 9 s at 8.5 s from the start of the pause. $C_{IP,1.5}$ is calculated like $C_{IP,8.5}$ but from an inspiratory pause of 1.5 s instead of 8.5 s. $C_{IP,sl}$ is the compliance estimate derived from the quasi-static P-V curve. The standard deviation of $C_{IP,sl}$ was derived from the linear regression analysis. All compliance estimates were calculated with the use of the two measurements of changes in lung volume: ΔV_{FL} and ΔV_{MC}.

were smaller than the compliance $C_{IP,sl}$ derived from the slope of quasi-static P-V curve when changes in volume were measured by the mercury strain gauge.

4.4 Discussion and conclusions.

We studied end-expiratory lung volume throughout the experiments because changes in lung volume as such affect the values of compliance. No systematic trends in the end-expiratory volumes were found. Therefore, the values of compliance obtained at different moments in the experiments were feasible for comparison.

4.4.1 ΔV_{MC} and P_T relationship during an inspiratory pause

The decrease in thoracic volume during an inspiratory pause could be attributed either to a decrease in intra-thoracic blood volume or to a decrease in lung volume or to both.

In other experiments in our laboratory a decrease in pulmonary blood volume was found during insufflation and the first two seconds of the inspiratory pause. Thereafter, cardiac output at the right and at the left side of the heart were similar again [104]. This supports the assumption that pulmonary blood volume is constant during the remaining part of an inspiratory pause. Therefore, it is unlikely that a sustained gradual decrease in pressure during a maintained inspiratory pause could depend on a further loss of intra-thoracic blood volume.

An explanation for a decrease in lung volume might be the continuous gas exchange [19,44,59,73,79]. Oxygen uptake from the lungs, in the presence of a high oxygen concentration due to $F_{I,O_2} = 0.95$ can be considered as constant throughout an inspiratory pause of 9 s. In the meantime the CO_2 transfer from blood to lungs will decrease due to the decreasing gradient between CO_2 tension in the blood and the alveolar gas. Therefore, eventually the decrease in lung volume will approximate the same rate as oxygen uptake [44,73]. Hong et al. [44] reported a lung volume decrease similar to the steady state oxygen consumption within 30 s, and Mithoefer [73] reported that the volume decrease was constant after 100 s. However, oxygen uptake during an inspiratory pause will not necessarily be similar to oxygen uptake ($\dot{V}_{O_2}$) during the preceding steady state ventilation.

Both oxygen uptake and CO_2 output will depend on several mechanisms. Exchange of these gases is expected to be decreased when the lung perfusion is reduced after inflation of a large volume, due to a high intra-thoracic

pressure [37,104]. Moreover, the gradient between the CO_2 tension in blood and alveolar gas is probably less reduced when the CO_2 buffer capacity of the gas volume is large at large volumes. Both mechanisms may explain the greater loss of lung volume during an inspiratory pause at low inflation volumes compared to the loss of volume during an inspiratory pause at larger inflation volumes.

In the present study oxygen uptake during steady state mechanical ventilation was on average 0.11 ± 0.02 (SD) $ml.s^{-1}.kg^{-1}$ (STPD) in 5 observations during each of the last three experiments (n=15). This value approximated the observed decrease in thoracic volume during inspiratory pauses at low volumes $(0.11 \pm 0.05$ (SD) $ml.s^{-1}.kg^{-1}$ (n=14) at 5 $ml.kg^{-1}$) (BTPS), indicating that 1) the respiratory exchange ratio was very low during inspiratory pauses at these volume levels 2) the blood flow through the lungs was not very much reduced.

We explained the gradual decrease in intra-thoracic volume to be mainly caused by continuous gas exchange. We tested this hypothesis in a detailed experimental study on the effect of gas exchange. This study is described in Chapter 6.

Part of the pressure decrease during inspiratory pauses at the higher inflation volumes could not be related to a decrease in thoracic volume. A number of additional mechanisms have been suggested to explain the time-dependence of tracheal pressure during an inspiratory pause.

Firstly, the fall in pressure has been attributed to an equilibration of the pressure gradients in the lungs. In normal lungs a sudden stop of insufflation during artificial ventilation will cause an almost instantaneous decrease in tracheal pressure. But in the presence of inhomogeneities in the lungs also a more gradual decrease in airway pressure could be observed as mentioned for the 'Pendelluft' phenomenon [10]. This effect on pressure fall is thought to end within 1 s [10,89].

Secondly, it has been suggested that opening of previously closed lung regions during an inspiratory pause will contribute to a decrease in airway pressure [49].

Thirdly, the viscoelastic properties of lungs and thorax may cause a decrease in recoil pressure -"stress relaxation"- after a stepwise increase of lung volume [10,22,49,66]. The decrease in recoil pressure during a maintained inspiratory pause is generally attributed to stress-relaxation, in particular in experiments with excised lungs [46,62]. The considerable decrease of tracheal pressure during the inspiratory pause after insufflation of large volumes in our experiments probably has some connection with this mechanism. A

more detailed analysis of this pressure decay in the absence of gas exchange is presented in Chapter 7.

Our data were not satisfactory to assess the contribution of each mechanism to the fall in pressure during the inspiratory pause.

4.4.2 *Overestimation of the plateau pressure*

The PV_{IP} curve through the P-V plots obtained after 8.5 s in the inspiratory pause could be regarded as the best approximation of the 'static' P-V relationship of the respiratory system in our study. This certainly holds true for the lower volume range where the changes in pressure and volume during the last part of the inspiratory pause coincided with the PV_{IP} curve (Fig. 4.4). It seems acceptable for the higher insufflated volumes that the real 'static' curve is shifted slightly to the left in the upper part of the PV_{IP} curve. We reason this from the lack in coincidence between the P-V relationship during an inspiratory pause and the PV_{IP} curve, except for the P-V point at 8.5 s. So a further decrease of pressure could have occurred beyond 8.5 s.

We have estimated the difference between the pressure at 1.5 s in the inspiratory pause ($P_{T,1.5}$) and the value on the PV_{IP} curve as the substitute for the static pressure at the insufflated volume ΔV_{FL}, in order to use this difference as a measure of overestimation of the static pressure when using $P_{T,1.5}$. In order to visualize the calculation a schematic drawing of a part of a dynamic pressure-volume curve and a part of the PV_{IP} curve is presented in Fig. 4.5. $P_{T,1.5}$ is projected via a horizontal line on the PV_{IP} curve which finds the static pressure P_{stat} corresponding to the insufflated volume. The total pressure decay from 1.5 to 8.5 s may be partitioned into a pressure loss ΔP_1, which is mainly due to stress-relaxation, and a pressure loss ΔP_2, which is mainly due to the loss of lung volume. The difference between $P_{T,1.5}$ and the value P_{stat} was expressed as a percentage of the difference between P_{stat} and the end-expiratory pressure P_{EE} according to

$$\text{overestimation} = \frac{(P_{T,1.5} - P_{stat})}{(P_{stat} - P_{EE})}.100\%. \tag{1}$$

At inflation volumes of 15 ml.kg^{-1} the pressure at 1.5 s ($P_{T,1.5}$) overestimated plateau pressure about 6.8 $\pm$ 2.1 (SD) %, n=32, at larger inflation volumes this overestimation was larger, e.g. 10.3 $\pm$ 2.3 (SD) %, n=26 at 25 ml.kg^{-1}. For inflation volumes less than 10 ml.kg^{-1} the overestimation of pressure at 1.5 s was 5.5 $\pm$ 2.5 (SD) %, n=16. However, due to the low absolute pressure values and the comparatively large cardiac interference on
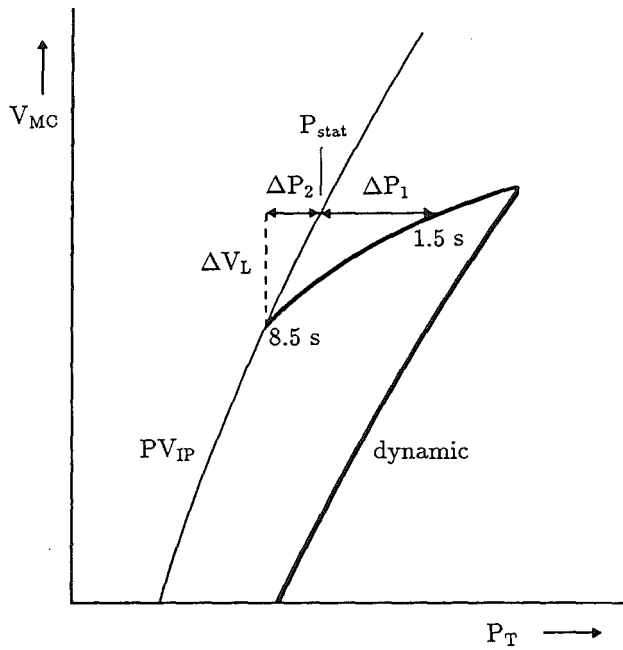
Figure 4.5 Schematic drawing of the partitioning of the pressure decay between 1.5 and 8.5 s into a pressure decrease (ΔP_1) which is mainly due to stress-relaxation and a pressure decrease (ΔP_2), which is mainly due to a loss of lung volume (ΔV_L). $P_{T,1.5}$ is the tracheal pressure at 1.5 s pause. P_{stat} represents the estimate of the quasi-static pressure at the volume corresponding to V_{MC} at 1.5 s.

the pressure signal the values for the overestimation at low inflation volumes were very sensitive to errors in the measurements.

4.4.3 *Compliance estimates based on the inspiratory pause method*

For consideration of the differences between the various compliance estimates we used $C_{IP,sl}$, in which the estimation of the change in lung volume was based on the mercury cord, as a reference. $C_{IP,sl}$ represents the slope of the linear part of the PV_{IP} curve. $C_{IP,sl}$ based on ΔV_{MC} did not differ much from $C_{IP,sl}$ based on ΔV_{FL}, because the decrease in volume during inspiratory pauses at volumes between 4-12 ml.kg^{-1} mainly caused a shift, instead of a change in slope, of the PV_{IP} curve.

The $C_{IP,1.5}$ values were not much influenced by stress-relaxation because we restricted the comparison of compliance estimates to the volumes range from 4 to 12 ml.kg^{-1} and moreover continuous gas exchange was of minor importance for the period of 1.5 s. For this reason we did not find a significant difference between the two $C_{IP,1.5}$ values obtained by the mercury strain gauge and by integration of the airflow, respectively.

The lower values of $C_{IP,1.5}$ compared to $C_{IP,sl}$ could be explained by the nonlinear part of the P-V curve occurring in the low volume range and reflecting opening of previously closed lung units [22,27,100].

When the change in lung volume was based on integration of the airflow the compliance estimate $C_{IP,8.5}$ derived from the inspiratory pause method was found to be significantly higher than $C_{IP,sl}$. This overestimation was caused by a pressure decrease partly due to a loss of lung volume during the inspiratory pause, undetected by the airflow integration technique. Therefore, in this situation the measurement of the real changes in lung volume, done by a mercury strain gauge, has to be preferred.

CHAPTER 5

THE PULSE METHOD AND THE SLOW INFLATION-DEFLATION METHOD

5.1 Introduction.

In this chapter additional observations and data-analyses are described, which were performed during the experiments as mentioned in Chapter 4, to evaluate two other methods for the estimation of C_{RS}, i.e. 1) the pulse method and 2) the slow inflation-deflation method. In the pulse-method C_{RS} is derived from the ratio between a constant flow rate and the slope of the pressure-time course during inflation (cf. section 2.3). In the slow inflation-deflation method C_{RS} is derived from the slope of the P-V loop of the respiratory system obtained by a slow inflation and subsequent deflation (cf. section 2.4). C_{RS} can be estimated from the inflation limb (C_{INFL}) as well as from the deflation limb (C_{DEFL}) of the P-V loop. In this chapter the 'pulse'-compliance and the compliances, C_{INFL} and C_{DEFL}, are compared with $C_{IP,sl}$, which was presented in Chapter 4.

In the majority of cases changes in lung volume in pressure-volume loops have been determined by assuming a change in lung volume equal to the tidal volume [43,64,68,69]. However, recent literature on the subject [21,30] suggests that continuous gas exchange might affect a proper estimation of changes in lung volume, in particular in slow inflation-deflation procedures. The mercury strain gauge, as described in Chapter 4, enabled us to differentiate between the input volume, estimated by integration of the airflow, and the real change in lung volume.

5.2 Methods.

5.2.1 *Introduction*

For the general conditions of the experiments we refer to the section on methods of Chapter 4. In this section we concentrate on the additional procedures and data-analyses which were performed for the 'pulse'-method and the slow inflation-deflation method.

5.2.2 Experimental protocol

The experimental protocol could be restricted to two types of special procedures (cf. Chapters 3 and 4) to derive the compliance estimates. These special procedures always started the inflation at the end of a normal expiratory phase in mechanical ventilation. Therefore, lung volume at the start of inflation was assumed to be equal to the end-expiratory lung volume in steady state ventilation.

Pulse method. For this method we have used the insufflation with constant flow in the inspiratory pause procedures, which were discussed in Chapter 4. Volume of inflation varied between 0 and 25 ml.kg^{-1} and inflation time between 1 and 5 s. Flow rates varied between 0 and 17.5 ml.s^{-1}.kg^{-1} in the different procedures. Although flow rate was constant during each inflation, only 10-12 inspiratory pause procedures from each series of 22 could be used to calculate 'pulse' compliance. This was caused by restrictions to the flow rate and the minimal required change in volume (cf. section 5.2.3).

Slow inflation-deflation method. The slow inflation-deflation procedures were performed in a series of three and in the same order. Because these procedures differed from each other we have called them slow inflation-deflation procedures 1, 2 and 3, or in abbreviation SID1, SID2 and SID3. In each procedure inflation volume was 25 ml.kg^{-1} and the total time period of the inspiratory phase was 35.0 s.

In SID1 the volume was insufflated in 10 equal volume steps of 2.5 ml.kg^{-1}. Each step took 3.5 s, including an inspiratory pause of 1.5 s. After the last step the inspiratory pause was 9 s. After this, the piglet was allowed to breathe out passively.

In SID2 inflation was the same as in SID1 but deflation was controlled by the ventilator and performed in 10 equal volume steps of 2.5 ml.kg^{-1} in 3.5 s per step including a pause of 1.5 s until the entire insufflated volume was recollected in the bellows of the ventilator.

In SID3 a volume of 25 ml.kg^{-1} was insufflated at a constant flow rate in 35 s and followed after a pause of 1.5 s by a controlled deflation of 25 ml.kg^{-1} in 35 s.

The imposed volume-time courses of procedures SID2 and SID3 have already been presented in Fig. 3.4 of Chapter 3, page 31.

Observations. The observations were started with two determinations of end-expiratory lung volume ($V_{L,EE}$). During the next 45 minutes three slow inflation-deflation procedures (SID1, SID2 and SID3) were performed at 15 minute intervals, followed by another determination of $V_{L,EE}$. Then, a series

of 22 inspiratory pause procedures was performed (series 'A') at 5 minute intervals, after which all observations were repeated (series 'B'). After these measurements $V_{L,EE}$ was measured once more.

5.2.3 Data-analysis

Pulse method. Pulse compliance C_P was calculated using the dynamic pressure-volume relationship during insufflation, which is a modified but not principally different analysis of the pressure-time relationship because flow rate was constant (cf. Chapter 2, page 16). C_P was only calculated from those inspiratory pause procedures in which the airflow of insufflation was less than 10 ml.s^{-1}.kg^{-1}. We applied a linear regression analysis to calculate $(\Delta V / \Delta P_T)$ in the volume interval from 4 to 12 ml.kg^{-1} with a minimum interval of 4-8 ml.kg^{-1}. The limitation of the airflow to 10 ml.s^{-1}.kg^{-1} and the volume interval between 4 and 12 ml.kg^{-1} are considered in the discussion section.

Slow inflation-deflation method. Changes in lung volume were obtained both from changes in thoracic volume measured with the mercury strain gauge and from integration of the flow rate. The calibration of these volume measurements was described in Chapter 4. When volume changes were obtained from integration of the airflow an accurate estimation of the zero flow level was important, because after a long period of integration a small drift in this level could cause substantial errors. In SID1 this zero level could be obtained during the pause of 9 s at end-inflation. Such a period with zero flow rate was not available in the SID2 and SID3 procedures. The 1.5 s pause periods could not be used for the determination of the zero flow level, because the inflation valve of the ventilator was not closed during those periods and the flow rate was still affected by cardiac interference and small adaptations in position of the piston. However, in these procedures the volume insufflated by the ventilator was equal to the inflation volume in SID1. In procedures SID2 and SID3 the zero level of the pneumotachometer could be defined from this similarity. The inflation volume was obtained by integration of the airflow and was corrected from ATPD to BTPS, i.e. corrected for differences in temperature, humidity and pressure. During deflation it was assumed that the temperature and humidity of the gas flowing through the flow head were similar to those of alveolar gas.

Changes in tracheal pressure and lung volume were averaged over the last cardiac cycles of each volume step. For the analysis of the continuous flow procedure of SID3, inflation and deflation were divided into 10 equal

volume steps. C_{INFL} and C_{DEFL} were derived from the slopes of rectilinear lines found by a linear regression method, through the P-V points in the volume interval between 4 and 12 ml.kg^{-1}. For reasons of comparison we chose for the same range of volume as was done in the analysis of $C_{IP,sl}$ in Chapter 4.

The area of each P-V loop was calculated to compare the amount of hysteresis in the P-V loop derived from ΔV_{FL} and that derived from ΔV_{MC}. The area was enclosed by the inflation and deflation limbs and the part of the Y–axis between the beginning of the inflation limb and the end of the deflation limb.

Compliance estimate CIP,sl. For the mutual comparison of C_{INFL}, C_{DEFL} and $C_{IP,sl}$ we used $C_{IP,sl}$ based on ΔV_{MC} as a reference. As was shown in Chapter 4, $C_{IP,sl}$ based on ΔV_{MC} was not significantly different from $C_{IP,sl}$ based on ΔV_{FL}.

5.2.4 *Statistical analysis*

Using the test procedure of Fisher-Behrens statistical analyses were performed, testing the equality of means with unequal sample size and possibly unequal variances [91]. p values of ≤ 0.05 were regarded as significant.

5.3 Results.

5.3.1 *Pulse Method*

The pressure-time course during an inflation at constant flow rate in normal mechanical ventilation is shown in Fig. 5.1. After a transient phase of about 0.5 s a linear pressure rise was observed. This linear increase in pressure was sometimes followed by a marked nonlinear rise in pressure depending on the inflation volume. To investigate the volume at which such a nonlinearity in the pressure-time course occurred, we compared the dynamic P-V curve during the inflations at constant flow rate with the quasi-static pressure volume (PV_{IP}) curve. The slope of the dynamic P-V curve (C_P) appeared to be different from the slope of the quasi-static P-V curve ($C_{IP,sl}$) in the volume range from 4 to 12 ml.kg^{-1}. Fig. 5.2A shows an individual example of a dynamic P-V curve and the corresponding quasi-static P-V curve. In Fig. 5.2B we plotted the relationship between the inflation volume and the pressure differences between the P-V curves for all inflations at the same airflow rate of 5 ml.s^{-1}.kg^{-1} in four experiments (line 1). Since the comparison of the P-V curves at the low levels of inflation volumes could also
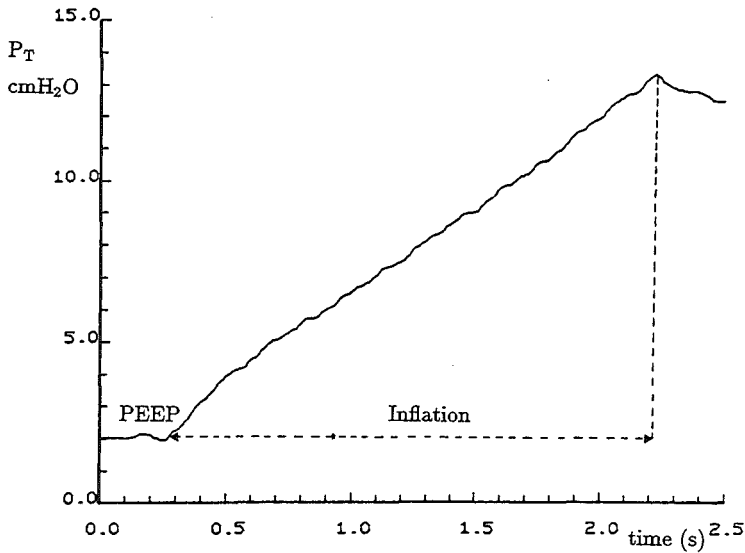
Figure 5.1 Tracheal pressure versus time during an inflation at constant flow rate. The pressure tracing starts at PEEP level. After a transient phase of about 0.5 s the pressure rise was linear, with a slight upward deflection in the upper part.
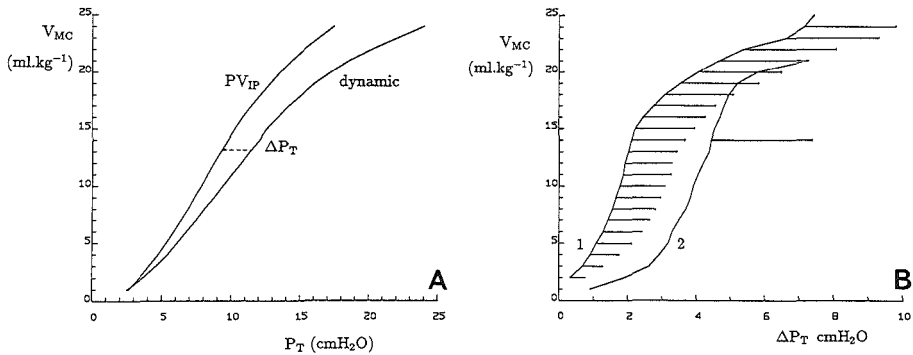
Figure 5.2 Differences between dynamic and quasi-static P-V curves.

A) Two pressure-volume curves are shown: a *quasi-static* P-V curve (PV_{IP}) through pressure-volume data at the end of the inspiratory pauses and a *dynamic* P-V curve during a typical inflation. ΔP_T indicates the difference in pressure at equal volumes.

B) The average difference in pressure ΔP_T between both tracings is presented for all procedures in which the flow rate was about 5 $ml.s^{-1}.kg^{-1}$ (line 1). The vertical lines indicate the standard deviation at each volume increment. In line 2 procedures are presented with an inspiratory flow rate of 17.5 $ml.s^{-1}.kg^{-1}$. Only one standard deviation line is plotted for comparison.

65

be performed in inflations with a larger volume more points of comparison were available at low levels of inflation volume (60 entries at 5 ml.kg^{-1}) than at high levels (16 entries at 25 ml.kg^{-1}).

The influence of flow rate on the estimation of compliance by the pulse method is illustrated in Fig. 5.2B. In this figure we also plotted the average differences in pressure between the P-V curves for inflations at the largest flow rate of 17.5 ml.s^{-1}.kg^{-1} (line 2). The difference between the dynamic and the quasi-static P-V curve at a flow rate of 17.5 ml.s^{-1}.kg^{-1} was larger than that obtained from inflations with a flow rate of 5 ml.s^{-1}.kg^{-1}. However, the slopes of both lines were similar in the volume range from 4 to 12 ml.kg^{-1}, indicating that the slopes, i.e. compliance estimates, were not airflow dependent. Because of the variability of the dynamic pressure-volume curve at large flow rates – as demonstrated by the large standard deviation in ΔP_T – we decided to restrict the pulse compliance analysis to inflations at flow rates less than 10 ml.s^{-1}.kg^{-1}.

5.3.2 *Slow Inflation deflation method*

In Fig. 5.3A a typical example of a pressure-volume curve is presented obtained from a slow inflation-deflation procedure SID2, in which changes in lung volume were derived from integration of the airflow. A volume of 25 ml.kg^{-1} (ATPD) was insufflated stepwise and subsequently deflated in about 70 s. Also the quasi-static pressure-volume curve (PV_{IP}) is presented in the figure. The slope of the deflation limb of the pressure-volume loop was found to deviate substantially from $C_{IP,sl}$, whereas C_{INFL} approximated $C_{IP,sl}$. Fig. 5.3B shows a pressure-volume loop, derived from the same observation as used in Fig. 5.3A, with volume based on the change in intrathoracic volume. In this case compliance estimates C_{INFL} and C_{DEFL} both approximated $C_{IP,sl}$.

The deflation limb in the P-V loops based on integration of the airflow was shown to give a marked positive intercept on the volume axis (Fig. 5.3A). This volume intercept was called 'unrecovered volume' by Gattinoni et al. [30], denoting a loss in lung volume during the procedure. This intercept on the volume axis was not observed when changes in volume based on the mercury strain gauge were plotted against P_T. In the last phase of the deflation in the slow inflation-deflation procedures the mercury strain gauge indicated a lung volume less than the end-expiratory volume, also suggesting a loss of (lung) volume during the procedure. Since the curve was plotted only for volumes above end-expiratory level and for pressure higher than
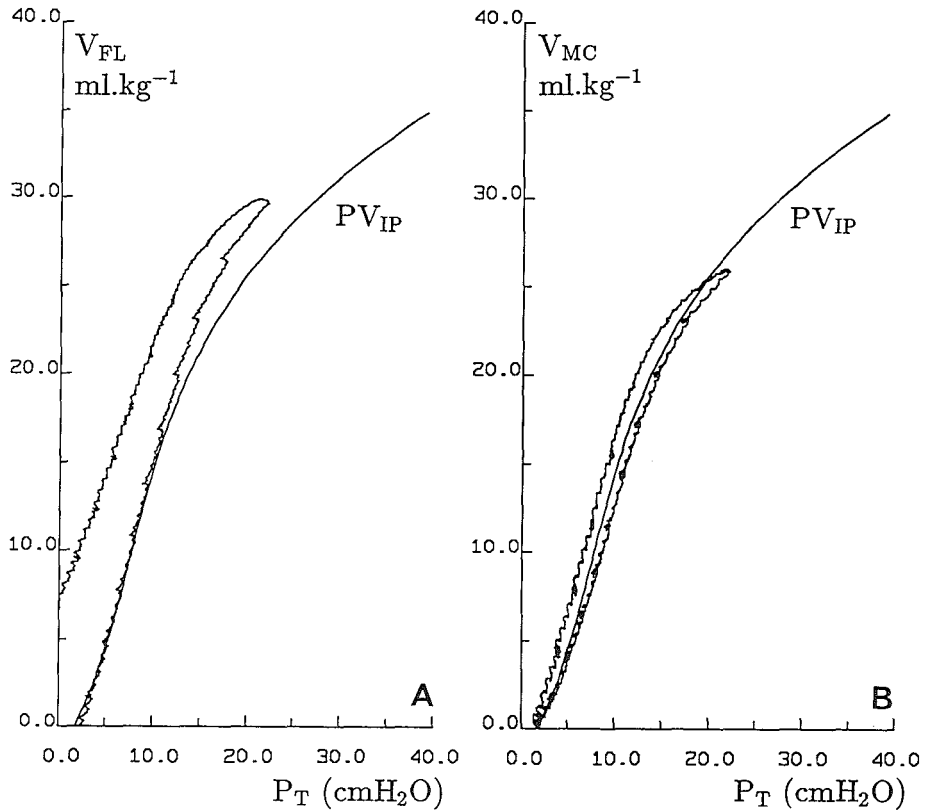
Figure 5.3 Slow inflation deflation procedures.

A) Pressure-volume loop obtained from a typical stepwise SID2 procedure. In this plot changes in volume were derived from integration of the airflow. The pressure starts at PEEP level and ends at a positive intercept on the volume axis ('unrecovered volume'). The single line (PV_{IP}) is the quasi-static pressure-volume curve derived from 22 inspiratory pause procedures.

B) The same SID2 procedure as in figure 5.3A. However, in this P-V curve changes in volume were derived from the mercury strain gauge. The single line is again the same quasi-static pressure volume curve as in panel A.
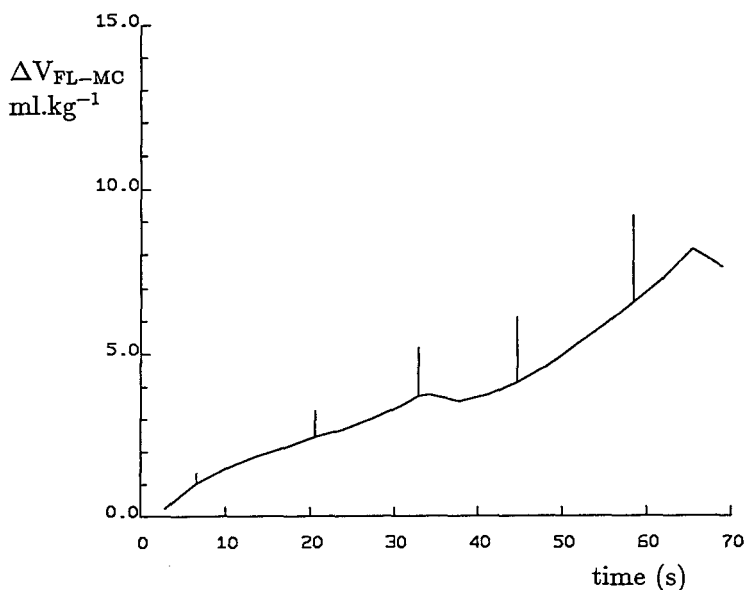
Figure 5.4 Difference between the volume estimates during SID procedures.
The difference between the change in volume derived from integration of the airflow and
the change in volume based on the mercury strain gauge ΔV_{FL-MC} as a function of time.
The vertical lines are standard deviations at the respective positions in the curve.

zero, i.e. higher than ambient air pressure, this last phase of deflation is
beyond the scope of Fig. 5.3A and B.

The amount of hysteresis was 160 ± 67 (SD) cm H_2O.ml.kg^{-1} (n=16),
when volume changes were based on V_{FL}. When the changes in volume
were based on V_{MC} this value decreased to 88 ± 43 (SD) cm H_2O.ml.kg^{-1}
(n=16). Because of the passive expiratory phase in the SID1 procedures,
these procedures could not be used to calculate the amount of hysteresis.

Fig. 5.4 shows the average differences between the estimated changes in
lung volume based on ΔV_{FL} and the actual changes in lung volume ΔV_{MC}
during inflation and deflation as a function of time for all P-V loops (i.e. the
SID2 and SID3 procedures). During inflation and the subsequent deflation
a gradually increasing difference in volume was found.

5.3.3 *Comparison of compliance estimates*

The choice of the volume interval between 4 and 12 ml.kg^{-1}, used in all
comparisons of compliance estimates in the present study was based on
1) the nonlinear increase in the difference in pressure between the dynamic

and the quasi-static pressure-volume curves at corresponding volumes above approximately 15 ml.kg^{-1} (Fig. 5.2B) and 2) the nonlinearity in the quasi-static pressure-volume curve as such.

The mean values of compliance obtained from the pulse method, the slow inflation-deflation method and the multiple inspiratory pause method ($C_{IP,sl}$), all normalized to body weight (ml.cm H$_2$O^{-1}.kg^{-1}), are shown in Table 5.1.

We obtained similar values of C_{INFL} from the SID procedures 1, 2 and 3 for the measurements based on integration of the airflow and those based on the mercury strain gauge. C_{DEFL} estimates derived from SID2 and SID3 were mutually similar for each of the two volume measurements. In the SID1 procedures C_{DEFL} could not be determined because in those procedure the pigs were allowed to breathe out passively. Therefore, we have averaged three C_{INFL} estimates and two C_{DEFL} per series for each type of volume measurement.

When *integration of the airflow* was used to determine the change in lung volume, C_{DEFL} was smaller than C_{INFL} and $C_{IP,sl}$ in all experiments. However, C_P and C_{INFL} were not significantly different from $C_{IP,sl}$.

When the *mercury strain gauge* was used the compliance estimates C_{INFL}, C_{DEFL} and C_P were not significantly different from each other. Pulse compliance was significantly lower ($p \leq 0.05$) than $C_{IP,sl}$. No significant differences were found between C_{INFL}, C_{DEFL} and $C_{IP,sl}$.

5.4 Discussion.

5.4.1 *Pulse method*

Considering the dependence on time of tracheal pressure during an inspiratory pause in particular at large inflation volumes, one of the basic assumptions, i.e. the absence of viscoelastic pressure [10,89,97], was not fulfilled in our analysis of the 'pulse compliance' C_P. This is probably the reason for the slight underestimation of compliance by the pulse method in comparison with $C_{IP,sl}$.

Reduction of the maximal flow rate from 10 ml.s^{-1}.kg^{-1} to 5 ml.s^{-1}.kg^{-1} did not change the estimate of C_P significantly. The nonlinear increase in airway pressure during inflations with constant flow rate up to inflation volumes larger than about 15 ml.kg^{-1} probably points to 1) an over-distention of the lungs [101] and 2) an increase of viscoelastic forces. This latter conclusion is confirmed by the results in Fig. 4.4, in which the pressure fall occurring after inflation of large volumes did not coincide with the PV$_{IP}$

TABLE 5.1

Pig	$C_{IP,sl}$	C_P		C_{INFL}		C_{DEFL}	
	ΔV_{MC}	ΔV_{FL}	ΔV_{MC}	ΔV_{FL}	ΔV_{MC}	ΔV_{FL}	ΔV_{MC}
1A	1.63	1.46	1.39	1.58	1.51	1.50	1.86
	(0.07)	(0.06)	(0.05)	(0.10)	(0.11)	(0.01)	(0.08)
1B	1.70	1.45	1.48	1.58	1.46	1.38	1.67
	(0.09)	(0.06)	(0.07)	(0.07)	(0.09)	(0.01)	(0.01)
2A	1.91	1.75	1.63	2.12	1.73	1.31	1.60
	(0.06)	(0.09)	(0.03)	(0.03)	(0.04)	(0.01)	(0.02)
2B	1.89	1.75	1.66	2.13	1.70	1.25	1.56
	(0.04)	(0.09)	(0.05)	(0.09)	(0.04)	(0.01)	(0.02)
3A	1.43	1.37	1.34	1.37	1.23	0.96	1.18
	(0.03)	(0.06)	(0.05)	(0.02)	(0.01)	(0.02)	(0.02)
3B				1.60	1.41	0.97	1.29
				(0.03)	(0.04)	(0.10)	(0.02)
4A	1.63	1.36	1.32	1.57	1.31	1.01	1.46
	(0.05)	(0.05)	(0.03)	(0.11)	(0.01)	(0.11)	(0.10)
4B	1.14	1.10	1.08	1.49	1.20	0.85	1.06
	(0.14)	(0.18)	(0.15)	(0.09)	(0.10)	(0.04)	(0.04)
mean	1.62	1.47	1.42	1.68	1.44	1.15	1.46
	(0.27)	(0.24)	(0.20)	(0.28)	(0.20)	(0.23)	(0.26)
	n=7	n=78	n=78	n=24	n=24	n=16	n=16

Comparison of compliance estimates.

In this table compliance estimates according to the pulse method C_P, and the slow inflation-deflation method (C_{INFL} and C_{DEFL}) are presented. To enable an easier comparison we also show the $C_{IP,sl}$ values, which were already presented in Table 4.1. Values are given in $ml.cmH_2O^{-1}.kg^{-1}$. The standard deviations are given in parentheses.

curve, except for the pressure-volume point at 8.5 s in the inspiratory pause. This was mainly attributed to viscoelasticity.

5.4.2   *Slow inflation-deflation method*

The flow rate in the slow inflation-deflation procedures was a compromise between the inflation volume of 25 $ml.kg^{-1}$ recommended in the literature [14] and the necessity to limit the duration of the entire procedure to prevent severe hypoxemia. The flow rate of 0.7 $ml.s^{-1}.kg^{-1}$ which was selected in all procedures was close to the flow rate of 0.5 $ml.s^{-1}.kg^{-1}$ ($=2$ $l.min^{-1}$) reported in studies on humans [14,43,68].

In most studies slow inflation-deflation procedures were performed after one or a series of large inflations to 'standardize' lung volume history. We did not perform any special lung volume standardizing procedure before measuring a slow inflation-deflation procedure, because of the large tidal volume during our mode of mechanical ventilation. This tidal volume, which was about 20.7 $ml.kg^{-1}$, was the consequence of the rather low ventilatory frequency of 10 min^{-1}. Moreover, we could not demonstrate any significant increase in compliance derived from the inflation limb of P-V curves in the first two procedures per series (SID1 and SID2), in contrast with other studies [15,45,68].

In this study an increasing difference is demonstrated between the change in lung volume estimated by integration of the airflow and the actual change in lung volume during slow inflation-deflation procedures. This difference has been attributed to gas exchange possibly in combination with changes in intra-thoracic blood volume [30]. A detailed analysis of the decrease in lung volume during an inspiratory pause due to continuous gas exchange is presented in the next chapter. The present study supports the findings of Gattinoni et al. [30] and D'All-Ava Santucci et al. [21], i.e. pressure-volume loops, hysteresis calculations and compliance estimates may give erroneous results, if they are derived from changes in lung volume measured at the airway opening instead of from changes in volume based on e.g. a mercury strain gauge.

The measurement of a P-V loop based on the measurement of the change in thoracic volume is rather complicated, particularly because of difficulties in obtaining an accurate calibration. Other disadvantages of the slow inflation-deflation procedure are potential risks of barotrauma, temporary haemodynamic instability, and hypoxemia. However, in our experiments the compliance estimates derived from the slow inflation-deflation procedures,

based on the change in thoracic volume, were not significantly different from $C_{IP,sl}$. The multiple inspiratory pause method to obtain $C_{IP,sl}$ is rather simple. Therefore, we prefer this method for the estimation of C_{RS}.

In summary we conclude that:

1. the 'pulse' method underestimates total respiratory compliance $C_{IP,sl}$ derived from the quasi-static P-V curve

2. the compliance estimates C_{INFL} and C_{DEFL}, derived from slow inflation-deflation procedures, yield values similar to $C_{IP,sl}$, provided the actual change in lung volume is measured (e.g. by means of a mercury strain gauge) and

3. the multiple inspiratory pause method $(C_{IP,sl})$ has to be preferred for the estimation of C_{RS}.

CHAPTER 6

THE LOSS OF LUNG VOLUME
BY GAS EXCHANGE DURING
AN INSPIRATORY PAUSE

6.1 Introduction.

The estimation of C_{RS} during artificial ventilation by the inspiratory pause method was based on the assumption of a stable plateau pressure. However, it was demonstrated in Chapter 4 that both tracheal pressure and intra-thoracic volume gradually decreased during the entire inspiratory pause. We ascribed the loss of lung volume to a continuous gas exchange at a respiratory exchange ratio less than 1.0. We observed the rate of decrease in lung volume to be inversely dependent on the volume of inflation, implying a large decrease at low inflation volumes and a markedly smaller loss of volume at large inflation volumes.

We hypothesized the large loss of volume at a small lung volume to be almost equal to oxygen consumption due to an equilibration between alveolar and mixed venous P_{CO_2}. At large volumes we assumed the uptake of oxygen from the alveoli into the blood partially compensated for by a sustained CO_2 exchange from the blood into the alveoli.

To test the hypothesis of a difference in loss of lung volume due to a difference in gas exchange we studied alveolar gas exchange during rebreathing cycles superimposed on inspiratory pause periods of 20 s at three different tidal volumes.

A potential problem in the quantitative comparison of the rebreathing technique superimposed on the inspiratory pause periods with the original inspiratory pause procedure in our former studies (cf. Chapter 4) could be the effect of the cyclic variation of lung volume on the gas exchange during rebreathing. Therefore, inequality of the loss of lung volume in both circumstances does not plead against the validity of the hypothesis. As a strict condition for verification we demanded the loss of lung volume to be of the same order of magnitude in both circumstances.

6.2 Methods.

6.2.1 *Surgical procedures and measurements*

Experiments were performed on 6 healthy piglets (weight 9.0 ± 0.9 (SD) kg). Surgical procedures, experimental conditions, data-acquisition and measurements were the same as described in Chapter 4. Only the additional methods are mentioned in this section.

End-expiratory lung volume $V_{L,EE}$ was estimated with the use of a closed system helium dilution technique. This technique was described in Chapter 3, page 38.

Respiratory exchange ratio R and oxygen consumption ($\dot{V}_{O_2}$) during base line mechanical ventilation were derived from the tidal volume and the inspiratory and mixed-expiratory gas concentrations during steady state baseline conditions. $\dot{V}_{O_2}$ was corrected for differences between the inspired and expired volumes, based on the assumption of a constant amount of N_2 in the lungs [81].

The animals were ventilated mechanically with a gas mixture of 40 % O_2 and 60 % N_2. At the beginning of each experiment tidal volume of normal mechanical ventilation was adjusted to achieve an arterial CO_2 tension (P_{a,CO_2}) between 35 and 45 Torr. After stabilizing P_{a,CO_2} tidal volume was kept constant at 22.4 ± 2.3 ml.kg^{-1}, (n=6) with a fixed respiratory rate of 10 per min and with an inspiration-expiration time ratio of 40:60. During the experiments a PEEP of about 2 cm H_2O was applied to avoid atelectasis.

6.2.2 *Ventilatory procedures*

Ventilator. Although the functioning of the ventilator has been described in Chapter 3 some features are repeated here to simplify the description of the rebreathing manoeuvres. Ventilation could be performed either by bellows 1 or by bellows 2 (Fig. 3.1 on page 24). In normal mechanical ventilation bellows 1 was used whereas bellows 2 was in flush mode. During the inspiratory phase the piston plate moved towards its front position. Because of the state of the valves (1A and 1C closed and 1B open) gas was driven out of the bellows 1 in the direction of the animal. During the expiratory phase valve 1C was open and provided a way for a passive expiration through a water seal, which was used for application of PEEP.
Rebreathing procedures. We modified the method previously described by Lanphier and Rahn [61] and Hong et al. [44] for spontaneously breathing subjects. The original method consisted of a period of breath holding

interrupted at intervals of 10-30 s by short expirations into a sampling bag followed by inspirations of the expired gas ('rebreathing'). The volume of this 'rebreathing'-gas was chosen large enough to obtain alveolar samples at end-expiration. The total period lasted for about 1 to 4 min.

To calculate the decrease in lung volume by gas exchange we studied the changes in composition of alveolar gas during a 20 s rebreathing period. We further adapted the method by shortening the time interval between the expirations to 2 s, which means a rebreathing ventilation at a rate of 30 per min. The rebreathing volume was 13.2 ml.kg^{-1}. The selection of this volume was partly due to a technical problem in the first experiment of the series of six, which caused the rebreathing volume to be about 30 % larger than was intended. We used the same volume in the other experiments for easier comparison of our experimental results in all six experiments.

The rebreathing procedures were performed at three different volume levels above end-expiratory lung volume. After a period of at least 10 min of normal mechanical ventilation, with bellows 1 of the ventilator, the procedure was started with an inflation (V_{RB1}) of either a small volume of 6.6 ml.kg^{-1}, a medium volume of 19.8 ml.kg^{-1} or a large volume of 33.0 ml.kg^{-1}, by bellows 2 of the ventilator. Inflation time was 2.5 s. The volume-time course of a rebreathing procedure at medium volume is presented in Fig. 6.1a. The gas mixture in the first inflation of the rebreathing procedure was the same as the gas mixture used during normal mechanical ventilation. During the rebreathing procedure bellows 1 was in 'flush' mode (1B and 1C closed, 1A open).

Immediately after the initial inflation the piston plate of the ventilator started a cyclic movement (one cycle in 2 s) with the same valve states as during the inflation, causing a cyclic variation of lung volume. In this way a volume V_{RBR} (13.2 ml.kg^{-1}) was rebreathed at three volume levels above end-expiratory lung volume. Although lung volume varied cyclically during the rebreathing period the volume level of rebreathing was defined as the average volume above the end-expiratory level, i.e. the initial level of rebreathing was equal to the difference between V_{RB1} and $0.5 \times V_{RBR}$. Therefore, rebreathing procedures were performed at volume levels of about 0.0, 13.2 and 26.4 ml.kg^{-1} above end-expiratory volume (i.e 6.6 - 0.5×13.2 = 0, 19.8 - 6.6 = 13.2 and 33.0 - 6.6 = 26.4 ml.kg^{-1}).

From the changes in composition of alveolar gas measured at the end of each deflation during the rebreathing procedure the decrease in lung volume due to gas exchange could be estimated based on the assumption of a constant amount of N_2.
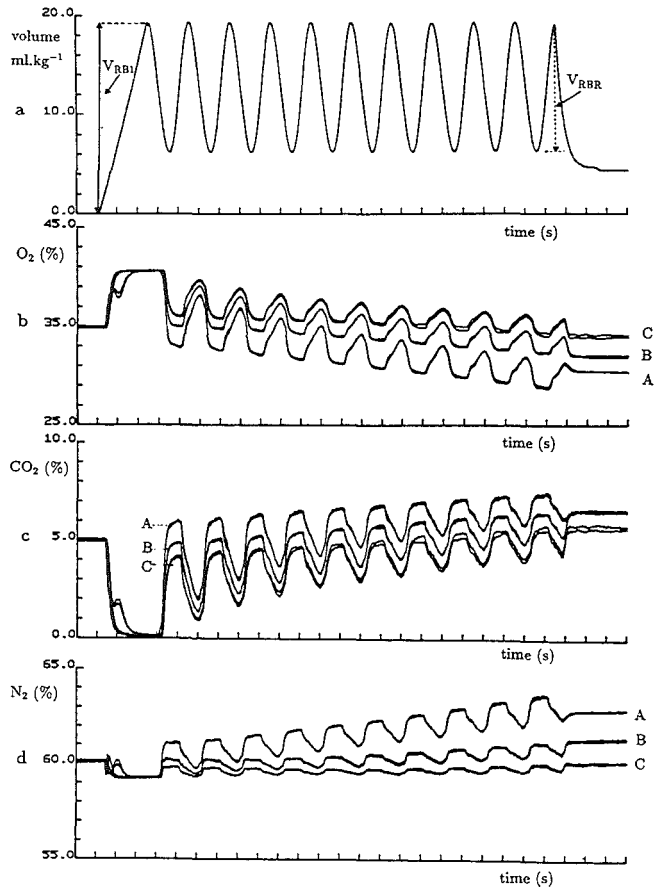
Fig. 6.1 Tracings of gas concentrations during rebreathing.

This figure shows the volume-time course of a rebreathing procedure at medium volume level (panel a) as a reference for the concentrations of the gases O_2, CO_2 and N_2 in panels b, c, and d respectively in 2 different rebreathing procedures at three different volume levels. Plotting of the signals was started 1 s before the first inflation in the rebreathing procedure V_{RB1}. After the first inflation rebreathing was performed during 10 cycles with a cycle time of 2 s.

(A): rebreathing at low volume level,

(B): rebreathing at medium volume level,

(C): rebreathing at high volume level.

After 20 s of rebreathing (10 cycles) the piglet was allowed to breathe out passively and normal mechanical ventilation was automatically resumed by bellows 1.

Inspiratory pause procedures. In the same experiments we performed procedures with an inspiratory pause (inflation volume 0-30 ml.kg^{-1}, inflation time 2.5 s, inspiratory pause 15 s). The aim of these procedures was 1) to compare the decrease in thoracic volume during inspiratory pauses with the loss of lung volume in the rebreathing procedures at corresponding volume levels above end-expiratory lung volume, 2) to calibrate the mercury strain gauge, and 3) to estimate $C_{IP,sl}$ (cf. Chapter 4, section 4.2.5).

During the inspiratory pauses the extra valve, which was positioned at the tracheal cannula was closed (cf. section 4.2.4). In contrast to the rebreathing procedures the mass-spectrometer did not sample gas from the airways during the inspiratory pause procedures, because we did not want to loose pulmonary volume by airflow to the mass-spectrometer.

6.2.3 *Observations*

After a stabilization period after surgery of at least 30 min the observations were started with base line measurements including determinations of $V_{L,EE}$. Then, a series of 12 inspiratory pause procedures was performed in a random sequence. Between the procedures normal mechanical ventilation was resumed for 5 min. In the next hour the three rebreathing procedures were performed twice at 10 min intervals, i.e. one measurement each 10 min. These measurements were followed by another set of base line measurements. Then, a second set of six rebreathing procedures, a second set of inspiratory pause procedures and again base line measurements were performed.

Ten minutes after killing the pig with an overdose of pentobarbital sodium six to eight inspiratory pause procedures were performed at different volumes at two minute intervals (cf. Chapter 7).

6.2.4 *Data acquisition and data analysis*

Estimation of the decrease in lung volume during the rebreathing procedure. The analysis of the alveolar gas exchange during the rebreathing procedure was based on the determination of the changes in the amounts of O_2, CO_2 and N_2 ($V_{O_2}{}^n$, $V_{CO_2}{}^n$, $V_{N_2}{}^n$ respectively) in the total system at each rebreathing cycle n. The first controlled deflation ($n = 1$) during the rebreathing was used as a reference for the calculation of changes in volume. The total amounts of O_2, CO_2, and N_2 at $n = 1$ were determined by adding

the amounts of these gases in each part of the rebreathing system, i.e. in A) the bellows nr. 2 of the ventilator, B) the tubing between lungs and ventilator and C) the lungs. All volumes were converted to STPD values.

The total amount of gas in bellows 2 at the end of a controlled deflation equals the sum of the dead space (Vd,bellows) in the bellows (ranging from 41.2 to 77.7 ml in the different experiments) and the rebreathing volume V_{RBR}. The volumes of the respiratory gases were estimated by multiplying the total volume in the bellows by the respective gas concentrations in the bellows, the latter being assumed to be equal to the concentrations measured during the subsequent inflation.

The O_2, CO_2 and N_2 volumes in the tubing were estimated by multiplying the effective tubing dead space (Vd,eff=29 ml) in these experiments, cf. Chapter 3 page 40, by the concentrations of each of the gases in the tubes. These concentrations were assumed to be approximately equal to the concentrations averaged between inflation and deflation.

The total lung volume V_L at the end of the first controlled deflation of the rebreathing procedure was calculated by adding the net insufflated volume (i.e. the insufflated volume V_{RB1} less V_{RBR}) to the end-expiratory lung volume. We took the mean value of the lung volume measurements before and after the series of rebreathing procedures as steady state end-expiratory lung volume level during the series.

The same calculation was performed for each cycle in the rebreathing procedure. However, it was assumed that the total amount of N_2 in the system ($V_{N_2}{}^{n=1}$) calculated at the first deflation remained constant during the subsequent rebreathing cycles [44,60,73], except for a small loss of N_2-volume due to the sampling of the mass-spectrometer.

In summary (Fig. 6.2), V_{N_2} was calculated for each deflation n from

$$V_{N_2}^n = (Vd,bellows + V_{RBR}).F_{I,N_2}^n + Vd,eff.\frac{1}{2}.(F_{I,N_2}^n + F_{E,N_2}^n) + (V_L^n).F_{E,N_2}^n \qquad (1)$$

where F_{I,N_2}, F_{E,N_2}: inspiratory and end-expiratory fractions of N_2. $V_L{}^{n=1}$ was calculated from

$$V_L^{n=1} = V_{L,EE} + (V_{RB1} - V_{RBR}) \qquad (2)$$

If necessary, the value V_L^n was adapted to satisfy the condition of a constant V_{N_2} in the total system during the rebreathing cycles $n=2\ldots10$

Changes in the amounts of O_2 and CO_2, ΔV_{O_2} and ΔV_{CO_2} respectively, between every two subsequent controlled deflations during the rebreathing period, i.e. in time intervals $\Delta t_{RBR}=2.0$ s, were used to estimate the oxygen uptake ($\Delta V_{O_2}/\Delta t_{RBR}$), the CO_2 output ($\Delta V_{CO_2}/\Delta t_{RBR}$) and the respiratory exchange ratio $R = \Delta V_{CO_2} / \Delta V_{O_2}$. In this analysis all volume changes
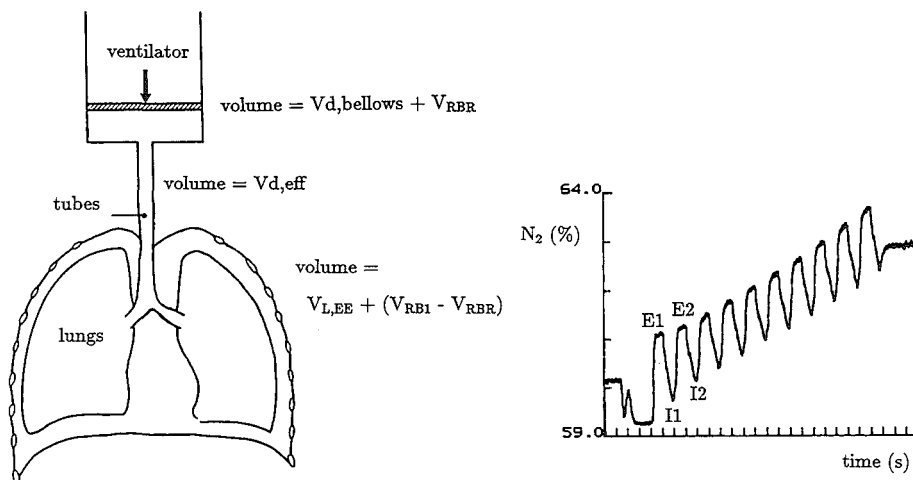
Fig. 6.2 Schematic presentation of the rebreathing analysis.
In this figure the calculation (equation 1) of the amount of N_2 in the system is illustrated. The inspiratory and end-expiratory N_2 fractions F_{I,N_2} and F_{B,N_2} are abbreviated as I1, I2 and E1, E2 respectively for the cycles $n = 1$ and $n = 2$ in the figure. For explanation see text.

were corrected for the loss of O_2, CO_2 and N_2 due to the sampling by the mass-spectrometer. Using ΔV_{O_2} and ΔV_{CO_2} the change in lung volume caused merely by gas exchange could be calculated.

6.2.5   *Statistical analyses*

Comparison of two empirical means of populations, which were assumed to be normally distributed, was performed using the two sample t-test for independent random samples (Sachs pg. 265 [91]). The comparison of the three different levels of rebreathing was performed using an analysis of variance and a technique of multiple comparison according to Student, Newman and Keuls [91]. In both tests differences were considered significant only when the p value was equal to or less than 0.05.

6.3   Results.

6.3.1   *General data*

In Table 6.1 the average values of the end-expiratory lung volume ($V_{L,EE}$), tidal volume (V_T), weight, total respiratory compliance ($C_{IP,sl}$), steady state

TABLE 6.1

Weight	9.0	(0.9)	kg	$n=6$	
$V_{L,EE}$	26.6	(4.0)	$ml.kg^{-1}$	$n=12$	BTPS
V_T	22.4	(2.3)	$ml.kg^{-1}$	$n=6$	BTPS
R	0.92	(0.06)		$n=39$	
$\dot{V}_{O_2}$	0.14	(0.01)	$ml.kg^{-1}.s^{-1}$	$n=39$	STPD
$C_{IP,sl}$	2.25	(0.13)	$ml.cm\ H_2O^{-1}.kg^{-1}$	$n=12$	BTPS

General data of the animals.

Values in parentheses are standard deviations.

oxygen consumption $(\dot{V}_{O_2})$ and steady state respiratory exchange ratio (R) are listed.

Lung volume estimates after each series of inspiratory pause procedures and rebreathing procedures were usually slightly higher than estimates of lung volume before the series. The maximal observed difference was 23.5 ml in experiment 2. Since $V_{L,EE}$ was 250 ml in that experiment this difference was less than 10%. We checked the influence of such differences in lung volume on the calculation of the decrease in volume due to gas exchange during a rebreathing procedure. When calculations were performed with a 10 % larger value of $V_{L,EE}$ the estimated loss of lung volume due to continuous gas exchange increased about 6 %. Therefore, we considered $V_{L,EE}$ sufficiently stable to perform our analyses

6.3.2 *Gas concentrations during rebreathing procedures*

Fig. 6.1 shows the respiratory gas concentrations O_2, CO_2 and N_2 as functions of time in panels b, c and d respectively. Both tracings of each gas concentration, obtained during the rebreathing procedures, were similar for the same volume level. However, at the three different volume levels they diverged from each other. This was observed in all corresponding observations. The lower the lung volume during rebreathing the higher the increase in concentration of CO_2 and N_2. The decrease in O_2 concentration was more prominent at low volume levels than at large volume levels.

6.3.3 *O_2 uptake, CO_2 output and respiratory exchange ratio (R)*

The oxygen uptake $\dot{V}_{O_2}$, the CO_2 output $\dot{V}_{CO_2}$ and the respiratory exchange ratio $(R = \Delta V_{CO_2}\ /\ \Delta V_{O_2})$ are presented as functions of time in Fig. 6.3,

in panels a, b and c respectively. The tracings A, B and C were derived from rebreathing procedures at low, medium and high volume levels of rebreathing respectively. Each point in that figure represents the mean value of 24 observations, i.e. 4 per animal. The start of the first inflation of the rebreathing procedure was chosen as $t = 0$. Again a divergence was found between the tracings of rebreathing procedures at different volume levels. Oxygen uptake during rebreathing was significantly different between the three different volume levels in the first 6 of the 9 values of $\dot{V}_{O_2}$ with the larger values for the oxygen uptake during rebreathing procedures at low inflation volumes. The opposite was observed for CO_2 output, which tended to be higher for rebreathing at larger inflation volumes. This tendency was only significant for the last 5 (of the 9) estimates of CO_2 output.

Combination of both oxygen uptake and CO_2 output yielded values for the respiratory exchange ratios which were significantly different for rebreathing procedures at different volume levels. The respiratory exchange ratio was lower during rebreathing at low volumes than during rebreathing at large inflation volumes.

6.3.4 Decrease in lung volume during rebreathing

The decrease in lung volume caused by continuous gas exchange was estimated from the increase in N_2-concentration. Then, the net loss of lung volume ΔV_L was calculated using the oxygen uptake $\dot{V}_{O_2}$ and the CO_2 output $\dot{V}_{CO_2}$. The ΔV_L values are presented in Table 6.2.

In Fig. 6.4 the decrease in lung volume during rebreathing procedures at low (panel a), medium (panel b) and high (panel c) volume levels above the end-expiratory volume level is presented (dash-dotted lines). The decrease in lung volume during rebreathing was larger for lower inflation volumes.

6.3.5 Decrease in lung volume during inspiratory pause procedures

The decrease in lung volume during the inspiratory pauses as such, as obtained from the mercury strain gauge, was measured on points of time corresponding to those in the rebreathing procedures. That is, we have determined the intra-thoracic volume (with respect to the end-expiratory level) at 7 points of time $(t_1 \ldots t_7)$, each at the moment the controlled deflation in the corresponding rebreathing procedure had ended. From these 7 values 6 volume differences were calculated with respect to the volume at t_1.

We corrected these values for the small changes in volume observed during post mortem manoeuvres at corresponding inflation volumes. During
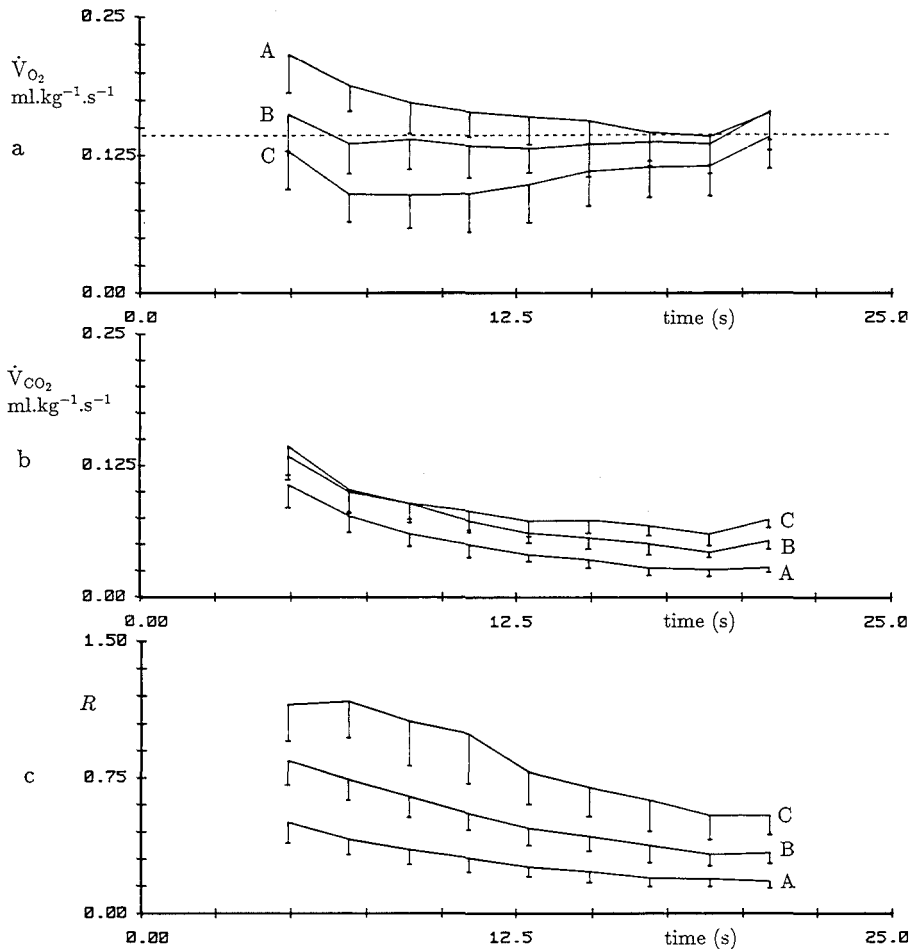
Fig. 6.3 O_2 uptake, CO_2 output and respiratory exchange ratio R.

Oxygen uptake $\dot{V}_{O_2}$ (panel **a**) was obtained by calculating the ratio $\Delta V_{O_2}/\Delta t_{RBR}$ per rebreathing cycle. CO_2 output $\dot{V}_{CO_2}$ was derived similarly from ΔV_{CO_2} (panel **b**). The values are expressed at STPD. Vertical lines are standard deviations (n=24). The steady state oxygen consumption during normal mechanical ventilation averaged over all experiments is indicated by the dotted line. The respiratory exchange ratio R (panel **c**) was derived from the ratio $\Delta V_{CO_2}/\Delta V_{O_2}$. Zero time was taken at the start of the first inflation in the rebreathing procedure. A, B and C: rebreathing at low, medium and high volume level, respectively

TABLE 6.2
Decrease in lung volume during an inspiratory pause and during rebreathing.

	Time	low volume			medium volume			high volume		
		ΔV_L rebr. ml.kg^{-1}	ΔV_L IP ml.kg^{-1}		ΔV_L rebr. ml.kg^{-1}	ΔV_L IP ml.kg^{-1}		ΔV_L rebr. ml.kg^{-1}	ΔV_L IP ml.kg^{-1}	
	s	n=24	n=24		n=24	n=24		n=24	n=24	
t_1	03.9	0.00 (0.00)	0.00 (0.00)		0.00 (0.00)	0.00 (0.00)		0.00 (0.00)	0.00 (0.00)	
t_2	05.9	-0.22 (0.08)	-0.30 (0.16)	*	-0.06 (0.05)	-0.10 (0.06)		0.03 (0.04)	-0.02 (0.06)	*
t_3	07.9	-0.44 (0.13)	-0.71 (0.22)	*	-0.13 (0.09)	-0.20 (0.09)		0.05 (0.07)	-0.01 (0.10)	
t_4	09.9	-0.67 (0.18)	-1.02 (0.30)	*	-0.23 (0.13)	-0.32 (0.12)		0.05 (0.10)	-0.02 (0.15)	
t_5	11.9	-0.90 (0.23)	-1.34 (0.30)	*	-0.36 (0.18)	-0.44 (0.16)		0.04 (0.15)	-0.05 (0.20)	
t_6	13.9	-1.14 (0.28)	-1.68 (0.34)	*	-0.50 (0.22)	-0.62 (0.20)		-0.02 (0.19)	-0.09 (0.25)	
t_7	15.9	-1.39 (0.32)	-1.93 (0.39)	*	-0.66 (0.26)	-0.79 (0.25)		-0.09 (0.24)	-0.16 (0.29)	

$t_1 \ldots t_7$: points in time after the start of insufflation both for the rebreathing procedures and the inspiratory pause procedures. ΔV_L (rebr.) is the decrease in lung volume caused by gas exchange, derived from the rebreathing analysis. ΔV_L (IP) is the decrease in lung volume during an inspiratory pause based on the mercury cord around the thorax. Values in parentheses are standard deviations. The sign * is added when the values were significantly different at $p \leq 0.05$.
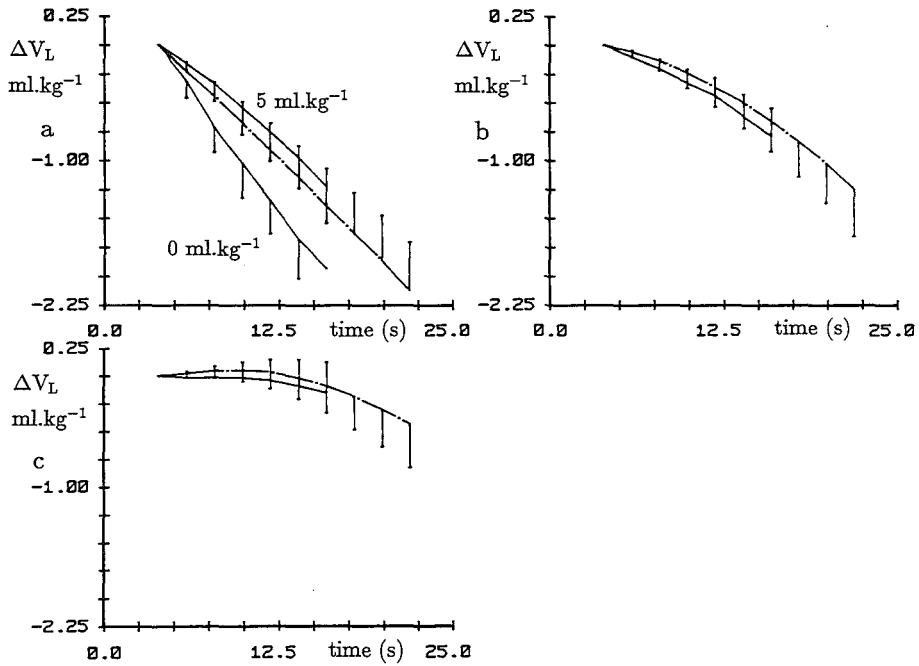
Fig. 6.4 Decrease in lung volume during rebreathing and during inspiratory pauses at different volumes.

Panels **a**, **b** and **c** show the decrease in lung volume at low, medium and high volume levels above end-expiratory lung volume respectively. In each panel the continuous line represents the average changes in lung volume detected by the mercury strain gauge during inspiratory pauses. In panel a the loss of volume during an inspiratory pause at 5 ml.kg^{-1} is presented too. The changes in lung volume during rebreathing procedures, estimated from oxygen uptake $\dot{V}_{O_2}$ and CO_2 output $\dot{V}_{CO_2}$ are also shown in each panel (dash-dotted lines). Vertical bars indicate the standard deviations.

inspiratory pauses which were performed post mortem we did not detect a significant decrease in lung volume ($\Delta V_{1...7}$) between t_1 and t_7 at low volumes (inflation 0 ml.kg^{-1}: $\Delta V_{1...7}$ = -0.07 ± 0.09 (SD) ml.kg^{-1}, n=6) and at medium volumes (inflation 13 ml.kg^{-1}: $\Delta V_{1...7}$ = 0.00 ± 0.10 (SD) ml.kg^{-1}, n = 6). However, at large inflation volumes (26 ml.kg^{-1}) a small decrease in lung volume was generally observed $\Delta V_{1...7}$ = -0.23 ± 0.11 (SD) ml.kg^{-1}, n = 18. This decrease in lung volume was thought to be caused by a small redistribution of blood from the thoracic into the abdominal compartment. This assumption was based on preliminary observations with two mercury strain gauges, one around the rib cage the other around the abdomen. We assumed that the same redistribution took place 'in vivo' and have subtracted the 'post mortem' volume decrease from the 'in vivo' decrease in intra-thoracic volume. These corrected values are presented in Fig. 6.4 (continuous lines) at each volume level and are listed in Table 6.2.

6.3.6   *Comparison of the changes in lung volume*

In Table 6.2 we have indicated the significant differences between the changes in lung volume derived from inspiratory pause procedures with the use of the mercury strain gauge and the changes in lung volume derived from the rebreathing procedures. At end-expiratory volume level the loss of lung volume during rebreathing was smaller than the loss of lung volume during the pause procedure. At the medium and high lung volume the decrease in volume during inspiratory pauses and during rebreathing procedures was not significantly different. Thus, at these volume levels the loss of volume during inspiratory pauses was equal to the loss of volume estimated from the gas exchanges during rebreathing.

6.4   Discussion.

6.4.1   *Gas exchange during breath holding*

The mechanisms affecting gas exchange during breath holding have been described in detail by Mithoefer [73] and Lanphier and Rahn [61]. Therefore, we will restrict our description to the most important aspects.

When a breath holding period is started after an insufflation the CO_2 output will be relatively large due to the low alveolar CO_2 tension (P_{A,CO_2}). Because of this input of CO_2 into the alveoli P_{A,CO_2} will rise. In the same period the amount of oxygen in the lungs is gradually decreasing due to the sustained oxygen uptake. Because of the constant amount of N_2 in the lungs

the lung volume decrease will be smaller in percentage of the initial volume than the uptake of oxygen in percentage of its initial fraction and therefore, the oxygen fraction will also decrease. During the first 20 s of breath holding, oxygen uptake is thought to remain constant [73] in the presence of a gas mixture of 40 % O_2 and 60 % N_2 in the lungs [73], provided lung perfusion is also constant. The dependence of oxygen uptake on perfusion is called circulation-limited O_2 exchange. Because of the rise in P_{A,CO_2} the gradient, i.e. the driving force for CO_2, between blood and alveolar gas will also diminish and CO_2-transfer will decrease. Therefore, the decrease in lung volume will gradually increase to the level of O_2 uptake. Another mechanism which will decrease CO_2 output will be the rise in P_{A,CO_2} by a concentrating effect due to the loss of lung volume.

6.4.2 Influence of the volume level on gas exchange

In Chapter 4 we hypothesized that the difference in gas exchange between inspiratory pause procedures at different inflation volumes is caused by

1. the difference in the volume of the first inflation, which does not contain CO_2,
2. the influence of the total lung volume on the gas exchange, and
3. the effect of the volume level, i.e. the intra-thoracic pressure on lung perfusion.

The first mechanism causes P_{A,CO_2} to start at a lower value after a larger inflation volume, which will augment CO_2 output. The absolute lung volume is important because for a given O_2 uptake and CO_2 output the changes in concentration will be more pronounced at smaller lung volumes than at larger volumes [61,50]. The effect of lung volume on gas exchange, in particular on arterial O_2-saturation, has also been described by Findley et al. [28]. These authors observed a gradual oxygen desaturation of arterial blood, during apnoeic periods of 30 s after inhalation of room air. At lower lung volumes the desaturation was more severe. Because of the higher inspiratory O_2 fraction (0.4) this effect was presumably negligible in our experiments.

During an inspiratory pause lung perfusion will be more reduced at larger inflation volumes, due to the reduced venous return caused by the higher intra-thoracic pressure as shown by Versprille and Jansen [104]. Cardiac output was about 30-50 % lower than mean cardiac output after inflations of 25 ml.kg^{-1}. Moreover, during prolonged end-expiratory pauses cardiac output was significantly higher than mean cardiac output [55]. Therefore,

we supposed the higher oxygen uptake during rebreathing at low inflation volumes to be a consequence of the higher lung perfusion. In accordance with Mithoefer et al. [73] and Hong et al. [44] we do not assume a change in metabolic oxygen consumption during the short (30 s) periods of rebreathing, and we consider the changes in oxygen uptake as non steady state effects caused by the temporary changes in blood flow due to the imposed inflation and rebreathing cycles.

6.4.3 Rebreathing and inspiratory pause

We used the rebreathing procedures for the estimation of the decrease in lung volume during inspiratory pause periods. These rebreathing procedures were similar to the procedures performed by Lanphier and Rahn [61] and Hong et al. [44]. In their experiments spontaneously breathing subjects were asked to breathe out a volume of about 600 ml from either TLC-level or FRC-level into a sampling bag, immediately followed by a re-inspiration (rebreathing) of the gas from the bag. Then, after a breath holding period of 10-30 s, the rebreathing procedure was repeated.

Because our aim was to estimate changes in lung volume during inspiratory pauses of about 15 s this 'rebreathing cycle' was performed more frequently in our experiments, i.e. every 2 s. The rebreathing volume we applied $(13.2 \text{ ml.kg}^{-1})$ was about three times the physiological dead space. This dead space was estimated in mechanically ventilated piglets by van Rooyen [88] in our laboratory. We assumed the end-expiratory gas free of dead space contamination, thus, the gas concentrations reflecting alveolar gas composition [103].

During rebreathing around end-expiratory lung volume the decrease in volume was smaller than the decrease during a prolonged end-expiratory pause (Fig. 6.4a). However, the decrease in volume during rebreathing at this volume level was significantly larger than the decrease during an inspiratory pause at 5 ml.kg^{-1} (Fig. 6.4a). The difference in loss of volume between both procedures at end-expiratory lung volume could be attributed to two mechanisms.

Firstly, we suppose that the rebreathing procedure per se increased the output of CO_2 over a longer period of time in comparison with a pause at end-expiration in which P_{A,CO_2} was presumably soon in equilibrium with the mixed venous concentration. The extra CO_2 output was probably due to a cyclically changing CO_2-gradient between blood and alveolar gas. This gradient, and therefore CO_2 transfer into the alveoli, increased periodically

during rebreathing when inflation diluted alveolar gas with gas from the ventilator, which has a lower P_{CO_2} than alveolar gas.

Secondly, mean cardiac output may have been smaller during the rebreathing procedure, because during insufflation a rather large decrease in venous return occurs [104], whereas cardiac output is hardly increased above the end-expiratory level during a deflation below end-expiratory lung volume. Below end-expiratory lung volume cardiac output is constant in spite of a decreasing intra-thoracic, and thus a decreasing central venous pressure [38]. Therefore, the effect of circulation limited O_2-exchange may have been larger during rebreathing than during the prolonged expiratory pause.

Rebreathing around higher lung volumes showed a decrease in lung volume which was less different from the decrease during inspiratory pauses at corresponding volumes. At higher lung volumes we suppose the CO_2 output into the alveoli to continue longer during the inspiratory pause. However the CO_2 output during an inspiratory pause is not necessarily equal to the CO_2 output during rebreathing.

6.4.4   Conclusions

We tested the hypothesis that the decrease in lung volume during an inspiratory pause depends on a difference between CO_2 output and O_2 uptake. The relevant findings for this test were the following.

1. During a rebreathing procedure lung volume gradually decreased, showing a change in the same direction as the change in lung volume during an inspiratory pause.

2. This decrease in lung volume was due to the difference in exchange between oxygen and carbon dioxide.

3. This difference was more prominent at lower lung volumes.

4. During rebreathing at the lowest volume level the decrease in lung volume was found to be smaller than during prolonged end-expiratory pauses (0 ml.kg^{-1} inflations). At medium and high volume levels the decrease in lung volume during rebreathing was almost equal to the decrease in volume during the inspiratory pause.

Thus, we regarded the hypothesis that the decrease in lung volume during an inspiratory pause depends on gas exchange to be verified.

CHAPTER 7

STRESS-RELAXATION IN
TRACHEAL PRESSURE

7.1 Introduction.

The marked gradual decrease in tracheal pressure as observed during inspiratory pauses (cf. Chapters 4 and 6) was attributed to viscoelasticity (stress-relaxation) and a loss of lung volume due to gas exchange.

At large inflation volumes, when the loss of lung volume was small, the gradual decay of tracheal pressure had a close similarity to that of an exponential function of time superimposed on a constant pressure level (cf. Chapter 4). We expected such an exponential decay also to be present at low inflation volumes, however, at these volumes a slow additional decrease in pressure occurred due to a rather large loss of lung volume.

In the present study we have analysed the decrease in pressure during an inspiratory pause in the absence of a loss of lung volume by performing 'post mortem' inspiratory pause procedures.

The objectives of this study were:

- to examine whether the P_T–decay could be described by a (multi)-exponential function of time and consequently whether the pressure decay could be extrapolated to a constant (static) recoil pressure of the respiratory system, corresponding to the volume of inflation,

- to consider whether such a characterization of the pressure decay could be applied in the 'in vivo' experiments.

Additionally, we separated the contribution of the lungs and that of the thorax to the total respiratory compliance and to the fall in tracheal pressure during an inspiratory pause. Therefore, we also measured intrathoracic pressure.

In order to elucidate the analysis and discussion of the 'post mortem' pressure decay some aspects concerning the modelling and description of stress-relaxation are discussed in the next section.

7.2 Stress-relaxation.

In some materials a sudden increase in strain, which is defined as the relative change in length ΔL of a material as a fraction of its resting length L_0, is associated with an initial increase in stress which is followed by a phase in which the stress asymptotically decays to a lower value (stress-relaxation). This feature has been recognized for many materials including human and animal tissues [19,45,46,47,49,62,92]. Since, a recovery in stress after a step-wise decrease in strain has also been described, some authors prefer to call this phenomenon stress-adaptation [19,92].

Stress-relaxation has been observed within the alveolar wall [29,94], in muscles and most arteries [5]. In the lungs, however, the decay in pressure after a stepwise increase in volume seems to be primarily caused (for about 70 %) by the air-liquid interface in the alveoli [46,47,62,70,77]. This was concluded from a markedly reduced stress-relaxation in excised saline filled lungs, in which the air-liquid interface was eliminated [6,8,47,62]. Moreover, viscoelastic properties were demonstrated in extracts of lung surfactant [16]. It has been postulated that the slow reversible movement of surfactant between the gas-liquid interface and the liquid sublayer is involved [48].

7.2.1 *Modelling of stress-relaxation*

Stress-adaptation, and part of the hysteresis in pressure-volume loops are considered to be phenomena which can be described by the theory of viscoelasticity. This theory combines descriptions of the properties of elasticity and viscosity [53]. However, some authors included another property which is analogous to dry friction to describe viscoelastic phenomena [24,42]. These three basic properties are defined below.
Elasticity. Elasticity is the property of a material which causes a reversible change in stress proportionally to the applied change in strain (equation 1). The relation between stress and strain is:

$$\sigma = \epsilon.\mathrm{E} \qquad (1)$$

where σ is the stress ($\mathrm{N.m^{-2}}$), ϵ the strain calculated by $\epsilon = (\mathrm{L-L_0})/\mathrm{L_0}$ ($\mathrm{L_0}$ resting length and L current length of the material (m)) and E is a constant which has been called the elastic modulus ($\mathrm{N.m^{-2}}$). An example of an elastic or Hooke element is a perfect spring, see Fig. 7.1A.
Viscosity. According to Newton's law a viscous element develops a stress σ always directly proportional to the rate of strain but independent of the
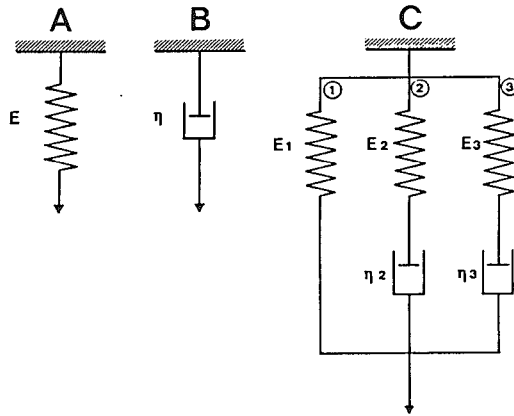
Figure 7.1. Model of viscoelasticity
An elastic element (E: 'spring', panel A) and a viscous element (η: 'dash-pot', panel B) are combined in a mechanical model of viscoelasticity (panel C), consisting of two maxwell elements and an elastic element. For explanation see text.

absolute value of the strain. The relation between the stress σ and the rate of strain $d\epsilon/dt$ is presented in equation 2

$$\sigma = \eta . \frac{d\epsilon}{dt} \qquad (2)$$

where η is the viscosity modulus (N.s.m^{-2}). An example of a mechanical element representing viscosity is the dash-pot, see Fig 7.1B.
Plasticity. Sometimes a third element is used to describe viscoelasticity. This element can be considered as a dry friction. No change in strain occurs until a certain threshold in the stress is reached. Thereafter, the element causes a constant opposing stress, which is finished when the threshold is passed in a reverse way. Due to this property the element is nonlinear.

Lorino et al. [62] demonstrated in excised rat lungs that for small pressure-volume loops the hysteresis could be explained entirely from elastic and viscous elements. However, Hildebrandt et al. [42] argued that about one-third of the lung hysteresis could be attributed to rate independent plastic strain. Although no general agreement exists about the relative contribution of these elements to viscoelastic properties of the respiratory system, the study in this chapter is confined to a linear mechanical model consisting of springs and dash-pots.

7.2.2 *Stepwise increase in strain in a mechanical model*

In an elastic element a stepwise applied strain is accompanied with a stepwise change in stress without any subsequent change in stress. In a viscous element, however, an infinite stress is associated with a stepwise strain, because $d\epsilon/dt \rightarrow \infty$. Models of viscoelasticity are all based on a combination of elastic and viscous components. From the two possible combinations of a spring and a dash-pot only the series combination, the Maxwell element, exhibits a decay in stress after a stepwise increase in strain. This decay is an exponential function of time and can be described by the mono-exponential function

$$\sigma(t) = P_1.e^{\left(\frac{-t}{\tau}\right)} \tag{3}$$

where σ is the stress in $N.m^{-2}$, P_1 is a constant $(N.m^{-2})$, and τ equals η/E where η and E are respectively viscosity and elasticity.

When the rate of extension $d\epsilon/dt$ is constant for a finite period of time, then the pressure developed in the Maxwell element is given by equation 4 during the period of extension.

$$\sigma(t) = \eta.\frac{d\epsilon}{dt}.(1 - e^{\frac{-t}{\tau}}) \tag{4}$$

Since the stress returns eventually to zero after the stepwise increase in strain this simple series combination cannot describe stress-relaxation in lungs in which pressure decays to an asymptotic level different from zero [95]. Therefore, the simplest description of stress-relaxation is the combination of a Maxwell element in parallel with a spring. If the viscoelastic properties of the lungs could be described by a model with one time constant then the area of hysteresis in small pressure-volume loops would be rate dependent, which is in contrast with studies on hysteresis in excised lungs [7,41]. Therefore, it is generally thought that two or more time constants are required for description of viscoelastic phenomena [7,41,45,62], implying a viscoelastic model with (at least) two Maxwell elements and a spring in parallel as is shown in Fig. 7.1C [20,67,108]. Such a model can account for the bi-exponential decay which has been reported in some studies on stress-relaxation [62,108]. However, the time-constants which were reported in such studies varied substantially. In a study of Nagao et al. [75] in rabbit lungs two parallel Maxwell elements were used to describe pressure adaptation. In that study the element with the shortest time constant ($\tau_1 = 30$ s), represented the 'fast' relaxation and the other element ($\tau_2 = 600$s) the 'slow' component. Lorino et al. [62] used three time constants for description of stress-relaxation curves in excised rat lungs ($\tau_1 = 0.6$ s, $\tau_2 = 6.5$s,

$\tau_3 = 95$ s). They attributed the shortest time constant mainly to a measurement artefact, the element with $\tau = 6.5$ s to tissue stress-relaxation and the longest time constant to stress-relaxation of the air-liquid interface. Sharp et al. [92] used in a different mechanical model consisting of springs and dash-pots a time constant of 5 s to describe the stress-adaptive properties of the human respiratory system.

7.2.3 *Linearity of the pressure decrease with logarithm of time*

It has been often noted that pressure decay due to stress-relaxation is linear when plotted as a function of the logarithm of time [41,45,46,93,96]. Hildebrandt [41] reported that the pressure decay in excised lungs could be described by the function

$$\frac{P(t)}{V_\mathrm{T}} = A - B.\log t \qquad (5)$$

where: V_T is tidal volume, t is time and A, B constants.

This description obviously fails both at the start $(t = 0)$ and for $t \rightarrow \infty$. Therefore, no plateau pressure can be estimated with this description of the pressure decay. The linearity of the pressure versus $\log t$ course was confirmed in our experiments. Besides, the tracheal pressure decay implied an exponential function of time superimposed on an asymptotic pressure level, predicted by the physical model shown in Fig. 7.1C. We have focused our attention to the latter description of the pressure decay.

7.3 Methods.

For the analyses of 'post mortem' stress-relaxation we used the same piglets as were used in the experiments mentioned in Chapter 6. At the end of those experiments the pigs were killed by an overdose of pentobarbital, injected intra-venously. The 'post mortem' observations were usually started ten minutes after the administration of the overdose. During this period and in between the 'post mortem' observations mechanical ventilation was continued at the same rate and volume as in the 'in vivo' situation. After the period of about ten minutes blood pressures were close to zero and no significant differences in concentration were found between inspiratory and expiratory gases, indicating absence of pulmonary gas exchange. The experimental set-up was identical to the set-up described in Chapter 6.

7.3.1 Measurements

Measurements of the changes in central venous pressure P_{cv} were used as a substitute for the changes in intra-thoracic pressure in the 'post mortem' situation. We did not use the relationship between P_{cv} and intra-thoracic pressure in the 'in vivo' studies because of the relatively large cardiac interference which was imposed on the small pressure fluctuations due to changes in lung volume. Besides, when relevant, changes in venous blood volume may cause changes in wall tension of the veins, which will jeopardize an accurate estimation of changes in intra-thoracic pressure via central venous pressure.

7.3.2 Observations

Ten minutes after killing the piglet we performed a series of 6-8 inspiratory pause procedures. The ventilatory pattern of these procedures was the same as in the 'in vivo' procedures: inflation time 2.5 s, inflation volumes ranging from 0 to 25 ml.kg^{-1} ATPD performed in a random sequence, and an inspiratory pause of 15 s. Inflation always started from the end-expiratory volume level. During the pause the extra valve X (Fig. 3.2) was used, as in the 'in vivo' observations.

End-expiratory lung volume $V_{L,EE}$ was not measured in the 'post mortem' observations. We have used the change in the signal of the mercury strain gauge between the end-expiratory level in the 'in vivo' observations and that in the 'post mortem' observations as an indication for changes in $V_{L,EE}$.

We have restricted all observations to the first 30 minutes after death in order to avoid effects of deterioration of the pulmonary tissues and alveolar lining fluid on the measurements, as well as possible.

7.3.3 Data analysis

Analysis of the tracheal pressure decay. By a semi-logarithmic plotting of the decay in P_T versus time it was observed that the pressure decay could not be described by a model with only one time-constant, see Fig 7.2. Therefore, an attempt was made to fit the pressure decay by a bi-exponential function superimposed on a constant pressure level

$$P = P_{\text{stat}} + P_1.e^{-t/\tau_1} + P_2.e^{-t/\tau_2} \tag{6}$$

where P_{stat} is the asymptotic pressure level, P_1 and P_2 are the magnitudes of the pressure decay $(cm\,H_2O)$ in the respective exponential functions and τ_1 and τ_2 are the respective time constants (s). In the analysis the first
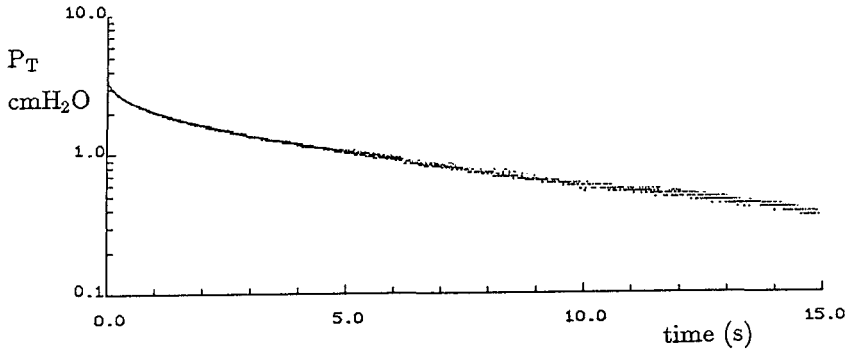
Figure 7.2. Semi-logarithmic plot of the pressure decay.
A tracing of the 'post mortem' decay in P_T with reference to the pressure estimated by exponential extrapolation of the pressure-time course during an inspiratory pause.

exponential function with parameters P_1 and τ_1 was linked to the slow decay in tracheal pressure whereas the second exponential function (P_2 and τ_2) was linked to the fast decay in pressure.

For the estimation of the 5 parameters of the bi-exponential model we used a nonlinear least squares technique suggested by Levenberg and introduced by Marquardt [65,78]. In this technique parameters are determined which minimize the quantity

$$\chi^2 = \sum_{1}^{N} (P_T(t_i) - P(t_i, P_{stat}, P_1, P_2, \tau_1, \tau_2))^2 \qquad (7)$$

where $P_T(t_i)$ are pressure values at time points t_i for i = 1...N, and $P(t_i, P_{stat}, P_1, P_2, \tau_1, \tau_2)$ is the function described in equation 6.

The Marquardt parameter estimation technique works adequately in practice and has become a standard of the nonlinear least square methods [78,107].

In the decay of the semi-logarithmic plotted P_T a part could be defined in which the decrease was approximately linear (from 6 to 15 s) in all inspiratory pause periods, which is also demonstrated in Fig. 7.2. By using a mono-exponential fitting procedure $P = P_{stat} + P_1.e^{-t/\tau_1}$ the parameters P_{stat}, P_1 and τ_1 of this function were estimated. These parameters were used as starting values for the 5-parameter fit.

95

We have limited the number of pressure data in the fit to maximally 500 in order to reduce computing time. To account for the influence of differences in time constants on the quantity χ^2 [62,107] more data points from the first part of the pressure decay were used than from the remaining part. In the fit procedure all data points from the first 1.5 s of the pressure decay (samples 1...150) were used and the remaining data points between 1.5 and 15 s (1350 samples) were compressed linearly into 350 entries. The choice of 1.5 s was arbitrary.

Goodness of fit. We quantified the goodness of fit

1. by calculating the variance s_2^2 in a short period of time (20 samples, 0.2 s) at the end of each pause. The variance was assumed to represent the variance in the pressure measurement, because pressure decrease due to stress-relaxation was sufficiently small in the considered time interval. The standard deviation of the pressure signal was estimated from $\sqrt{s_2^2}$ and was found to be about 0.02 cmH$_2$O. This standard deviation was about equal to the accuracy of the analogue to digital converter used in this study. The variance in the pressure signal was unaffected by the absolute value of the pressure as well as by the moment in the inspiratory pause.

2. by calculating the variance s_1^2 of the difference between P$_T$ and the exponential function by using all data points between 0 and 14.8 s. This variance will be close to the variance in the pressure signal if the exponential function properly fits to the pressure-decay curve. It may be considerable larger in case of a lack of fit.

3. by calculating the ratio $F = s_1^2/s_2^2$ and by testing the equality of variances s_1^2 and s_2^2.

Compliance estimates. C$_{RS}$ was estimated from the multiple inspiratory pause method (C$_{IP,sl}$), which was described in section 4.2.5. Thoracic and lung compliance were derived similarly from the quasi-static pressure-volume relationship with pressure based on P$_{cv}$ (with respect to ambient pressure) and P$_T$ minus P$_{cv}$, respectively.

The separation of lung and thoracic viscoelasticity. We did not perform the bi-exponential analysis on P$_{cv}$ because the pressure decay was relatively small and not as smooth as the P$_T$ decay.

Yet, to distinguish the contributions of lungs and thorax to the decay in P_T during an inspiratory pause, we calculated the difference in P_T between 1.5 s and 15 s and similarly for P_{cv}. We chose for 1.5 s because we assumed the pressure fall from 1.5 s to the end of the pause to be mainly caused by viscoelasticity (stress-relaxation), in contrast with the pressure fall in the first 1.5 s, which was assumed to be influenced also by other mechanisms as equilibration of gas pressures. The difference in P_{cv} between 1.5 s and 15 s was thought to be representative for the pressure decay of the thoracic compartment in that period of time. The change in the tracheal pressure was assumed to be equal to the sum of the fall in pressures in lungs and thorax, enabling the estimation of the change in pressure in the lungs.

7.4   Results.

7.4.1   Comparison of 'post-mortem' and 'in vivo' observations

$V_{L,EE}$ was lower in the 'post mortem' observations than in the 'in vivo' observations. The decrease in lung volume, 1.8 ± 0.9 (SD) ml.kg^{-1}, n = 6, was estimated from the change in end-expiratory level detected by the mercury strain gauge. This decrease in $V_{L,EE}$ was accompanied with an increased peak pressure at end-inflation in 'post mortem' ventilation compared with the 'in vivo' ventilation. The decrease in lung volume will have caused a larger change in recoil pressure for the same tidal volume due to an increase in curvilinearity of the P-V curve at low lung volume. In spite of this increase in peak-pressure, $C_{IP,sl}$ did not change significantly between the 'in vivo' and the 'post mortem' observations. In the last series of inspiratory pause procedures which was performed 'in vivo', $C_{IP,sl}$ was on average 2.1 ± 0.4 (SD) ml.cmH$_2$O^{-1}.kg^{-1} in the six experiments, whereas in the 'post mortem' observations $C_{IP,sl}$ was on average 2.3 ± 0.3 (SD) ml.cmH$_2$O^{-1}.kg^{-1}.

Because of the differences in peak pressure we checked whether the fall in pressure during the inspiratory pause was comparable in both situations. Fig 7.3 shows a tracing of P_T during a typical 'in vivo' inspiratory pause in combination with a tracing during a pause at the same inflation volume performed 'post mortem'. The pressure decay 'in vivo' was much larger than 'post mortem'.

In Fig 7.4 the fall in P_T between 1.5 and 15 s in the inspiratory pause is presented as a function of the inflation volume both for the 'in vivo' situation and for the 'post mortem' situation. The fall in P_T was larger in the 'in vivo' inspiratory pauses than in the 'post mortem' inspiratory pauses,
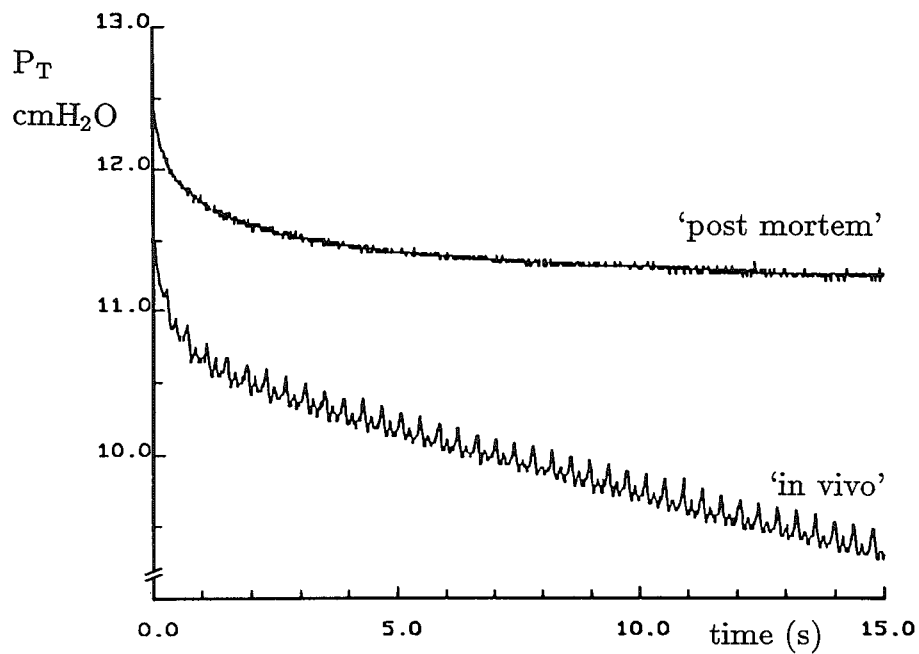
Figure 7.3. Pressure decay during an inspiratory pause.
Two tracings are presented during 'in vivo' and during 'post-mortem' circumstances respectively. The volume of inflation was 14 ml.kg^{-1} (BTPS) for both tracings.
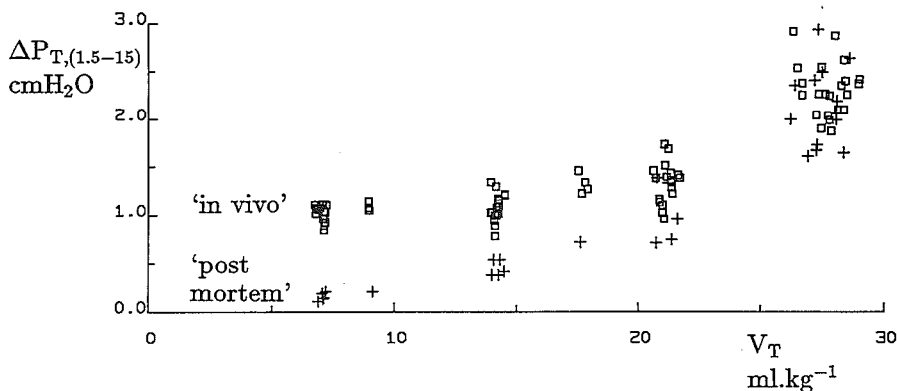
Figure 7.4. Fall in P_T between 1.5 and 15 s in an inspiratory pause.
The difference in P_T between 1.5 and 15 s in an inspiratory pause $\Delta P_{T,(1.5-15)}$ is plotted versus inflation volume V_T at BTPS conditions under 'in vivo' ($\square$) and 'post-mortem' ($+$) circumstances. For explanation see text.

in particular at low inflation volumes. We assumed this difference to be caused by the loss of lung volume in the 'in vivo' experiments. Since at large inflation volumes the difference lost statistical significance we assumed the 'post mortem' stress-relaxation to be comparable with the 'in vivo' stress-relaxation.

7.4.2   The description of the pressure decay during an inspiratory pause

A typical example of a fit of the five parameters of the bi-exponential function (equation 6) to the decay in P_T during an inspiratory pause is presented in Fig 7.5. The bi-exponential description of the P_T decay during the inspiratory pause did not always yield an acceptable fit according to the goodness of fit criterium, in particular for medium and large inflation volumes. However, a close agreement between fit and data was observed in the second half of the inspiratory pause, indicating that a reliable estimate of the asymptotic pressure level was obtained. We calculated the overestimation of P_{stat} by the pressure after an inspiratory pause of only 1.5 s from $(P_{T,1.5} - P_{stat})/(P_{stat} - P_{EE})$ similar to the analysis presented in Chapter 4, equation 1. Fig. 7.6 shows this overestimation as a function of tidal volume. At an inflation volume of 20 ml.kg^{-1} the overestimation of the asymptotic pressure level was about 10%, which is similar to the data
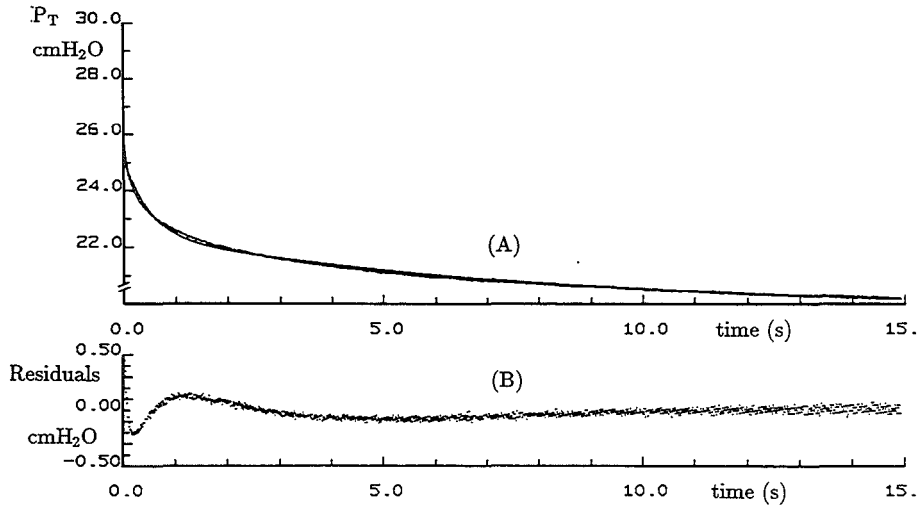
Figure 7.5. A five parameter fit of the pressure decay during an inspiratory pause. Example of a 5 parameter fit using equation 6. The P_T signal and the curve of the bi-exponential function are presented in panel A, the residual errors are presented in panel B.

presented in Chapter 4.

In Fig. 7.7 the parameters P_1, which is the 'magnitude' of slow exponential decay, and τ_1, which is the time constant of the slow decay, and the parameters P_2 and τ_2 of the fast decay are presented as functions of inflation volume.

The magnitude of the slow exponential decay P_1 (Panel A) was larger for larger tidal volumes. A similar relationship with volume was found for the magnitude of the fast decay, P_2. It has to be emphasized, however, that these parameters may be also dependent on the rate of airflow during the inflation, because inflation time was constant (2.5 s) in all procedures.

The ratio P_1/P_{stat} was larger for larger volumes, which might also be an indication for a relative increase of viscoelasticity at increasing tidal volumes. The ratio increased from about 0.04 at 5 ml.kg^{-1} inflations to about 0.15 at about 25 ml.kg^{-1} inflations.

Parameter τ_1, the time constant of the slow pressure decay, was on average 8.2 $\pm$ 2.5 (SD) s, n=30 (Panel B) in all inspiratory pause procedures. The time constant was lower at inflation volumes below 10 ml.kg^{-1} than at volumes between 10 and 30 ml.kg^{-1} (BTPS). The short time constant τ_2 was on average 0.6 $\pm$ 0.15 (SD) s, n=30 (Panel D).
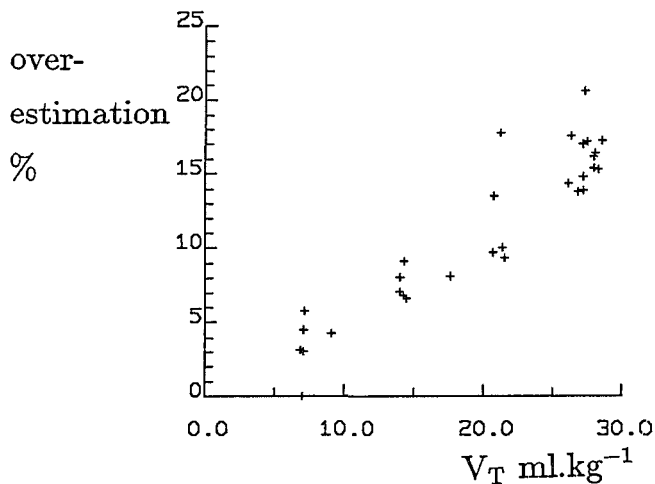
100

Figure 7.6. Overestimation of P_{stat} by $P_{T,1.5}$. The overestimation of P_{stat} by the measurement of the pressure after an inspiratory pause of only 1.5 s (expressed in %) as a function of inflation volume.

7.4.3 Compliance and pressure fall in lungs and thorax

Compliance of the chest wall, being 19.4 ± 2.3 (SD) $ml.cmH_2O^{-1}.kg^{-1}$, n=6, was much larger than the compliance of the lungs, being 2.4 ± 0.4 (SD) $ml.cmH_2O^{-1}.kg^{-1}$, n=6. The fall in pressure between 1.5 and 15 s was also significantly different between thorax and lungs. Fig 7.8 shows this difference in pressure versus inflation volume, normalized to the weight of the pig. Both the pressure decrease in the thoracic compartment and the pressure decrease in the lungs between 1.5 and 15 s pause are presented. At small and medium volume the fall in pressure in the lungs was twice as large as that in the thoracic compartment. At larger inflation volumes the fall in pressure was disproportionally larger in the lungs.

7.5 Discussion.

7.5.1 Comparison of thoracic and lung compliance

The compliance of the chest wall is often reported to be about equal or slightly larger than the compliance of the lungs in healthy adult man and full-grown animals [18,39,92]. The large difference in compliance between lungs and thorax in the present investigation might be caused by 1) the age of the pigs, since thoracic compliance is much larger than lung compliance
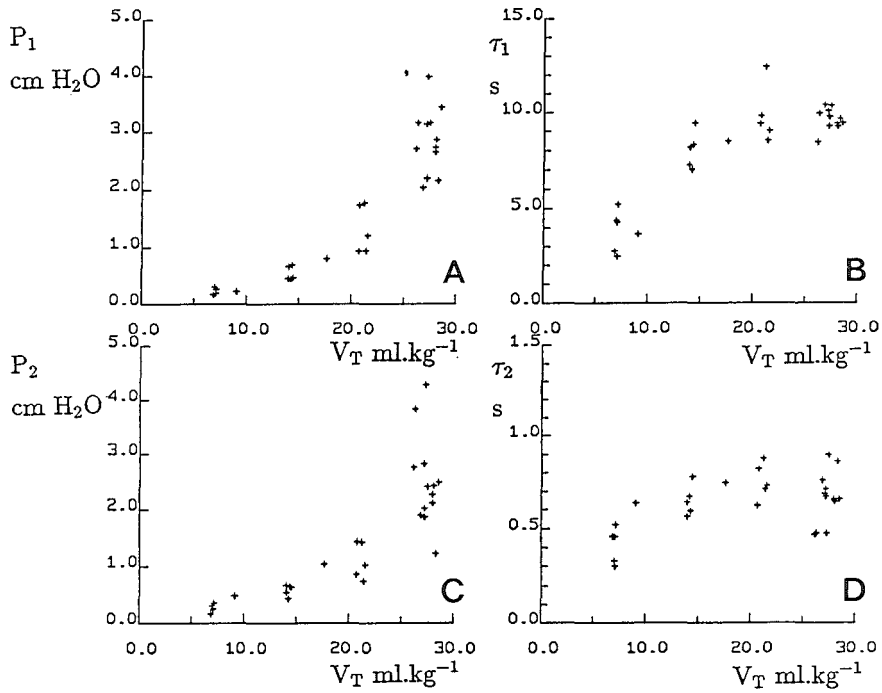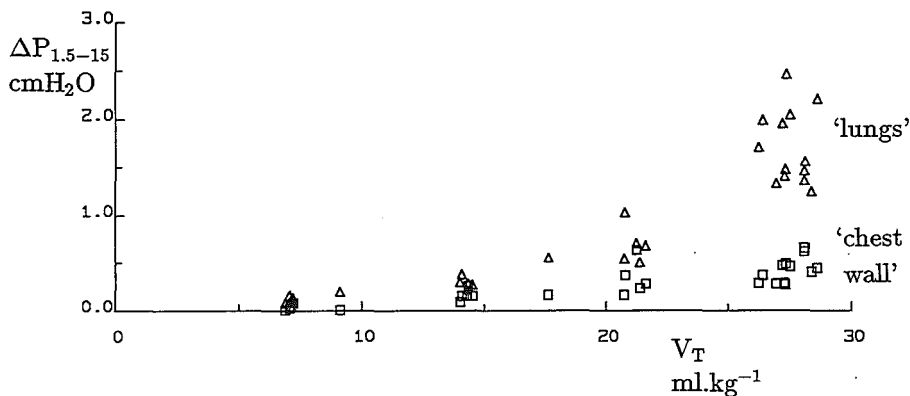
Figure 7.7. Parameter values of the bi-exponential decay.
Panels A and B show the parameters P_1 and τ_1 of the slow decay. Panels C and D show the parameters P_2 and τ_2 of the fast decay. All parameters are plotted as functions of the inflation volume, normalized to bodyweight.

Figure 7.8. Fall in transpulmonary pressure and transthoracic pressure during 'post mortem' inspiratory pauses.

The decrease in P_T between 1.5 and 15 s in the inspiratory pause is subdivided into a lung ($\triangle$) and a chest wall component ($\square$). Values of $\Delta P_{1.5-15}$ are expressed cm H_2O.

in newborns and infants [2,4], 2) the difference in species with respect to humans.

7.5.2 *Description of the decay in pressure during an inspiratory pause*

A bi-exponential fit approximated the gradual pressure decay during the inspiratory pause, but a lack of fit was a common finding.

Usually we could not recognize the sharp decrease in pressure due to equilibration of gas pressures in the initial phase of an inspiratory pause reported by many investigators [3,89,90]. Moreover, the transient phase in the pressure-time course at the start of an inflation was also small (Fig. 5.1 page 65) and, therefore, airway resistance was probably small. This might be the reason why the entire pressure-time course during inspiratory pauses in our study had a close similarity to a smooth bi-exponential function superimposed on a constant pressure level. Our data were not satisfactory to divide the pressure decay during an inspiratory pause into a part due to equilibration of gas pressures and a part due to merely stress-relaxation. We suppose, however, that P_1 and a substantial part of P_2 are linked to the fall in pressure due to stress-relaxation.

In accordance with the study of Hughes et al. [49] in rabbit lungs, stress-relaxation was found to increase nonlinearly with volume. This nonlinearity was more prominent in the lungs than in the thorax. Therefore, the non-

linear increase in tracheal pressure during inflations at constant flow rate to volumes higher than about 15 ml.kg^{-1}, mentioned in Chapter 5, is probably related to the nonlinear increase in stress-relaxation of the lungs.

The time constants of the slow exponential decay were similar for all 'post mortem' procedures except for the inspiratory pause procedures at about 5 ml.kg^{-1}. This might be due to the small stress-relaxation combined with the measurement errors in the pressure signal. Although the slow decay in pressure was adequately described by an exponential function it is expected, based on findings of other investigators that greater time constants will be found when the time interval is prolonged (cf. references in section 7.2.2).

In the section on stress-relaxation it was mentioned that an exponential decay after a sudden increase in strain could be described by a mechanical model (Maxwell element) consisting of a series combination of a dash-pot and a spring. Assuming similar parameters in the Maxwell element both during inflation and inspiratory pause, a time constant of about 8 s will be found during inflation too. Considering equation 4, which describes the pressure rise in the Maxwell element, when it is strained at a constant rate, the dynamic component of the pressure does not become constant during a rather short inflation period. This might be the reason for the differences between the slope of the dynamic pressure-volume curves during the inflation and the slope of the quasi-static pressure-volume PV_{IP} curve (cf. Chapter 5, Fig 5.2, page 65), explaining the lower values of pulse compliance with respect to $C_{IP,sl}$.

For several reasons we considered the analysis of the pressure decay with the use of a model based on two Maxwell elements in parallel not suitable for the 'in vivo' situation, because:

- A marked cardiac interference was usually observed on the tracheal pressure signal (cf. Fig. 7.3) causing a poor signal-to-noise ratio, which could hardly be improved by filtering techniques,

- A reliable fit of the parameters of the bi-exponential function to the P_T tracing requires a sufficiently long inspiratory pause, considering the slow decay with a τ_1 of $\approx$ 8 s. However, during prolonged inspiratory pauses in the 'in vivo' situation a decrease in pressure occurred due to a loss of lung volume.

- It is obvious that we are dealing with a nonlinear viscoelastic effect, based on the curvilinear relationship between parameters P_1 and P_2 and the volume of inflation (Fig. 7.7A). Therefore, the parameters

104

of the mechanical model, described in Fig. 7.1C, are dependent on the inflation volume, and consequently not very useful to characterize lung tissue condition. For measurements of viscoelasticity very small inflation volumes have to be used to avoid such an nonlinear effect [62]. However, at low inflation volumes stress-relaxation is also lower, causing a lower signal-to-noise ratio

We conclude that in the post mortem situation in mechanically ventilated piglets the static recoil pressure during an inspiratory pause can be estimated by fitting a bi-exponential function of time superimposed on a constant pressure level to the P_T-decay curve. The bi-exponential decay approximates the pressure decay during the whole inspiratory pause. However, in the 'in vivo' experiments such an analysis is thought to be too complex to be carried out, in particular because of the gradual loss of lung volume during the inspiratory pause.

Summary

Chapter 1

In this chapter aspects of the pressure-volume (P-V) relationship of the respiratory system reported in the literature are discussed. The compliance C_{RS} of the total respiratory system can be estimated by calculating the ratio between a change in lung volume (ΔV) and a change in recoil pressure (ΔP_{RS}) of lungs and thorax. During mechanical ventilation P_{RS} is usually obtained by measurement of the airway pressure, P_{AW}. This pressure, might be affected by a dynamic pressure component due to airway resistance and inhomogeneities in ventilation. Moreover, the recoil pressure of the respiratory system will gradually change after a sudden change in lung volume due to viscoelastic properties of the respiratory system.

During mechanical ventilation C_{RS} can be estimated with the use of inspiratory pause procedures. A stable difference between P_{AW} after an inspiratory pause of 1.5 s and P_{AW} at end-expiration has been reported in several studies.

In preliminary studies, however, we observed a gradual decrease in P_{AW} during inspiratory pauses of several seconds, suggesting potential errors in the estimation of C_{RS}. In this thesis we considered primarily the mechanisms which contribute to these errors as viscoelasticity and a loss of volume due to gas exchange. Moreover, we evaluated several methods for the estimation of C_{RS} during mechanical ventilation.

Chapter 2

Five methods for the estimation of C_{RS} during mechanical ventilation are discussed. The inspiratory pause method is described first (Fig 2.1, page 14). C_{RS} can be obtained from $\Delta V/\Delta P$ during each inspiratory pause procedure. The volume and pressure data of inspiratory pause procedures with different inflation volumes yield a quasi-static P-V relationship of the respiratory system. This is called the multiple inspiratory pause method (Fig. 2.2, page 16). The slope of the approximately linear part of the quasi-static P-V curve (between 0.5 and 1.0 l above end-expiratory lung volume in human beings) has been advocated as an estimate of C_{RS}. In the pulse method, C_{RS} is estimated by calculating the ratio between the rate of airflow ($\dot{V}$) during an inflation at constant flow rate and the slope of the pressure-time course ($\Delta P/\Delta t$) according to: $C_{RS} = \dot{V}/(\Delta P/\Delta t)$ (Fig. 2.3, page 17).

In a single slow inflation-deflation (SID) procedure a quasi-static P-V relationship of the respiratory system can be obtained in which again the slope of the approximately linear part represents C_{RS} (Fig. 2.4, page 20). The last method which is mentioned is the interrupter method, in which the quasi-static P-V relationship of the respiratory system is measured during short repeated interruptions (100 ms) of the airflow in passive expirations.

Chapter 3

In the experiments we used a computer controlled research ventilator consisting of two bellows, synchronously driven by an electromagnetic motor. Mechanical ventilation and a series of special ventilatory procedures could be performed by varying the volume of the bellows and by opening and closing electromagnetic valves in the tubes between ventilator and lungs (Fig. 3.2, page 28). Only one of the bellows was ventilating the lungs, the other was flushed with a gas mixture containing 5% He. Mechanical ventilation could be switched to this bellows at the end of a normal expiration, for the estimation of end-expiratory lung volume $V_{L,EE}$. In our study we used the 'open wash-in' method (Fig. 3.5, page 34) to check stability of lung volume and the 'closed wash-in' method (Fig. 3.9, page 39) for estimation of the absolute volume.

Chapter 4

In a series of 4 experiments with healthy, anaesthetized and paralysed piglets, inspiratory pause procedures (with a pause of 9 s) were performed at different inflation volumes, between 0 and 25 ml.kg^{-1}. Four estimates of C_{RS} were obtained from the inspiratory pause method. Pressure was determined both at 1.5 s and at the end of the pause and changes in lung volume were determined both by integration of the airflow (volume change ΔV_{FL}) and by means of a calibrated mercury cord around the rib cage (volume change ΔV_{MC}). C_{RS} was also estimated by means of the multiple inspiratory pause method, by calculating the slope of a line through the volume and pressure points at the end of the inspiratory pauses in the approximately linear part of the quasi-static P-V curve (Fig.4.3, page 52). The compliance estimate represented by the slope was called $C_{IP,sl}$. By means of the mercury cord a gradual loss of lung volume was demonstrated in all inspiratory pauses (Fig. 4.2, page 50), which was greater for lower inflation volumes. We hypothesized this gradual loss of lung volume to be caused by a sustained oxygen uptake and a decreasing CO_2 output from blood to alveolar gas. At low inflation volumes the pressure decrease during an inspiratory

pause could be mainly attributed to the decrease in lung volume, whereas at large inflation volumes a substantial pressure decay was observed which was mainly attributed to viscoelastic properties of the respiratory system (Fig. 4.1, page 50 and Fig. 4.4, page 52). The airway pressure after an inspiratory pause of only 1.5 s implied an overestimation of the static recoil pressure of the respiratory system of about 10% when 20 ml.kg^{-1} was insufflated.

Chapter 5

Two other methods for the estimation of C_{RS} were evaluated: the pulse method based on the dynamic P-V curve during inflation (compliance estimate C_P) and the slow inflation-deflation method (compliance estimates C_{INFL} and C_{DEFL})

We considered $C_{IP,sl}$ as reference in the comparison with the two methods. C_P was lower than $C_{IP,sl}$ (Fig. 5.2, page 65) and therefore the assumption of a constant dynamic pressure component in P_{AW} during inflations at constant flow rate, which should not affect the slope of the P-V relationship, appeared to be invalid in our experiments.

In the majority of the SID procedures reported in the literature the relationship between P_{AW} and the insufflated volume was measured. During slow inflation-deflation procedures of 70 s in our study an increasing difference was found between the imposed inflation volume and the actual change in lung volume measured by means of the mercury cord (Fig. 5.4, page 68). This difference was attributed to a continuous gas exchange, and was shown to cause a marked underestimation of C_{RS} when compliance was derived from the deflation limb of the P-V loop based on the imposed inflation volume (Fig. 5.3). When volume changes were based on measurements with the mercury cord C_{INFL} and C_{DEFL} were not significantly different from $C_{IP,sl}$.

Chapter 6

In Chapter 4 we hypothesized that the gradual loss of lung volume during an inspiratory pause was caused by a continuous gas exchange. This hypothesis was tested in 6 experiments. In these experiments inspiratory pause procedures were performed (with a pause of 15 s) to detect the loss of lung volume during the inspiratory pauses by using the mercury cord. In addition, 'rebreathing' procedures were performed (10 'rebreathing' cycles of 2 s) at corresponding volume levels. The rebreathing procedures enabled the semi-continuous monitoring of gas exchange.

We expected a slight difference between the loss of lung volume esti-

mated from the rebreathing analysis and the loss of lung volume during an inspiratory pause, because during rebreathing alveolar volume and gas concentrations changed cyclically, affecting gas exchange. During an inspiratory pause gas exchange is dependent on more gradually changing gas concentrations.

Indeed, at a low lung volume the loss of lung volume was larger during an inspiratory pause in comparison with the loss during the rebreathing. This was attributed to a larger exchange of CO_2 into the lungs during rebreathing. At larger volumes hardly any difference in loss of lung volume was found (Fig. 6.4, page 84). Therefore, we regarded the hypothesis that the loss of lung volume during an inspiratory pause depends on gas exchange to be verified.

Chapter 7

Inspiratory pause procedures were also performed 'post mortem' to study the gradual decay in pressure in the absence of a change in lung volume due to gas exchange. Although differences in the pressure decay were observed between the 'in vivo' and the 'post mortem' inspiratory pauses (Fig. 7.3 on page 98 and Fig. 7.4, page 99) we attributed these differences to the loss of lung volume in the 'in vivo' situation and we argued that the pressure decay due to stress-relaxation was similar in both conditions.

The total recoil pressure was partitioned into recoil pressures of lungs and thorax by measuring intra-thoracic pressure via the central venous pressure. The compliance of the thorax of the piglets was found to be about eight times larger than the compliance of the lungs and therefore almost the entire total recoil pressure was caused by the recoil pressure of the lungs.

The pressure decay during an inspiratory pause was described by a mechanical model with two Maxwell elements in parallel to an elastic element (Fig. 7.1C, page 91). The bi-exponential function superimposed on a constant (plateau) level, predicted by the model, approximated the pressure decay in the whole inspiratory pause (Fig. 7.5, page 100). However at medium and high inflation volumes a lack of fit was a common finding. The time constant of the slow decay in pressure was estimated to be about 8 s (Fig. 7.7B, page 102). In the 'in vivo' situation the estimation of the parameters of the model was considered too complex in particular because of the gradual pressure decay due to the loss of lung volume.

Samenvatting

Hoofdstuk 1

De mate van rekbaarheid (compliantie) van het totale ademhalingssysteem, dat wil zeggen van de combinatie van longen en thorax, kan tijdens beademing bepaald worden door een longvolumeverandering (ΔV) op te leggen en de verandering in tegendruk (ΔP_{RS}) van het ademhalingssysteem te bepalen. De totale compliantie C_{RS} kan worden afgeleid uit de verhouding $\Delta V / \Delta P_{RS}$.

Tijdens beademing kan P_{RS} bepaald worden door meting van de druk aan de mond, P_{AW}. Deze druk wordt echter niet alleen bepaald door de elastische eigenschappen van longen en thorax maar ook door een drukcomponent tijdens of net na een insufflatie als gevolg van een drukverschil over de luchtwegen door luchtwegweerstand en inhomogeniteiten in de ventilatie van de verschillende longgebieden. Bovendien kunnen visco-elastische eigenschappen van longen en thorax bijdragen tot een foutieve bepaling van de elastische tegendruk van het ademhalingssysteem.

Ook activiteit van de ademhalingsspieren kan P_{AW} beinvloeden. In dit proefschrift worden echter alleen experimenten beschreven waarbij de ademhalingsspieren verlamd waren door middel van spierverslappers, zodat deze invloed verder onbesproken blijft.

Tijdens beademing kan C_{RS} geschat worden met behulp van een inspiratoire pauze. Een constant drukverschil ΔP_{AW} tussen de druk na een pauze van 1.5 s en de eind-expiratoire druk werd door verschillende onderzoekers waargenomen. In voorafgaande onderzoeken in beademde biggen bleek de druk ook na een pauze van 1.5 s nog geleidelijk te dalen. Dit zou kunnen wijzen op een systematische fout in de schatting van de totale compliantie wanneer de druk na 1.5 s verondersteld wordt gelijk te zijn aan de elastische tegendruk van het respiratoire systeem. Het onderzoek waarover in dit proefschrift gerapporteerd wordt handelt voornamelijk over de invloed van mechanismen als visco-elasticiteit en een mogelijke longvolumeverandering, als gevolg van continue gasuitwisseling, op de geleidelijk drukafname tijdens een inspiratoire pauze. Bovendien worden nog enkele andere methoden om C_{RS} te bepalen tijdens beademing geëvalueerd.

Hoofdstuk 2

Er zijn verschillende methoden om de totale compliantie C_{RS} tijdens beademing te bepalen. In de inspiratoire pauze methode wordt de insufflatie direct gevolgd door een periode waarin geen luchtstroom aan de mond mogelijk is. Aan het einde van een inspiratoire pauze van 1.5 s wordt in het algemeen aangenomen dat de druk aan de mond gelijk is aan de elastische tegendruk van longen en thorax behorend bij het geïnsuffleerde volume. C_{RS} wordt dan bepaald uit de verhouding $\Delta V/\Delta P$ (Fig. 2.1, pag. 14). Een andere methode om C_{RS} te bepalen is een combinatie van inspiratoire pauze procedures met verschillende inflatievolumes ('meervoudige inspiratoire pauze methode'). Door combinatie van de druk-volume waarden aan het einde van de pauzes in deze procedures kan een quasi-statische P-V curve van longen en thorax verkregen worden. De helling van het bij benadering lineaire deel van deze druk-volume curve is ook een maat voor de totale compliantie (Fig. 2.2, pag. 16). In de pulse methode (Fig. 2.3, pag. 17) wordt C_{RS} berekend uit de verhouding tussen de luchtstroomsterkte ($\dot{V}$) en de helling van de druk-tijd relatie gedurende een 'pulse' insufflatie (constante $\dot{V}$). In deze methode wordt aangenomen dat de dynamische component van de druk die aan de mond gemeten wordt constant is gedurende dat deel van de inflatie dat voor deze methode wordt gebruikt. Door het uitvoeren van een langzame inflatie-deflatie (SID) procedure kan de P-V curve van het ademhalingssysteem verkregen worden. C_{RS} wordt in deze methode bepaald door berekening van de helling van het meest lineaire deel van de P-V curve (Fig. 2.4, pag. 20). Tenslotte lijkt het mogelijk om tijdens een passieve expiratie de tegendruk van longen en thorax te bepalen door op verschillende tijdstippen de expiratie voor korte tijd te onderbreken (100 ms).

Hoofdstuk 3

Voor ons onderzoek werd gebruik gemaakt van een computergestuurde research ventilator. De ventilator bestond in essentie uit twee balgen, die dezelfde volumevariatie kregen opgelegd door middel van een electromagnetische motor (Fig. 3.1, pag. 24). Met behulp van de volume variatie in de balgen kon, door het openen en sluiten van de juiste kleppen in de slangen tussen ventilator en longen, een volume in de long worden gebracht (inflatie) of er juist geleidelijk aan worden onttrokken (gecontroleerde expiratie). In de normale beademing en de meeste speciale beademingsprocedures volgde echter na de periode van insufflatie een fase waarin de longen in directe verbinding kwamen met de buitenlucht (evt. via een positief expiratoire druk

niveau, PEEP) waardoor het longvolume weer afnam, via een passieve expiratie, tot aan het eind-expiratoire volume niveau (Fig. 3.2, pag. 28). De normale beademing en vrijwel alle speciale procedures werden uitgevoerd met één van de twee balgen.

Twee methoden werden gebruikt om het eind-expiratoire longvolume te bepalen. In de 'open inwas' methode werd aan het eind van een normale passieve expiratie overgeschakeld van de balg met het normale beademingsgas naar de tweede balg die gevuld was met een gasmengsel met circa 5% helium, zonder dat enige verandering in de beademing optrad (Fig. 3.5, pag. 34). Door nauwkeurige meting van 1) de hoeveelheid helium die werd geïnsuffleerd, 2) de hoeveelheid die werd geëxpireerd en 3) de gemiddelde helium fractie in de long, kon het eind-expiratoire longvolume berekend worden. In de 'gesloten inwas' methode werd ook op het eind-expiratoire niveau overgeschakeld op de 'andere' balg van de ventilator die een beademingsmengsel met ongeveer 5% He bevatte. Na insufflatie van dit gasmengsel werd de uitademing echter wederom opgevangen in de balg ('rebreathing'). Deze procedure werd enige malen herhaald. Het aanvankelijk helium vrije gas in de longen raakte gedurende deze 'inwas' geleidelijk gemengd met het helium mengsel uit de balg (Fig. 3.9, pag. 39). Met behulp van een massabalans voor helium kon het eind-expiratoire longvolume berekend worden. De 'open inwas' methode werd in dit onderzoek alleen gebruikt om de stabiliteit van het eind-expiratoire longvolume te controleren. Voor de schatting van het absolute longvolume werd gebruik gemaakt van de 'gesloten inwas' methode.

Hoofdstuk 4

In een serie van vier experimenten met gezonde genarcotiseerde biggen werden procedures met een inspiratoire pauze uitgevoerd tijdens normale beademing. De duur van de inspiratoire pauze bedroeg in onze experimenten 9 s. De inflatievolumes varieerden van 0 tot 25 ml per kg. Vier schattingen van C_{RS} werden verkregen per procedure met een inspiratoire pauze. De trachea druk (P_T) werd zowel op 1.5 s als aan het eind van de inspiratoire pauze bepaald, en de verandering in longvolume werd bepaald door middel van integratie van de luchtstroomsterkte (volumeverandering ΔV_{FL}) en door middel van een kwikkoordje rond de thorax van de big (volumeverandering ΔV_{MC}). Tevens werd de totale compliantie bepaald met de 'meervoudige inspiratoire pauze methode' ($C_{IP,sl}$, Fig. 4.3 op pag. 52). Dankzij de meting van longvolumeveranderingen met het kwikkoordje kon tijdens de inspiratoire pauze een geleidelijke afname van het intra-thoracale

113

volume vastgesteld worden (Fig. 4.2, pag. 50). Beargumenteerd werd dat deze volumevermindering waarschijnlijk werd veroorzaakt door een afname van het longvolume, en niet door een intra-thoracale bloedvolumeverandering. Tijdens de inspiratoire pauze na een insufflatie met een klein volume werd een grotere afname van het longvolume waargenomen dan tijdens de pauze na een inflatie met een groot volume. De drukdaling tijdens de pauze op laag volume niveau bleek vrijwel geheel verklaard te kunnen worden uit de afname van het longvolume. Dit was niet het geval voor de drukdaling op hoog volume niveau (Fig. 4.4, pag. 52). Er werden sterke aanwijzingen gevonden dat deze drukdaling primair een gevolg was van de visco-elastische eigenschappen van longen en thorax. Meting van P_T na een inspiratoire pauze van slechts 1.5 s hield in dat de elastische tegendruk van het ademhalingssysteem met circa 10 % werd overschat, bij een inflatievolume van 20 $ml.kg^{-1}$.

Als hypothese werd geformuleerd dat de geleidelijke vermindering van het longvolume een gevolg is van een continue zuurstof opname en een geleidelijk afnemende CO_2 afgifte vanuit het bloed naar het alveolaire gas en dat de afname van het longvolume door continue gasuitwisseling toeneemt bij kleinere inflatievolumes.

Hoofdstuk 5

Twee andere methoden om de totale compliantie van longen en thorax te bepalen werden geëvalueerd, namelijk: de 'pulse' methode (compliantie C_P) en, de langzame (slow) inflatie-deflatie (SID) methode met een schatting van C_{RS} tijdens de inflatie (C_{INFL}) en deflatie (C_{DEFL}). De compliantie $C_{IP,sl}$ werd als referentie voor de andere methoden gebruikt.

De pulse compliantie C_P bleek een geringe onderschatting te geven van de totale compliantie ($C_{IP,sl}$), zie Fig. 5.2 op pag. 65. Deze onderschatting werd waarschijnlijk veroorzaakt door visco-elastische eigenschappen van long en thorax die tijdens de insufflatie een toename van de dynamische drukcomponent in P_{AW} veroorzaakten, in tegenstelling tot de veronderstelde constante dynamische druk component.

In vrijwel alle langzame inflatie-deflatie procedures die beschreven zijn in de literatuur werd de relatie tussen de druk en het opgelegde volume gemeten. Ons onderzoek wijst echter uit dat in een langzame inflatie-deflatie procedure de reële verandering van het longvolume bepaald moet worden, zoals met een kwikkoordje rond de thorax, omdat gedurende de procedure, die 70 s duurde, een toenemend verschil tussen het opgelegde volume en het reële actuele longvolume werd waargenomen (Fig. 5.4, pag. 68). Dit verschil

in volume werd waarschijnlijk veroorzaakt door continue gasuitwisseling. De bepaling van C_{DEFL} uit de P-V relatie die werd gebaseerd op het opgelegde volume leidde tot een significante onderschatting van C_{RS} (Fig. 5.3, pag. 67).

Bij meting van de actuele verandering in longvolume waren C_{INFL} en C_{DEFL} echter gelijk aan $C_{IP,sl}$.

Hoofdstuk 6

De hypthese dat longvolumeafname een functie is van het inflatievolume (Hoofdstuk 4) werd getoetst in een serie van 6 experimenten met gezonde beademde biggen. In deze experimenten werd 1) de afname van het intrathoracaal volume gedurende inspiratoire pauzes van 15 s met behulp van een kwikkoordje rond de thorax gemeten, en 2) de verandering in longvolume berekend uit de veranderingen in gasconcentraties gedurende procedures waarin cyclisch een volume in- en uitgeademd werd in een gesloten systeem ('rebreathing' procedure, Fig 6.1, pag. 76). Deze rebreathing procedures werden op 3 volume niveaus boven het eind-expiratoire longvolume uitgevoerd om de invloed van het inflatievolume op de afname in longvolume te meten. Hoewel de afname van het longvolume gedurende deze 'rebreathing' procedures en die tijdens de inspiratoire pauze procedures slechts beperkt vergelijkbaar was, gezien de verschillen in procedures, bleek de berekende longvolumeafname inderdaad toe te nemen bij kleinere inflatievolumes en van dezelfde orde van grootte als de longvolumedaling die werd waargenomen in inspiratoire pauze procedures (Fig. 6.4, pag. 84). Deze resultaten werden beschouwd als een verificatie van de hypothese.

Hoofdstuk 7

Dit hoofdstuk handelt over een serie inspiratoire pauze procedures, die kort na het intreden van de dood bij de proefdieren ('post mortem') werd uitgevoerd. In deze situatie is het longvolume gedurende de inspiratoire pauze constant doordat geen gasuitwisseling meer optreedt. Hoewel in de inspiratoire pauzes een verschil in drukafname werd waargenomen tussen de 'in vivo' en 'post mortem' metingen, werd beargumenteerd dat de drukafname door 'stress-relaxatie' vergelijkbaar was (Fig. 7.3 en 7.4 resp. op pag. 98 en op pag. 99).

De drukafname gedurende een inspiratoire pauze werd beschreven met een mechanisch model waarin twee Maxwell elementen en een elastisch element parallel geschakeld waren (Fig. 7.1, pag. 91). Dit model beschrijft de drukafname gedurende een inspiratoire pauze als een bi-exponentiele functie van de tijd boven op een constant drukniveau. Deze functie bleek een goede

benadering van de drukafname als functie van de tijd te geven (Fig. 7.5, pag. 100). In dit hoofdstuk wordt tevens de haalbaarheid van een dergelijke analyse in de 'in vivo' metingen bediscussieerd.

Door middel van meting van de centraal-veneuze druk werd een schatting gemaakt van de bijdrage van long en thorax afzonderlijk aan de totale druk die aan de mond werd gemeten. De bijdrage van de thorax aan de totale tegendruk bleek heel gering door een grote thorax compliantie. Een mogelijke oorzaak hiervoor is de afwezigheid van spiertonus. Ook is het denkbaar dat bij varkens van deze leeftijd de normale elastische tegendruk van de thorax klein is.

References

[1] Agostini, E. and J. Mead, Statics of the respiratory system, In: *Handbook of Physiology, section Respiration*, edited by W.O. Fenn and H. Rahn. Washington D.C.: American Physiological Society, 1965, sec. 3, vol. 2, pp 387-409.

[2] Agostini, E., Volume-pressure relationship of thorax and lung in the newborn, *J. Appl. Physiol.*, 14: 909, 1959.

[3] Al-Saady, N. and D. Bennett, Decelerating inspiratory flow waveform improves lung mechanics and gas exchange in patients on intermittent positive-pressure ventilation, *Intensive Care Med.*, 11: 68-75, 1985.

[4] Avery, M.E., and C.D. Cook, Volume-pressure relationships of lungs and thorax in fetal, newborn and adult goats, *J. Appl. Physiol.*, 16, 1034-1038, 1961.

[5] Azuma, T. and M. Hasegawa, A rheological approach to the architecture of arterial walls, *Japan. J. Physiol.*, 21: 27-47, 1971.

[6] Bachofen, H., J. Hildebrandt and M. Bachofen, Pressure-volume curves of air- and liquid-filled excised lungs — surface tension in situ, *J. Appl. Physiol.*, 29: 422-431, 1970.

[7] Bachofen, H., and J. Hildebrandt, Area analysis of pressure-volume hysteresis in mammalian lungs, *J. Appl. Physiol.*, 30: 493-497, 1971.

[8] Barrow, R.E., Volume-pressure cycles from air and liquid filled *intact* rabbit lungs, *Resp. Physiol.*, 63: 19-30, 1986.

[9] Bates, J.H.T., G.K. Prisk, T.E. Tanner and A.E. McKinnon, Correcting for the dynamic response of a respiratory mass spectrometer, *J. Appl. Physiol.*, 55: 1015-1022, 1983.

[10] Bates, J.H.T., A. Rossi and J. Milic-Emili, Analysis of the behavior of the respiratory system with constant inspiratory flow, *J. Appl. Physiol.*, 58: 1840-1848, 1985.

[11] Bates, J.H.T., M. Decramer, D. Chartrand, W.A. Zin, A. Boddener and J. Milic-Emili, Volume-time profile during relaxed expiration in the normal dog, *J. Appl. Physiol.*, 59: 732-737, 1985.

[12] Bates, J.H.T., P. Baconnier and J. Milic-Emili, A theoretical analysis of interrupter technique for measuring respiratory mechanics, *J. Appl. Physiol.*, 64: 2204-2214, 1988.

[13] Behrakis, P.K., B.D. Higgs, A. Baydur, W.A. Zin and J. Milic-Emili, Respiratory mechanics during halothane anesthesia and anesthesia-paralysis in humans, *J. Appl. Physiol.*, 55: 1085-1092, 1983.

[14] Benito, S., F. Lemaire, B. Mankikian and A. Harf, Total respiratory compliance as a function of lung volume in patients with mechanical ventilation, *Intensive Care Med.*, 11: 76-79, 1985.

[15] Bernstein, L., The elastic pressure-volume curves of the lungs and thorax of the living rabbit, *J. Physiol.*, 138: 473-487, 1957.

[16] Bienkowski, R. and M. Skolnick, Dynamic behavior of surfactant films, *J. Colloid. Interface Sci.*, 39: 323-330, 1972.

[17] Bone, R.C., Diagnosis of causes for acute respiratory distress by pressure-volume curves, *Chest*, 70: 740-746, 1976.

[18] Butler, J., and B.H. Smith, Pressure-volume relationships of the chest in the completely relaxed anaesthetised patient, *Clin. Sci.*, 16: 125-146, 1957.

[19] Butler, J., The adaptation of the relaxed lungs and chest wall to changes in volume, *Clin. Sci.*, 16: 421-433, 1957.

[20] Coolsaet, B.L.R.A., W.A. van Duyl, R. van Mastrigt and A. van der Zwart, Visco-elastic properties of the bladder wall, *Urol. int.*, 30: 16-26, 1975.

[21] Dall'Ava-Santucci, J., A. Armaganidis, F. Brunet, J.F. Dhainaut, G.L. Chelucci, J.F. Monsallier and A. Lockhart, Causes of error of respiratory pressure-volume curves in paralyzed subjects, *J. Appl. Physiol.*, 64: 42-49, 1988.

[22] Don, H.F., and J.G. Robson, The mechanics of the respiratory system during anesthesia, *Anesthesiology*, 26: 168-178, 1965.

[23] Don, H., The mechanical properties of the respiratory system during anesthesia, *Int. Anaesthesiol. Clin.*, 15: 113-136, 1977.

[24] Duyl van, W.A., A.T.M. van der Zon and A.C. Drogendijk, Stress relaxation of the human cervix: a new tool for diagnosis of cervical incompetence, *Clin. Phys. Physiol. Meas.*, 5: 207-218, 1984.

[25] Emmanuel, G., W.A. Briscoe and A. Cournand, A method for the determination of the volume of air in the lungs. Measurements in chronic pulmonary emphysema, *J. Clin. Invest.*, 40: 329-337, 1961.

[26] Falke, K.J., H. Pontoppidan, A. Kumar, D.E. Leith, B. Geffin and M.B. Laver, Ventilation with end-expiratory pressure in acute lung disease, *J. Clin. Invest.*, 51: 2315-2323, 1972.

[27] Falke, K.J., Do changes in lung compliance allow the determination of "optimal PEEP", *Anaesthesist*, 29: 165-168, 1980.

[28] Findley, L.J., A.L. Ries, G.M. Tisi and P.D. Wagner, Hypoxemia during apnea in normal subjects: mechanisms and impact of lung volume, *J. Appl. Physiol.*, 55: 1777-1783, 1983.

[29] Fukaya, H., C.J. Martin, A.C. Young and S. Katsura, The mechanical properties of alveolar walls, *J. Appl. Physiol.*, 25: 689-695, 1968.

[30] Gattinoni, L., D. Mascheroni, E. Basilico, G. Foti, A. Pesenti and L. Avalli, Volume/pressure curve of total respiratory system in paralysed patients: artefacts and correction factors, *Intensive Care Med.*, 13: 19-25, 1987.

[31] Gattinoni, L., A. Pesenti, L. Avalli, F. Rossi and M. Bombino, Pressure-volume curve of total respiratory system in acute respiratory failure, *Am. Rev. Respir. Dis.*, 136: 730-736, 1987.

[32] Gibson, G.J., and N.B. Pride, Lung distensibility, The static pressure-volume curve of the lungs and its use in clinical assessment, *Br. J. Dis. Chest*, 70: 143-184, 1976.

[33] Glaister, D.H., R.C. Schroter, M.F. Sudlow and J. Milic-Emili, Bulk elastic properties of excised lungs and the effect of a transpulmonary pressure gradient, *Resp. Physiol.*, 17: 347-364, 1973.

[34] Gottfried, S.B., B.D. Higgs, A. Rossi, F. Carli, P.M. Mengeot, P.M.A. Calverley, L. Zocchi and J. Milic-Emili, Interrupter technique for measurement of respiratory mechanics in anesthetized humans, *J. Appl. Physiol.*, 59: 647-652, 1985.

[35] Gottfried, S.B., A. Rossi, B.D. Higgs, P.M.A. Calverley, L. Zocchi, C. Bozic and J. Milic-Emili, Noninvasive determination of respiratory system mechanics during mechanical ventilation for acute respiratory failure, *Am. Rev. Respir. Dis.*, 131: 414-420, 1985.

[36] Gray, B.A., D.R. McCaffree, E.D. Sivak and H.T. McCurdy, Effect of pulmonary vascular engorgement on respiratory mechanics in the dog, *J. Appl. Physiol.*, 45: 119-127, 1978.

[37] Guyton, A.C., A.W. Lindsey and B.N. Kaufmann, Effect of mean circulatory filling pressure and other peripheral circulatory factors on cardiac output, *Am. J. Physiol.*, 180: 463-468, 1955.

[38] Guyton, A.C., C.E. Jones and T.G. Coleman, In: *Circulatory Physiology: Cardiac output and its regulation*, Philadelphia: W.B. Saunders Company, 2nd ed., 1973.

[39] Heaf, P.J.D., and F.J. Prime, The compliance of the thorax in normal human subjects, *Clin. Sci.*, 15: 319-327, 1956.

[40] Hickham, J.B., E. Blair and R. Frayser, An open circuit helium method for measuring functional residual capacity and defective intra-pulmonary gas mixing, *J. Clin. Invest.*, 33: 1277-1286, 1954

[41] Hildebrandt, J., Comparison of mathematical models for cat lung and viscoelastic balloon derived by Laplace transform methods from pressure-volume data, *Bull. Math. Biophysics*, 31: 651-667, 1969.

[42] Hildebrandt, J., Pressure-volume data of cat lung interpreted by a plastoelastic, linear viscoelastic model, *J. Appl. Physiol.*, 28: 365-372, 1970.

119

[43] Holzapfel, L., D. Robert, F. Perrin, P.L. Blanc, B. Palmier and C. Guerin, Static pressure-volume curves and effect of positive end-expiratory pressure on gas-exchange in adult respiratory distress syndrome, *Crit. Care Med.*, 11: 591-597, 1983.

[44] Hong, S.K., Y.C. Ling, D.A. Lally, B.J.B. Yim, N. Kominami, P.W. Hong, and T.O Moore, Alveolar gas exchanges and cardiovascular functions during breath holding with air, *J. Appl. Physiol.*, 30: 540-547, 1971.

[45] Hoppin, F.G., and J. Hildebrandt, Mechanical properties of the lung, In: *Bioengineering aspects of the lung*, edited by J.B. West. New York: Dekker, 1977, vol. 3,pp 83-162 (Lung Biol. Health Dis. Ser.)

[46] Horie, T., and J. Hildebrandt, Dynamic compliance, limit cycles and static equilibria of excised cat lung, *J. Appl. Physiol.*, 31: 423-430, 1971.

[47] Horie, T., and J. Hildebrandt, Volume history, static equilibrium and dynamic compliance of excised cat lung, *J. Appl. Physiol.*, 33: 105-112, 1972.

[48] Horn, L.W., Evaluation of some alternative mechanisms for interface-related stress relaxation in lung, *Respir. Physiol.*, 34: 345-357, 1978.

[49] Hughes, R., A.J. May and J.G. Widdicombe, Stress relaxation in rabbits' lungs, *J. Physiol.*, 146: 85-97, 1959.

[50] Hurewitz, A.N. and M.G. Sampson, Voluntary breath holding in the obese, *J. Appl. Physiol.*, 62: 2371-2376, 1987

[51] Hylkema, B.S., P. Barkmeyer-Degenhart, R.G. Grevink, T.W. v.d. Mark, R. Peset and H.J. Sluiter, Lung mechanical profiles in acute respiratory failure: Diagnostic and prognostic value of compliance at different tidal volumes., *Crit. Care Med.*, 13: 637-640, 1985.

[52] Jackson, A.C., H.T. Milhorn and J.R. Norman, A reevaluation of the interrupter technique for airway resistance measurement, *J. Appl. Physiol.*, 36: 264-268, 1974.

[53] Jamison, C.E., R.D. Marangoni and A.A. Glaser, Viscoelastic properties of soft tissue by discrete model characterization, *J. Biomech.*, 1: 33-46, 1968.

[54] Jansen, J.R.C., J.J. Schreuder, J.M. Bogaard, W. van Rooyen and A. Versprille, Thermodilution technique for measurement of cardiac output during artificial ventilation, *J. Appl. Physiol.*, 51: 584-591, 1981.

[55] Jansen, J.R.C., J.M. Bogaard and A. Versprille, Extrapolation of thermodilution curves obtained during a pause in artificial ventilation, *J. Appl. Physiol.*, 63: 1551-1557, 1987.

[56] Jansen, J.R.C., E. Hoorn, J. van Goudoever and A. Versprille, A computerized respiratory system for ventilation, lung function and circulation testing, *J. Appl. Physiol.*, accepted for publication, 1989

[57] Katz, J.A., S.E. Zinn, G.M. Ozanne and H. Barrie Fairley, Pulmonary, chest wall, and lung-thorax elastances in acute respiratory failure, *Chest*, 80: 304-311, 1981.

[58] Katz, J.A., G.M. Ozanne, S.E. Zinn and H. Barrie Fairly, Time course and mechanisms of lung-volume increase with PEEP in acute pulmonary failure, *Anesthesiology*, 54: 9-16, 1981.

[59] Kim, T.S., H. Rahn and L.E. Fahri, Estimation of true venous and arterial P_{CO_2} by gas analysis of a single breath, *J. Appl. Physiol.*, 21: 1338-1344, 1966.

[60] Klocke, F.J., and H. Rahn, Breath holding after breathing of oxygen, *J. Appl. Physiol.*, 14: 689-693, 1959.

[61] Lanphier, E.H., and H. Rahn, Alveolar gas exchange during breath holding with air, *J. Appl. Physiol.*, 18: 478-482, 1963.

[62] Lorino, A.M., A. Harf, G. Atlan, H. Lorino and L. Laurent, Role of surface tension and tissue in rat lung stress relaxation, *Resp. Physiol.*, 48: 143-155, 1982.

[63] Mancebo, J., N. Calaf and S. Benito, Pulmonary compliance measurement in acute respiratory failure, *Crit. Care Med.*, 13: 589-591, 1985.

[64] Mankikian, B., F. Lemaire, S. Benito, C. Brun-Buisson, A. Harf, J.P. Maillot and J. Becker, A new device for measurement of pulmonary pressure-volume curves in patients on mechanical ventilation, *Crit. Care Med.*, 11: 897-901, 1983.

[65] Marquardt, D.W., An algorithm for least squares estimation of nonlinear parameters, *J. Soc. Ind. Appl. Math.*, 11: 431-441, 1963.

[66] Marshall, R., and J.G. Widdicombe, Stress relaxation in the human lung, *Clin. Sci.*, 20: 19-31, 1960.

[67] Mastrigt van, R., B.L.R.A. Coolsaet and W.A. van Duyl, Passive properties of the urinary bladder in the collection phase, *Med. Biol. Eng. Comput.*, 16: 471-482, 1978

[68] Matamis, D., F. Lemaire, A. Harf, C. Brun-Buisson, J.C. Ansquer and G. Atlan, Total respiratory pressure-volume curves in the adult respiratory distress syndrome, *Chest*, 86: 58-66, 1984.

[69] Mathe, J.C., A. Clement, J.Y. Chevalier, C. Gaultier and J. Costil, Use of total inspiratory pressure-volume curves for determination of appropriate positive end-expiratory pressure in newborns with hyaline membrane disease, *Intensive Care Med.*, 13: 332-336, 1987.

[70] Mead, J., J.L. Whittenberger and E. P. Radford jr., Surface tension as a factor in pulmonary volume-pressure hysteresis, *J. Appl. Physiol.*, 10: 191-196, 1957.

[71] Mead, J. and E.A. Gaensler, Esophageal and pleural pressure in man, upright and supine, *J. Appl. Physiol.*, 14: 81-83, 1959.

[72] Milic-Emili, J., J. Mead, J.M. Turner and E.M. Glauser, Improved technique for estimating pleural pressure from esophageal balloons, *J. Appl. Physiol.*, 19: 207-211, 1964.

[73] Mithoefer, J.C., Mechanism of pulmonary gas exchange and CO_2 transport during breath holding, *J. Appl. Physiol.*, 14: 706-710, 1959.

[74] Murciano, D., M. Aubier, S. Bussi, J.P. Derenne, R. Pariente and J. Milic-Emili, Comparison of esophageal, tracheal and mouth occlusion pressure in patients with chronic obstructive pulmonary disease during acute respiratory failure, *Am. Rev. Resp. Dis.*, 126: 837-841, 1982.

[75] Nagao, K., R. Ardila and J. Hildebrandt, Rheological properties of excised rabbit lung stiffened by repeated hyperinflation, *J. Appl. Physiol.*, 47: 360-368, 1979.

[76] Neergaard von, K., and K. Wirz, Die Messung der Strömungswiderstände in den Atemwegen des Menschen, insbesondere bei Asthma und Emphysem, *Z. Klin. Med.*, 105: 51-82, 1927.

[77] Neergaard von, K., Neue Auffassungen über einen Grundbegriff der Atemmechanik. Die Retraksionskraft der Lunge, Abhängig von der Oberflächenspannung in den Alveolen. *Z. Ges. Exp. Med.*, 66: 373-394, 1929.

[78] Press, W.H., B.P. Flannery, S.A. Teukolsky, and W.T. Vetterling, Numerical recipes: the art of scientific computing, Cambridge University Press, U.S.A., 1986.

[79] Otis, A.B., H. Rahn and W.O. Fenn, Alveolar gas changes during breath holding, *Am. J. Physiol.*, 152: 674-686, 1948.

[80] Otis, A.B. and D.F. Proctor, Measurement of alveolar pressure in human subjects, *Am. J. Physiol.*, 152: 106-112, 1948.

[81] Otis, A.B., Quantitative relationships in steady-state gas exchange, In: *Handbook of Physiology, section Respiration*, Washington D.C.: Am. Physiol. Soc., 1964, sect. 3, vol. I, chapter 27.

[82] Pedley, T.J., M.F. Sudlow, and J. Milic-Emili, A non-linear theory of distribution of pulmonary ventilation, *Respir. Physiol.*, 15: 1-38, 1972

[83] Pepe, P.E., and J.J. Marini, Occult positive end-expiratory pressure in mechanically ventilated patients with airflow obstruction, *Am. Rev. Respir. Dis.*, 126: 166-170, 1982.

[84] Peslin, R., J. Morinet-Lambert, C. Duvivier, Étude de la réponse de fréquence de pneumotachographes, *Bull. Europ. Physiopath. Resp.*, 8: 1363-1376, 1972.

[85] Rahn, H., A.B. Otis, L.E. Chadwick and W.O. Fenn, The pressure-volume diagram of the thorax and lung, *Am. J. Physiol*, 146: 161-178, 1946.

[86] Rattenborg, C.C., and D.A. Holaday, Constant flow inflation of the lungs, *Acta Anaesthesiol. Scand.*, 23: 211-223, 1967.

[87] Rohrer, F., Der Zusammenhang der Atemkräfte und ihre Abhängigkeit vom Dehnungszustand det Atmungsorgane, *Pflügers Arch. ges. Physiol.*, 165: 419-444, 1916

[88] Rooyen van, W., Respiratory and hemodynamic effects of diminished expiratory flow during artificial ventilation, Thesis, Erasmus University Rotterdam, 1986.

[89] Rossi, A., S.B. Gottfried, B.D. Higgs, L. Zocchi, A. Grassino and J. Milic-Emili, Respiratory mechanics in mechanically ventilated patients with respiratory failure, *J. Appl. Physiol.*, 58: 1849-1858, 1985.

[90] Rossi, A., S.B. Gottfried, L. Zocchi, B. Higgs, S. Lennox, P. Calverley, P. Begin, A. Grassino and J. Milic-Emili, Measurement of static compliance of the total respiratory system in patients with acute respiratory failure during mechanical ventilation, *Am. Rev. Respir. Dis.*, 131: 672-677, 1985.

[91] Sachs, L., Applied statistics (2nd ed.), New York: Springer-Verlag, 1984.

[92] Sharp, J.T., F. N. Johnson, N. B. Goldberg and P. van Lith, Hysteresis and stress adaptation in the human respiratory system, *J. Appl. Physiol.*, 23: 487-497, 1967.

[93] Stromberg, D.D., and C.A. Wiederhielm, Viscoelastic description of a collagenous tissue in simple elongation, *J. Appl. Physiol.*, 26: 857-862, 1969.

[94] Sugihara, T., J. Hildebrandt and C.J. Martin, Viscoelastic properties of alveolar wall, *J. Appl. Physiol.*, 33: 93-98, 1972.

[95] Sullivan, K.J., and J.P. Mortola, Dynamic lung compliance in newborn and adult cats, *J. Appl. Physiol.*, 60: 743-750, 1986.

[96] Sullivan, K.J. and J.P. Mortola, Age related changes in the rate of stress-relaxation within the respiratory system, *Respir. Physiol.*, 67: 295-309, 1987.

[97] Suratt, P.M., D.H. Owens, W.T. Kilgore, R.R. Harry and H.S. Hsiao, A pulse method of measuring respiratory system compliance, *J. Appl. Physiol.*, 49: 1116-1121, 1980.

[98] Suratt, P.M., and D.H. Owens, A pulse method of measuring respiratory system compliance in ventilated patients, *Chest*, 80: 34-38, 1981.

[99] Suratt, P.M., D.H. Owens, H. Hsiao, D.L. Kaiser, and D.F. Rochester, Lung compliance and its transient elevations measured with pulse-flow method, *J. Appl. Physiol.*, 50: 1318-1324, 1981.

[100] Suter, P.M., H.B. Fairley and M.D. Isenberg, Effect of tidal volume and positive end-expiratory pressure on compliance during mechanical ventilation, *Chest*, 73: 158-162, 1978.

[101] Thomas, L., D. Robert and M. Gerard, Routine use of pressure-volume loops during mechanical ventilation, *Chest*, 75: 743-744, 1979.

[102] Trop, D., R. Peeters and K. P. van de Woestijne, Localization of recording site in the esophagus by means of cardiac artifacts, *J. Appl. Physiol.*, 29: 283-287, 1970.

[103] Tsunoda, S, A.C. Young and C.J. Martin, Emptying pattern of lung compartments in normal man, *J. Appl. Physiol.*, 32: 644-649, 1972.

[104] Versprille, A., and J.R.C. Jansen, Mean systemic filling pressure as a characteristic pressure for venous return, *Pflügers Arch.*, 405: 226-233, 1985.

[105] Versprille, A., Pulmonary blood flow and blood volume during positive pressure ventilation, In: *Update in Intensive Care and Emergency Medicine*, ed. J.L. Vincent, Berlin Heidelberg: Springer-Verlag, 3, pp 234-239,(update) 1987.

[106] Walling, P.T., and T.M. Savege, A comparison of oesophageal and central venous pressures in the measurement of transpulmonary pressure change, *Br. J. Anaesth.*, 48: 475-479, 1976.

[107] Wesseling, K.H., G.J. Langewouters, A. Zwart and W.J.A. Goedhard, Log-time fitting Apter / Westerhof models to creep curves of human aortas measured in vitro, *Progress Report Inst. Med. Phys. TNO, Utrecht*, 6: 174-188, 1978.

[108] Westerhof, N., and A. Noordergraaf, Arterial viscoelasticity: A generalized model, *J. Biomech.*, 3: 357-379, 1970.

[109] Woestijne van de, K.P., D. Trop and J. Clément, Influence of the mediastinum on the measurement of esophageal pressure and lung compliance in man, *Pflügers Arch.*, 323: 323-341, 1971.

[110] Zin, W.A., L.D. Pengelly and J. Milic-Emili, Single-breath method for measurement of respiratory mechanics in anesthetized animals, *J. Appl. Physiol.*, 52: 1266-1271, 1982.

[111] Zwart, A., Modelling of gas transfer in the lung, a study of prediction and falsification, *Thesis*, Katholieke Universiteit te Nijmegen, The Netherlands.

Nawoord

Bij de opzet en de analyse van de experimenten en bij de uiteindelijke totstandkoming van dit proefschrift heb ik veel steun gehad van de medewerkers van de afdeling.

Zeer dankbaar ben ik Prof. Dr. A. Versprille en Dr. J.M. Bogaard voor de plezierige en goede begeleiding gedurende mijn gehele onderzoek.

Dr. J.R.C. Jansen ben ik zeer erkentelijk voor zijn kundige en vindingrijke hulp bij het oplossen van veel problemen.

Aan A. Drop heb ik in belangrijke mate de uiteindelijke nauwkeurigheid van de observaties te danken. Bovendien heb ik het samenwerken met hem bijzonder op prijs gesteld. Ook drs. A. Logmans, arts, wil ik bij deze bedanken voor de enthousiaste steun bij het uitvoeren van de experimenten zoals beschreven in hoofdstukken 4 en 5.

Bij het schrijven van de computerprogramma's voor de analyse van de experimenten heb ik dankbaar gebruik gemaakt van de grote hoeveelheid, goed gedocumenteerde, 'software' die werd ontwikkeld door Ing. E. Hoorn.

Lenie Hebly, tenslotte, ben ik zeer dankbaar voor haar betrokkenheid bij mijn onderzoek en promotie.

Curriculum Vitae
van
Jeroen van Goudoever

1958	20 augustus, geboren te Leiden
1977	Diploma Gymnasium B, Barlaeus Gymnasium, Amsterdam.
1977	Studie Natuurkunde aan de Universiteit van Amsterdam.

Doctoraal stage, gedurende $2\frac{1}{2}$ jaar voor de helft van de werktijd, bij het Nationaal Instituut voor Kernfysica en Hoge-Energie Fysica (NIKHEF), sectie Kernfysica, in de werkgroep "Pionen en Muonen Fysica" (PiMu) te Amsterdam.

1984	Doctoraal diploma "Experimentele Natuurkunde" aan de Universiteit van Amsterdam, met bijvakken Capita Wiskunde en Meteorologie.
1984-1989	Onderzoeksmedewerker in dienst van de Nederlandse Organisatie voor Wetenschappelijk Onderzoek, N.W.O. voorheen Z.W.O., bij de Stichting voor Biofysica, op het pathofysiologisch laboratorium van de afdeling Longziekten aan de Erasmus Universiteit te Rotterdam (E.U.R.) in het kader van een projekt getiteld "Statisch mechanische eigenschappen van long en thorax" onder begeleiding van Prof. Dr. A. Versprille en Dr. J.M. Bogaard.